Long-Term Effects of Precipitation Extremes on Ecosystem Processes:

From Plant Phenology to Nutrient Cycling

by

Courtney McCann Currier

A Dissertation Presented in Partial Fulfillment
of the Requirements for the Degree
Doctor of Philosophy

Approved April 2023 by the
Graduate Supervisory Committee:

Osvaldo Sala, Chair
Scott Collins
Sasha Reed
Heather Throop

ARIZONA STATE UNIVERSITY

May 2023

ABSTRACT

Drylands cover over 40% of the Earth's surface, account for one third of global carbon cycling, and are hotspots for climate change, with more frequent and severe droughts coupled with deluges of novel magnitude and frequency. Because of their large terrestrial extent, elucidating dryland ecosystem responses to changes in water availability is critical for a comprehensive understanding of controls on global aboveground net primary productivity (ANPP), an important ecosystem service. The focus of this dissertation is to investigate cause-effect mechanisms between altered water availability and ecosystem processes in dryland ecosystems. Across a network of experimental rainfall manipulations within a semiarid Chihuahuan Desert grassland, I examined short- and long-term dynamics of multiple ecosystem processes—from plant phenology to nitrogen cycling—in response to directional precipitation extremes.

Aboveground, I found herbaceous plant phenology to be more sensitive in greenup timing compared to deep-rooted, woody shrubs, implying that precipitation extremes will disproportionately affect grass-dominated compared to woody ecosystems. Surprisingly, after 14 years of experimentally adding water and N, I observed no effect on ANPP. Belowground, bulk soil N dynamics remained stable with differing precipitation amounts. However, mineral associated organic N (MAOM-N) significantly increased under chronic N inputs, indicating potential for dryland soil N sequestration. Conversely, the difference between low- and high-N soil N content may increase a drawdown of N from all soil N pools under low-N conditions whereas plants source N from fertilizer input under high-N conditions. Finally, I considered ecosystem-level acclimation to climate change. I found that N availability decreased with annual

precipitation in space across continents, but it posed initially increasing trends in response to rainfall extremes at the Jornada that decreased after 14 years. Mechanisms for the acclimation process are thus likely associated with differential lags to changes in precipitation between plants and microorganisms.

Overall, my dissertation demonstrates that examining linkages between multiple ecosystem processes, from aboveground phenological cycles to belowground N cycling dynamics, can provide a more integrative understanding of dryland response to climate change. Because dryland range is potentially expanding globally, water limited systems provide a unique and critical focus area for future research that revisit and revise current ecological paradigms.

DEDICATION

To my family,

especially da and mom,

thanks a million.

ACKNOWLEDGMENTS

It is absolutely necessary for me to first thank those who contributed to my endeavor of preparing and completing a Ph.D. Many special people made this possible, and any omissions are a fumble of hand, not of heart. I thank my advisor, Osvaldo Sala, for providing the support to investigate important questions about long-term changes to dryland ecosystems. I enjoyed learning from him the important art of scientific storytelling and finding meaning in data. I also extend my utmost gratitude to my committee members—Heather Throop, Sasha Reed, and Scott Collins—whose guidance, knowledge, and encouragement supported my growth as a young scientist. A number of other scientists also provided valuable mentorship and nurtured my research interests: Michala Phillips, Sharon Hall, Arianne Cease, Liz Makings, Dom Chaloner, and Jim Elser. I am grateful for their thoughtfulness and wisdom.

In the field, laboratory, and office, many people were critical for the success of my research by providing space, resources, training, and assistance. At the Jornada Basin LTER, I thank: Dave Thatcher, Joe Ramirez, John Anderson, Greg Maurer, Deb Peters, Brandon Bestelmeyer, and Niall Hanan. In the lab, working with Natalya Zolotova (ASU METAL Lab) was a joy and highlight of my experience at ASU; thank you. I also thank: Sarah McGregor (ASU METAL Lab); Leah Gaines-Sewell (Nancy Grimm Lab); Adrien Finzi, Marc Giasson, and Bob Michener (Boston University Stable Isotope Lab). Within SOLS, I thank: Krista Hartrick and Maricel Scalzo (ASU SOLS Business Office); Kylie Franse, Amanda Vigil, and Gillian Rodriguez (ASU SOLS Graduate Office); David Bello, Miguel Carrillo, and Judy Swartz (ASU SOLS Facilities).

I am grateful for my fellow current and former lab members who provided intellectual, field, or laboratory support: Abbey Chatwin, Chris Vito, Kelsey Duffy-McGurrin, Lara Reichmann, and many undergraduates (Sam Allbee, Gretel Baur, Zoe Bergman, Andrew Hallberg, Sally Jung, Noah Oas, Jules Petty, Sam Smith, Alex Stettner, Miranda Vega, and Claire Yager).

Moreover, words cannot express the depth of my gratitude and respect for Luis Weber-Grullon, Marcos Sauceda, and Owen McKenna. Not only did these friends offer tangible help with my research, but they also provided peer mentorship and loving kindness that carried me through challenges. I especially thank Sam Jordan for his comradery, trust, and many conversations on and off the bicycle about dryland ecology. Finally, I cannot thank Lau Gherardi enough for his belief in my abilities, his endless encouragement, his love, and so much more.

Outside of the laboratory, I thank my talented peers who I am honored to call friends: Edauri Navarro Perez, Liz Dietz, Ruth Armbruster, Maddy Kelley, Aldo Brandi, and Némesis Ortiz-Declet. To my friends with beautiful imaginations: Meredith G. Johnson, Hannah Berco, Jessie Bersson, Grayson Glazer, Craig Perl, and Mitch Phillips. Finally, to: Tempe Casual Crew, my neighbors at Villa Arsitas, and Farley's Finest.

Most importantly, I thank my family whose unconditional love provide constant strength: mom, dad, Mary, Jeff, Meghan, Timmy, Toby, and cat Artie.

Funding for this research came from the National Science Foundation for the Jornada Basin Long-Term Ecological Research Program Grant DEB 2025166 and the National Science Foundation LTREB Grant DEB 1754106. I was also financially

supported by the ASU Graduate College, the ASU Graduate and Professional Student Association, the ASU School of Life Sciences, the Jornada Basin LTER.

Finally, I acknowledge that I am a visitor to the land where this research was conducted, land that belongs to many indigenous communities. Field and laboratory research took place on the historic homelands of the Mescalero Apache, Manso, Akimel O'odham and Piipaash peoples and their ancestors. I thank these communities, who stewarded this land and continue to care and keep it.

TABLE OF CONTENTS

LIST OF TABLES

LIST OF FIGURES

CHAPTER 1

INTRODUCTION

Theoretical background

Drylands are distinguished from other ecosystems by having an aridity index—the ratio of mean annual precipitation and potential evapotranspiration (MAP/PET)—of less than 0.65 (Atlas 1992). These water-limited ecosystems cover 45% of the global terrestrial surface (Prăvălie 2016), contribute the most to global variability in the C cycle (Poulter et al. 2014, Ahlström et al. 2015, MacBean et al. 2021), and support approximately one third of the world's human population (Safriel et al. 2005, F. A. O. 2019). Drylands include deserts, grasslands, savannas, steppes, and dry forests. Compared to well-studied temperate systems, drylands are equally important yet constitute a younger branch of ecology with patterns that do not necessarily conform to theories developed in mesic ecosystems.

Precipitation is the dominant control of biological processes in drylands. Dryland precipitation patterns are typically characterized as discrete events of varying duration and magnitude. This rainfall pulse concept, first developed by Westoby (1972) and Noy-Meir (1973), theorizes that discontinuous and highly variable rainfall inputs of desert ecosystems recharge ecosystem reserves, which are gradually depleted through time between rainfall events (c.f., "pulse-reserve paradigm"). Precipitation pulse patterns and subsequent effects on ecosystem processes may be further organized hierarchically (Schwinning and Sala 2004), where the rainfall input size is proportional to the biological process that is activated. For example, small rainfall events (< 5 mm) primarily trigger

microbial processes (Collins et al. 2008), as microorganisms occupying the pore space between soil particles are able to use small amounts of water. Conversely, larger organisms, such as plants, require more water to stimulate biological functions, such as seed germination (Beatley 1974). Long-term patterns in small-scale rainfall pulses ultimately determine ecosystem-level processes, such as community dynamics and ecosystem acclimation to climate change, that emerge over decadal timescales. The majority of rainfall in desert ecosystems is comprised of small rainfall pulses, whereas infrequent but large rainfall events determine inter-annual rainfall variability (Sala and Lauenroth 1982). Because the frequency of extreme precipitation events is increasing globally due to anthropogenic climate change (Pörtner et al. 2022), this dissertation focuses primarily on the implications of long-term directional precipitation changes on dryland ecosystem functioning.

Aboveground net primary productivity (ANPP) is an important process in drylands that provides multiple ecosystem services, including carbon sequestration (Lal 2004), forage for rangelands (Briske 2017), and biodiversity support across multiple biomes (Whittaker and Niering 1965, Maestre et al. 2012). The importance of precipitation as the primary control of production in drylands should not be understated; ANPP is tightly linked to mean annual precipitation in water-limited systems, ranging from arid deserts to sub-humid grasslands (Churkina and Running 1998, Sala et al. 2012). Compared to mean annual precipitation (MAP), mean annual temperature (MAT) has relatively smaller effects on ANPP (Epstein et al. 1996). ANPP tends to decrease with increasing temperature, but vegetation responses to MAP and MAT are asymmetrical.

This trend opposes most biological systems that suggest that the temperature effect occurs through changes in the water balance. Underpinning productivity are multiple ecosystem processes, such a plant phenology and nutrient cycling, which interact with water availability and are modified by precipitation extremes.

Phenology, deriving from the Greek word phaino ("to appear"), is the seasonal timing of life cycle events (Rathcke and Lacey 1985). For plants, phenology is distinguished by phenophases, which include the start of season growth (greenup), the timing of maturity, the maximum vegetative output at maturity (maximum greenness), and onset of senescence. Much of phenological understanding comes from regions where water is not often limiting for growth, and phenology is modulated mainly by a combination of photoperiod and temperature (Kramer et al. 2000, Jackson et al. 2001, Zhang et al. 2003), with the exception of tropical forests where variability in photoperiod and temperature is low (Reich 1995, Morellato 2003). However, the determinants and sensitivities of phenophase timing in relationship to climate change are less clear in water-limited ecosystems. As the name suggests, dryland phenology is tightly controlled by both precipitation and temperature. Climate change will result in novel temperature and precipitation regimes that may shift the duration that plants are green in drylands, which consequently will impact carbon fixation and productivity globally (Peñuelas et al. 2009, Bandieri et al. 2020). Understanding ecosystem-level responses to precipitation or temperature can be further dissected by determining causal mechanisms behind phenological shifts at the plant community level. Plant functional types, for example, vary in their response to changes in environmental conditions or resources (Grime 1973).

Functional traits—such as photosynthetic pathways or mean rooting depth—may be correlated with differential phenological sensitivities to shifts in typical temperature or water availability niches. Drylands are projected to probably accelerate expansion over the next century (Yao et al. 2020, Berg and McColl 2021). Thus, understanding the mechanisms of precipitation and temperature controls on phenology will be important to better integrate the role of drylands in global ecological processes, with implications for phenological feedbacks to Earth's water and carbon balance.

Changes to water availability may extend or shorten dryland vegetation growing season length, which in turn affect rates of litter input and nutrient turnover. After water, nitrogen (N) availability is the most important limiting factor for plant productivity (Vitousek and Howarth 1991, Marschner and Rengel 2007). Relatively small rainfall inputs characteristic of drylands regulate low annual rates of organic matter and nutrient cycling (Noy-Meir 1973). Precipitation in drylands is generally spatially heterogeneous as well as temporally variable (Osborne et al. 2022), resulting in rainfall pulses that range in magnitude. Depending on the event size, a rainfall pulse will trigger biological activities at different spatiotemporal scales, resulting in "hot spot" and "hot moment" activities of productivity (Schwinning and Sala 2004, Collins et al. 2008). Thus, nutrient cycling in drylands is dependent on both the magnitude and timing of precipitation events. Because organisms respond hierarchically to rainfall event size based on body size and physiology (Schwinning and Sala 2004), rates of N transformations and losses are also dependent on rainfall pulse size and overall water availability (Austin et al. 2004, Yahdjian and Sala 2010). N mineralization, for example, tends to linearly increase in

coarse-textured soils of arid regions with rainfall pulse frequency (Austin et al. 2004). Periods of drought, conversely, decouple these cycles; inorganic N supply may accumulate (Reichmann et al. 2013, Homyak et al. 2017), depending on the time scale and magnitude of organic inputs. Biological activity associated with N cycling, therefore, is tightly linked to the hydrologic cycle, and this varies according to biological scale and even among functional groups at the same scale. Thus, understanding the causes and consequences of coupling or decoupling of nutrient cycles with water availability is critical for a comprehensive approach to the controls of dryland productivity.

Dissertation overview

Research objectives

The overall research objective of this dissertation is concerned with understanding precipitation controls on dryland phenology and N cycling, which underpin ANPP, at the Jornada Basin Long Term Ecological Research (LTER) site.

Research objective 1 (Chapter 2): Determine the relative contribution of precipitation extremes versus temperature on plant functional type phenology.

Research objective 2 (Chapter 3): Determine how long-term, directional changes to precipitation amount and N availability affect soil N stocks within bulk soil and among two density soil fractions. Further, to elucidate how these N stock dynamics may explain the lack of ANPP response to high N and high-water availability at the Jornada.

Research objective 3 (Chapter 4): Assess the long-term patterns in ecosystem acclimation of the N cycle to directional changes in precipitation amount.

Study site description

The research approach for this dissertation was experimental and based on long-term rainfall manipulation studies at the Jornada Basin LTER site. The Jornada Basin LTER is located at 32.56 latitude, -106.78 longitude (Las Cruces, NM, USA) and receives a mean precipitation amount of 250 mm annually. Seventy six percent of this mean annual precipitation comes in the form of summer monsoonal storms derived from the Gulf of Mexico (Havstad et al. 2006). During the summer, which constitutes the main growing season for dominant vegetation, mean maximum temperature is 36°C. Dominant vegetation consists of the C_3 perennial shrub, *Prosopis glandulosa* (honey mesquite) and the C_4 perennial grass, *Bouteloua eriopoda* (black grama). Soils are classified as Cacique loamy fine sand with weakly developed textural B (argillic) horizons overlaying semi-indurated to indurated caliche at approximately 30–60 cm in depth (Gile 1981, Monger 2006). My specific study location was located within Pastures 9 and 13, which contain the most continuous and intact black grama grass patches remaining at the Jornada LTER. Overall, the Jornada LTER presents an ideal study site for dryland ecosystem processes due to its closed-basin topography, monsoonal rainfall system, and common plant genera that are found worldwide.

Approach

To address my research objectives, the main approach for my dissertation consists of long-term field experiments at the Jornada Basin LTER. These experiments consist of rainfall manipulations that passively intercept and actively apply incoming rainfall in

amounts ranging from 50–80% ambient precipitation. Specifically, automated rainfall manipulation systems (ARMS; Yahdjian and Sala 2002, Gherardi and Sala 2013) operate by passively intercepting incoming precipitation using an array of acrylic "shingles" constructed at angles that allow water to flow into catchment containers. Concurrent with a rain event, collected water activates a float switch within each container, and solar-powered battery activates a pump that moves water through a PVC-sprinkler system onto irrigated plots. Chapters 2 and 3 utilized data from the oldest long-term experiment, which commenced in 2006, and alters experimental water availability by ± 80%. This amount is representative of historic rainfall extremes at the Jornada Basin LTER, equivalent to a 1/100-year drought. Chapter 4 utilized multiple experiments with differing start dates and rainfall manipulation intensities. In addition to altering water availability by ± 80%, I also utilized experiments that altered incoming precipitation by ± 50%. Within these experiments, I conducted field and laboratory measurements at multiple temporal scales—ranging from daily to annually—to assess ecosystem responses to directional precipitation extremes.

Complementary to the field approach, I also include data from existing sources in my analyses. These include meteorological data made at the Jornada Basin LTER and large ecological spatial datasets from the literature and National Ecological Observatory Network (NEON). Synthesizing observational data with experimentation provided for my research a powerful means to assess causal mechanisms behind ecological responses to precipitation extremes.

Dissertation structure

To address the outlined research objectives above, my dissertation contributes three novel data chapters to the field of dryland ecology and one concluding chapter summarizing the main findings.

Chapter 2 entitled "Precipitation versus temperature as phenology controls in drylands" addresses Research Objective 1. Incoming precipitation was experimentally manipulated at the Jornada Basin LTER for over a decade. I analyzed plant phenology responses at the daily scale for seven years within in response to precipitation extremes and ambient temperature patterns and compared shifts in phenology to estimated long-term phenology patterns.

Chapter 3 entitled "Unresponsive drylands to nitrogen availability: Access to alternative sources?" addresses Research Objective 2. After observing no ANPP response by the dominant grass to high N and high-water availability, I tested the hypothesis that under low N availability plants derive N from different soil fractions and switch to N derived from fertilizer when N amendments are present. I analyzed N stocks among bulk soil, the particulate organic matter soil fraction, and the mineral associated organic matter fraction from a long-term rainfall manipulation crossed with N fertilization experiment at the Jornada Basin LTER.

Chapter 4, entitled "Acclimation of the nitrogen cycle to changes in precipitation," addresses Research Objective 3. To assess how prolonged shifts in water availability facilitate acclimation of the N cycle, I used the natural abundances of stable nitrogen isotopes for plants and soils 5–14 years after directional precipitation shifts were

initiated. I then compared these temporal patterns within one site to spatial patterns at the continental scale.

Chapter 5 integrates the major conclusions from Chapters 2–4 and presents closing remarks for the entire dissertation.

References

Ahlström, A., M. R. Raupach, G. Schurgers, B. Smith, A. Arneth, M. Jung, M. Reichstein, J. G. Canadell, P. Friedlingstein, A. K. Jain, E. Kato, B. Poulter, S. Sitch, B. D. Stocker, N. Viovy, Y. P. Wang, A. Wiltshire, S. Zaehle, and N. Zeng. 2015. "The dominant role of semi-arid ecosystems in the trend and variability of the land CO_2 sink." *Science* 348:895–899.

Atlas, U. 1992. *World Atlas of Desertification*, Vol. 80. Kent: UNEP and E. Arnold Ltd.

Austin, A. T., L. Yahdjian, J. M. Stark, J. Belnap, A. Porporato, U. Norton, D. A. Ravetta, and S. M. Schaeffer. 2004. "Water pulses and biogeochemical cycles in arid and semiarid ecosystems." *Oecologia* 141:221–235.

Bandieri, L. M., R. J. Fernández, and A. J. Bisigato. 2020. "Risks of neglecting phenology when assessing climatic controls of primary production." *Ecosystems* 23:164–174.

Beatley, J. C. 1974. "Phenological events and their environmental triggers in Mojave Desert ecosystems." *Ecology* 55:856–863.

Berg, A., and K. A. McColl. 2021. "No projected global drylands expansion under greenhouse warming." *Nature Climate Change* 11:1–7.

Briske, D. D., editor. 2017. *Rangeland Systems: Processes, Management and Challenges*. New York, NY: Springer International Publishing.

Churkina, G., and S. W. Running. 1998. "Contrasting climatic controls on the estimated productivity of global terrestrial biomes." *Ecosystems* 1:206–215.

Collins, S. L., R. L. Sinsabaugh, C. Crenshaw, L. Green, A. Porras-Alfaro, M. Stursova, and L. H. Zeglin. 2008. "Pulse dynamics and microbial processes in aridland ecosystems: Pulse dynamics in aridland soils." *Journal of Ecology* 96:413–420.

Epstein, H. E., W. K. Lauenroth, I. C. Burke, and D. P. Coffin. 1996. “Ecological responses of dominant grasses along two climatic gradients in the Great Plains of the United States.” *Journal of Vegetation Science* 7:777–788.

F. A. O. 2019. “Forests and Land Use in Drylands: The First Global Assessment—Full Report.” *FAO Forestry Paper* 184.

Gherardi, L. A., and O. E. Sala. 2013. “Automated rainfall manipulation system: a reliable and inexpensive tool for ecologists.” *Ecosphere* 4:art18.

Gile, L. H. 1981. “Soils and geomorphology in the basin and range area of southern New Mexico: Guidebook to the Desert Project, New Mexico.” *Bureau of Mines and Mineral Resources Memoir* 39:222.

Grime, J. P. 1973. “Competitive exclusion in herbaceous vegetation.” *Nature* 242:344–347.

Havstad, K. M., L. F. Huenneke, and W. H. Schlesinger, editors. 2006. *Structure and Function of a Chihuahuan Desert Ecosystem: The Jornada Basin Long-Term Ecological Research Site*. New York, NY: Oxford University Press.

Homyak, P. M., S. D. Allison, T. E. Huxman, M. L. Goulden, and K. K. Treseder. 2017. “Effects of drought manipulation on soil nitrogen cycling: A meta-analysis.” *Journal of Geophysical Research: Biogeosciences* 122:3260–3272.

Jackson, R. B., M. J. Lechowicz, X. Li, and H. A. Mooney. 2001. “Phenology, growth, and allocation in global terrestrial productivity.” In *Terrestrial Global Productivity*, edited by J. Roy, B. Saugier, and H. A. Mooney, 61–82. Cambridge, MA: Academic Press.

Kramer, K., I. Leinonen, and D. Loustau. 2000. “The importance of phenology for the evaluation of impact of climate change on growth of boreal, temperate and Mediterranean forests ecosystems: An overview.” *International Journal of Biometeorology* 44:67–75.

Lal, R. 2004. “Carbon sequestration in dryland ecosystems.” *Environmental Management* 33:528–544.

MacBean, N., R. L. Scott, J. A. Biederman, P. Peylin, T. Kolb, M. E. Litvak, P. Krishnan, T. P. Meyers, V. K. Arora, V. Bastrikov, D. Goll, D. L. Lombardozzi, J. E. M. S. Nabel, J. Pongratz, S. Sitch, A. P. Walker, S. Zaehle, and D. J. P. Moore. 2021. “Dynamic global vegetation models underestimate net CO_2 flux mean and inter-annual variability in dryland ecosystems.” *Environmental Research Letters* 16:094023.

Maestre, F. T., J. L. Quero, N. J. Gotelli, A. Escudero, V. Ochoa, M. Delgado-Baquerizo, M. Garcia-Gomez, M. A. Bowker, S. Soliveres, C. Escolar, P. Garcia-Palacios, M. Berdugo, E. Valencia, B. Gozalo, A. Gallardo, L. Aguilera, T. Arredondo, J. Blones, B. Boeken, D. Bran, A. A. Conceicao, O. Cabrera, M. Chaieb, M. Derak, D. J. Eldridge, C. I. Espinosa, A. Florentino, J. Gaitan, M. G. Gatica, W. Ghiloufi, S. Gomez-Gonzalez, J. R. Gutierrez, R. M. Hernandez, X. Huang, E. Huber-Sannwald, M. Jankju, M. Miriti, J. Monerris, R. L. Mau, E. Morici, K. Naseri, A. Ospina, V. Polo, A. Prina, E. Pucheta, D. A. Ramirez-Collantes, R. Romao, M. Tighe, C. Torres-Diaz, J. Val, J. P. Veiga, D. Wang, and E. Zaady. 2012. "Plant species richness and ecosystem multifunctionality in global drylands." *Science* 335:214–218.

Marschner, P., and Z. Rengel, editors. 2007. *Nutrient Cycling in Terrestrial Ecosystems*. New York, NY: Springer.

Monger, H. C. 2006. "Soil development in the Jornada Basin." In *Structure and Function of a Chihuahuan Desert Ecosystem: The Jornada Basin Long-Term Ecological Research Site*, edited by K. M. Havstad, L. F. Huenneke, and W. H. Schlesinger, 81–106. New York, NY: Oxford University Press.

Morellato, L. P. C. 2003. "South America." in *Phenology: An Integrative Environmental Science*, edited by M. D. Schwartz, 75–92. Dordrecht: Kluwer Academic Press.

Noy-Meir, I. 1973. "Desert ecosystems: Environment and producers." *Annual Review of Ecology and Systematics* 4:25–51.

Osborne, B. B., B. T. Bestelmeyer, C. M. Currier, P. M. Homyak, H. L. Throop, K. Young, and S. C. Reed. 2022. "The consequences of climate change for dryland biogeochemistry." *New Phytologist* 236:15–20

Peñuelas, J., T. Rutishauser, and I. Filella. 2009. "Phenology feedbacks on climate change." *Science* 324:887–888.

Pörtner, H. O., D. C. Roberts, H. Adams, C. Adler, P. Aldunce, E. Ali, R. A. Begum, R. Betts, R. B. Kerr, and R. Biesbroek, editors. 2022. *Climate Change 2022: Impacts, Adaptation and Vulnerability. Contribution of Working Group II to the Sixth Assessment Report of the Intergovernmental Panel on Climate Change*. Geneva, Switzerland: IPCC.

Poulter, B., D. Frank, P. Ciais, R. B. Myneni, N. Andela, J. Bi, G. Broquet, J. G. Canadell, F. Chevallier, Y. Y. Liu, S. W. Running, S. Sitch, and G. R. van der Werf. 2014. "Contribution of semi-arid ecosystems to interannual variability of the global carbon cycle." *Nature* 509:600–603.

Prăvălie, R. 2016. “Drylands extent and environmental issues. A global approach.” *Earth-Science Reviews* 161:259–278.

Rathcke, B., and E. P. Lacey. 1985. “Phenological patterns of terrestrial plants.” *Annual Review of Ecology and Systematics* 16:179–214.

Reich, P. B. 1995. “Phenology of tropical forests: patterns, causes, and consequences.” *Canadian Journal of Botany* 73:164–174.

Reichmann, L. G., O. E. Sala, and D. P. Peters. 2013. “Water controls on nitrogen transformations and stocks in an arid ecosystem.” *Ecosphere* 4:1–17.

Safriel, U., Z. Adeel, D. Niemeijer, J. Puigdefabregas, R. White, R. Lal, and D. Mcnab. 2005. “Dryland Systems, Millenium Ecosystem Assessment.” in *Ecosystems and Human Well-Being: Current State and Trends*, 623–662. Washington D.C.: Island Press.

Sala, O. E., L. A. Gherardi, L. Reichmann, E. Jobbagy, and D. Peters. 2012. “Legacies of precipitation fluctuations on primary production: Theory and data synthesis.” *Philosophical Transactions of the Royal Society B: Biological Sciences* 367:3135–3144.

Sala, O. E., and W. K. Lauenroth. 1982. “Small rainfall events: An ecological role in semiarid regions.” *Oecologia* 53:301–304.

Schwinning, S., and O. E. Sala. 2004. “Hierarchy of responses to resource pulses in arid and semi-arid ecosystems.” *Oecologia* 141:211–220.

Vitousek, P. M., and R. W. Howarth. 1991. “Nitrogen limitation on land and in the sea: How can it occur?” *Biogeochemistry* 13:87–115.

Westoby, M. 1972. “Problem-oriented modelling: A conceptual framework.” *Page IBP/Desert Biome*, Information Meeting, Tempe, Arizona.

Whittaker, R. H., and W. A. Niering. 1965. “Vegetation of the Santa Catalina Mountains, Arizona: A gradient analysis of the south slope.” *Ecology* 46:429–452.

Yahdjian, L., and O. E. Sala. 2002. “A rainout shelter design for intercepting different amounts of rainfall.” *Oecologia* 133:95–101.

Yahdjian, L., and O. E. Sala. 2010. “Size of precipitation pulses controls nitrogen transformation and losses in an arid Patagonian ecosystem.” *Ecosystems* 13:575–585.

Yao, J., H. Liu, J. Huang, Z. Gao, G. Wang, D. Li, H. Yu, and X. Chen. 2020. "Accelerated dryland expansion regulates future variability in dryland gross primary production." *Nature Communications* 11:1665.

Zhang, X., M. A. Friedl, C. B. Schaaf, A. H. Strahler, J. C. F. Hodges, F. Gao, B. C. Reed, and A. Huete. 2003. "Monitoring vegetation phenology using MODIS." *Remote Sensing of the Environment* 84:471–475.

CHAPTER 2

PRECIPITATION VERSUS TEMPERATURE AS PHENOLOGY CONTROLS IN DRYLANDS

Abstract

Cycles of plant growth, termed "plant phenology," are tightly linked to environmental controls. The length of time spent growing, bounded by the start and end of season, is an important determinant of the global carbon, water, and energy balance. Much focus has been given to global warming and consequences for shifts in growing season length in temperate regions. In conjunction with warming temperatures, altered precipitation regimes are another facet of climate change that have potentially larger consequences than temperature in dryland phenology globally. We experimentally manipulated incoming precipitation in a semiarid grassland for over a decade and recorded plant phenology at the daily scale for seven years. We found precipitation to have a strong relationship with the timing of grass greenup and senescence but temperature had only a modest effect size on grass greenup. Pre-season drought strongly resulted in delayed grass greenup dates and shorter growing season lengths. Spring and summer drought corresponded with earlier grass senescence whereas higher precipitation accumulation over these seasons corresponded with delayed grass senescence. However, extremely wet conditions diluted this effect and caused a plateaued response. Deep-rooted woody shrubs showed few effects of variable precipitation or temperature on phenology and displayed consistent annual phenological timing compared to grasses. While rising temperatures have already elicited phenological consequences and extended

growing season length for mid and high-latitude ecosystems, precipitation change will be the major driver of phenological change in drylands that cover 40% of land surface with consequences for the global carbon, water, and energy balance.

Introduction

Annual cycles of plant growth, termed plant "phenology," are sensitive to variation in their environmental cues, such as temperature or precipitation, which will be modified by anthropogenic climate change. Phenology affects net ecosystem productivity and global carbon cycling since carbon fixation dominates over ecosystem respiration during the phase when plants are green, and respiration dominates over carbon fixation during the time when ecosystems are bare (Kikuzawa 1995, Goulden et al. 1996, Schlesinger 2005). The length of the green period is one of the determinants of the carbon balance. Additionally, phenology affects the energy balance of our planet. When canopy shifts from bare to green, the albedo decreases, therefore increasing the amount of energy absorbed (Richardson et al. 2013). Duration of the phase in which ecosystems remain green affects energy partitioning with ultimate feedbacks to the global energy balance. A longer duration of the green phase will enhance the effect of increased greenhouse gas emissions on temperature. Phenology also controls ecosystem water balance. During inactive parts of the year, when more bare ground is exposed, water losses occur through soil evaporation, deep percolation, or run-off. When plants and ecosystems leaf out, transpiration then acts as an additional, major water loss from the ecosystem. Therefore,

changes in the green period may affect the amount of water reaching streams, recharging water tables, and ultimately affecting precipitation patterns (Shukla et al. 1990).

Many phenological studies focus on mesic, temperate, and alpine ecosystems, demonstrating that phenology is controlled primarily by temperature in these regions (Goulden et al. 1996, Kramer et al. 2000, Jackson et al. 2001, Zhang et al. 2003, Richardson et al. 2018b, Collins et al. 2021). Indeed, scientists have observed increased global net primary production (NPP) due to warming temperature-driven extension of growing season length in recent decades, mostly in mid and northern latitude regions (Nemani et al. 2003). However, the determinants and sensitivities of the timing and magnitude of greenness in relationship to climate are less clear in water-limited ecosystems. Drylands are characterized by having an aridity index, the ratio of mean annual precipitation and potential evapotranspiration (MAP/PET), of less than 0.65 (Atlas 1992). Drylands have been relatively overlooked in phenology, yet these important ecosystems cover over 40% of the terrestrial earth surface (Prăvălie 2016), account for 30% of global carbon fixation (Field et al. 1998), and explain most of the interannual variability of the carbon cycle (Poulter et al. 2014). As the name suggests, these systems are biologically sensitive to water availability. Climate change in drylands is expected to decrease precipitation, probably expand the global dryland area (but see Berg and McColl 2021), and increase interannual precipitation variability (Gherardi and Sala 2019) with more frequent and severe droughts coupled with deluges of novel magnitude and frequency (Petrie et al. 2014, Ault 2020). Given the large terrestrial extent of drylands, phenological sensitivity of plants within these ecosystems to directional changes in

precipitation amount could have large consequences from local forage production to carbon, water, and energy balance of our planet.

Our study addressed three questions. First, we asked: Within a dryland community, how do two dominant plant species differ in their phenology patterns? Specifically, we focused on a perennial, deciduous shrub (*Prosopis glandulosa*) and a perennial grass (*Bouteloua eriopoda*). These two dominant plant species account for most (67%) of aboveground net primary production (ANPP) at our study site (Huenneke et al. 2002, Reichmann et al. 2013b). The *Prosopis* and *Bouteloua* genera represent common plant-functional types found in drylands worldwide, shrubs and grasses, and thus we refer to our study organisms as "shrub" and "grass" respectively. Second question, what are the determinants of those phenological patterns? Given the morphological and physiological differences, we expect our study species to respond differentially to changes in phenological controls, such as seasonal water availability or temperature. *P. glandulosa*, a C_3, N-fixing shrub, exhibits extensive rooting systems that can sometimes reach 5 m in depth while *B. eriopoda* is a C_4, shallow-rooted, stoloniferous grass (Gibbens and Lenz 2001). Ecophysiologically, *P. glandulosa* typically outperforms *B. eriopoda* under drought stress, maintaining a more favorable leaf-water potential and higher photosynthetic rates for a longer fraction of the growing season (Throop et al. 2012). Because of the large spatial extent of our study species within North American deserts and grasslands ("Occurrence records of Bouteloua eriopoda (Torr.) Torr." 2021, "Occurrence records of Prosopis glandulosa Torr." 2021) and the ubiquity of the *Bouteloua* and *Prosopis* genera in drylands worldwide ("Occurrence records of

Bouteloua Lag." 2021, "Occurrence records of Prosopis L." 2021), our third question asks: What are the consequences of a changing climate for phenology of drylands?

Our approach to understanding the effects of temperature and precipitation on dryland phenology combines long-term precipitation manipulative field experiments with temperature observations. Here, we present a multi-year experimental study at the Jornada Basin LTER (New Mexico, USA) that combines rainfall manipulation in the field and phenocameras to address our three objectives while elucidating cause-effect relationships between precipitation, temperature, and phenology patterns of two plant functional groups, woody shrubs and grasses. The vegetation habitat types of our field site are representative of the northern Chihuahuan Desert, which covers a total spatial extant of 501,895 km^2 and is the largest desert of North America (Havstad et al. 2006). Mean annual rainfall of 250 mm, measured potential evaporation of about 2200 mm yr^{-1}, and the closed-basin topography typical of the southwestern United States make this site an ideal, representative study system for understanding dryland ecosystem processes (Havstad et al. 2006, Maestre et al. 2021). Because it is impossible to detect long-term trends based on short-term observations (Collins et al. 2011), our study provides novel perspectives on precipitation-temperature-phenology interactions in drylands by synthesizing seven years of data from a long-term rainfall manipulation experiment in a multi-functional group system. This plot-level scale provides an advantage because community composition could amplify or offset the effects of climate change if plant groups respond differently (Ibrahim et al. 2021). Finally, one study estimates that climate change has already advanced plant greenup by 2.3–5.1 days $decade^{-1}$ for the Northern

Hemisphere (Parmesan 2007) and could extend growing season length in some ecosystems by 1–2 weeks under current warming trends by the end of this century (Richardson et al. 2018b). Our study presents a temporal resolution at the daily scale, matching the timescale of future climate-change impacts.

Methods

Overview

Our objective was to investigate temperature and precipitation controls on the phenology of a dryland ecosystem co-dominated by two plant types. To address our questions, phenocameras were installed just outside of a long-term rainfall manipulation experiment in which incoming precipitation was subtracted or added by 80%, located at the Jornada Basin Long Term Ecological Research site (New Mexico, USA). Daily images were analyzed for changes in greenness through time. We extracted greenup (start of season) and senescence (end of season) dates from the greenness vs. time curves for each plant species and explored their relationships with temperature and precipitation using linear mixed effects models.

Study Site Description

This study was conducted at the Jornada Basin Long Term Ecological Research (LTER) site, located at 32.56 latitude, -106.78 longitude (Las Cruces, NM, USA). The Jornada Basin receives a mean precipitation amount of 250 mm annually. Seventy six percent of this mean annual precipitation comes in the form of summer monsoonal storms

derived from the Gulf of Mexico (Havstad et al. 2006). During the summer, which constitutes the main growing season for dominant vegetation, mean maximum temperature is 36°C. Dominant vegetation consists of the C_3 perennial shrub, *Prosopis glandulosa* (honey mesquite) and the C_4 perennial grass, *Bouteloua eriopoda* (black grama). Soils are classified as Cacique loamy fine sand with weakly developed textural B (argillic) horizons overlaying semi-indurated to indurated caliche at approximately 30–60 cm in depth (Gile 1981, Monger 2006).

Climate Variables

Climate data were obtained from the meteorological stations nearest to the experimental plots. Gap-filled daily precipitation sums were obtained from the Jornada G-BASN long-term NPP site (32.53 latitude, -106.79 longitude; approximately 3.3 km southwest from experimental plots) (Yao et al. 2020). Daily temperature means were obtained from the Jornada Experimental Range Headquarters NOAA station (32.62 latitude, -106.74 longitude; approximately 7.5 km northeast from study plots), calculated as the mean of the daily minimum and maximum.

Experimental Design and Image Capture

Water treatments were achieved using rainout shelters that decreased incoming precipitation by 80% and automated irrigation systems that simultaneously applied 80% of incoming precipitation (Yahdjian and Sala 2002, Gherardi and Sala 2013). During precipitation events, shelters intercepted and redirected incoming rainfall to a PVC

irrigation system surrounding +80% treatment plots by means of a solar-powered pump; control plots received ambient precipitation (with no shelter or irrigation system) throughout the duration of the experiment. Manipulation intensities were based on extremes of historical precipitation data for the region. Rainfall manipulation treatments were started in 2006 along with control plots that received ambient rainfall (n=6; N=18 2.5 x 2.5 m plots) (Reichmann et al. 2013b).

To address our questions, Wingscape TimeLapse Pro (WCT 00125) "phenocams" were installed just outside of nine plots (n=3 per treatment) in year 8 (2014) and an additional nine (to increase our replication to n=6 per treatment) were installed in year 12 of the experiment (2018). All cameras were installed facing west/southwest, horizontal and aimed to the center of each plot (Fig. S2.1). Images taken before 2018 were captured once during peak sunlight at noon, and images taken after 2018 were captured every 30 minutes between 11:00 and 14:00.

Image Analyses

Daily images from each plot were analyzed for changes in greenness through time. Three regions of interest (150 x 150 pixels) were situated on each dominant grass patch (*B. eriopoda*) and central shrub (*P. glandulosa*) using a Matlab-based graphical user interface, PhenoAnalyzer (patent pending), developed by the Craig Tweedie System Ecology Lab (University of Texas, El Paso) (Ramirez et al. 2021). The regions of interest were placed on portions of each plant and plant patch that qualitatively had the most consistent leaf cover in order to avoid analyzing extraneous parts of the image, such as

soil, sky, obstruction from other plants, or woody stems. Pixelated information were extracted and composited, resulting in output that contained date, and red, blue, and green color channel information. The green chromatic coordinate (g_{cc}), analogous to NDVI in other phenology studies, was calculated as:

$$g_{cc} = \frac{(green\ digital\ number)}{[(red\ digital\ number)+(blue\ digital\ number)+(green\ digital\ number)]} \qquad eq.\ 2.1$$

The g_{cc} index has been found to be a suitable color index for phenology studies at the landscape and plot level (Sonnentag et al. 2012, Richardson et al. 2018a). From these time series data for each plot, we followed the double logistic model curve-fitting and phenophase extraction approach using the per90 g_{cc} after Sonnentag et al. (2012) and the phenopix package (Filippa et al. 2016) in R version 4.0.3 (R Core Team 2018). Within this package, images that were below a brightness threshold of 0.2 (due to cloudy days or camera obstruction) did not pass quality control and were automatically discarded using the "night" filter within the autoFilter() function. A rolling window of 7 days for images taken before 2018 (one image per day) and 3 days for images taken after 2018 (multiple images per day) were applied to the 90th percentile of g_{cc} data time series. Shrub data were fit with a klosterman curve (Klosterman et al. 2014) using the gu extraction method (Gu et al. 2009) while grasses were best fit with a gu curve (Gu et al. 2009) using the klosterman extraction method (Klosterman et al. 2014). Some plots were missing data due to camera failure or installation of new cameras mid-season (Table S2.1).

Statistical Analyses

The independent variables, precipitation amount (mm) and mean air temperature (°C), were categorized into the following seasons: winter (Jan 01–Mar 31), spring (Apr 01–Jun 30), summer (Jul 01–Sept 31, the typical monsoon season at the Jornada Basin LTER), and fall (Oct 01–Dec 31). We selected the winter season as the independent variable for greenup analyses, as these are the months immediately preceding typical greenup events observed long-term at this site. We selected the spring and summer seasons for senescence analyses, specifically using rainfall sums across these months as the precipitation variable. For the temperature variable in senescence analyses, we used mean air temperature from the fall following the typical growing season. We used maximum likelihood to compare the fixed effects (Bolker et al. 2009) of precipitation amount and mean air temperature on plant greenup and senescence with the following linear mixed effects models :

$$Y_{si} = \beta_0 + S_{0s} + \beta_1 X_i + e_{si} \qquad \textit{eq. 2.2}$$

$$Y_{sj} = \beta_0 + S_{0s} + \beta_2 X_j + e_{si} \qquad \textit{eq. 2.3}$$

$$Y_{sj} = \beta_0 + S_{0s} + \log(\beta_2 X_j + 2) + e_{sj} \qquad \textit{eq. 2.4}$$

$$Y_{sij} = \beta_0 + S_{0s} + \beta_1 X_i + \beta_2 X_j + e_{sij} \qquad \textit{eq. 2.5}$$

$$Y_{sij} = \beta_0 + S_{0s} + \beta_1 X_i + \log(\beta_2 X_j + 2) + e_{si} \qquad \textit{eq. 2.6}$$

$$Y_{sij} = \beta_0 + S_{0s} + \beta_1 X_i + \beta_2 X_j + \beta_1 X_i \beta_2 X_j + e_{sij} \qquad \textit{eq. 2.7}$$

$$Y_{sij} = \beta_0 + S_{0s} + \beta_1 X_i + \beta_2 X_j + \beta_1 X_i \log(\beta_2 X_j + 2) + e_{sij} \qquad \textit{eq. 2.8}$$

$S_{0s} \sim N(0, \tau_{00}^2\ )$,

$e_{sij} \sim N(0, \sigma^2)$

Where Y_{sij} = response (greenup or temperature), β_0 = intercept, S_{0s} = random effect (year), $\beta_1 X_i$ = fixed effect 1 (mean temperature), $\beta_2 X_j$ = fixed effect 2 (precipitation amount), e_{sij} = residuals. Because some seasons may have zero or less than 1 mm of rainfall, logarithmic models included addition of a constant to the precipitation variable. All linear mixed effects models were analyzed using the lmer() function in the lme4 package (Bates et al. 2014). We used Akaike Information Criterion (AIC) to select the best model (Sakamoto et al. 1986). Models that met our criteria had the lowest AIC with $\Delta AIC > 2$, otherwise the most parsimonious model was selected. Residuals of selected models were tested for and exhibited normality.

Results

Overview

We found that woody shrubs greenup earlier in the summer growing season, around day of year 96 (early April) whereas grasses greenup later, with a mean greenup day of year of 157 (mid-June) (Fig. 2.1). These results are typical of the Jornada Basin and match landscape-level observations made previously (Browning et al. 2017). In general, growing season length for shrubs is longer than that for grasses; mean growing season length was 187 and 97 days for shrubs and grasses, respectively.

The division of temporal niches for these two plant species may reflect responses to the cue that varies the most at the annual scale (Okin et al. 2018). In drylands, that cue is precipitation (Trenberth et al. 2003, Gherardi and Sala 2019), which varied the most annually at our site both over the long-term (105 years) (Fig. 2.2a) and during our study

period (7 years; Fig. 2.2b). The long-term coefficient of variation (CV) for annual precipitation was approximately 39% whereas the CV for air temperature (calculated using temperature in Kelvin) was approximately 0.34% (Table S2.1). At the intra-annual scale, transitions in seasonal temperature are essential triggers that plants also may use to shift between phenological stages of growth. We explored the relative effects of temperature and precipitation, two important phenological cues and components of environmental change, on grass and shrub phenology.

Model Selection

For grass greenup response, the additive model with both temperature and precipitation (equation 2.5) met our criteria and was selected. For shrub greenup response, the model with temperature alone (equation 2.2) met our criteria and was selected. Grass senescence was best explained by the logarithmic precipitation model (equation 2.4). Shrub senescence was best explained by the non-logarithmic precipitation model (equation 2.3). For all selected models, except that for shrub senescence, the random effect variances were estimated as zero. While singularity indicates a mixed model that is over-fitted, we felt that it was important to retain the random effect term (year) to reflect the repeated nature of our experimental design. Bolker et al. (2009) affirm that in cases like this, the results remain unchanged and the random effect parameter may be retained. The Supporting Information contains statistical output for AIC comparisons (Table S2.2) and results from each mixed model (Tables S2.3–S2.6).

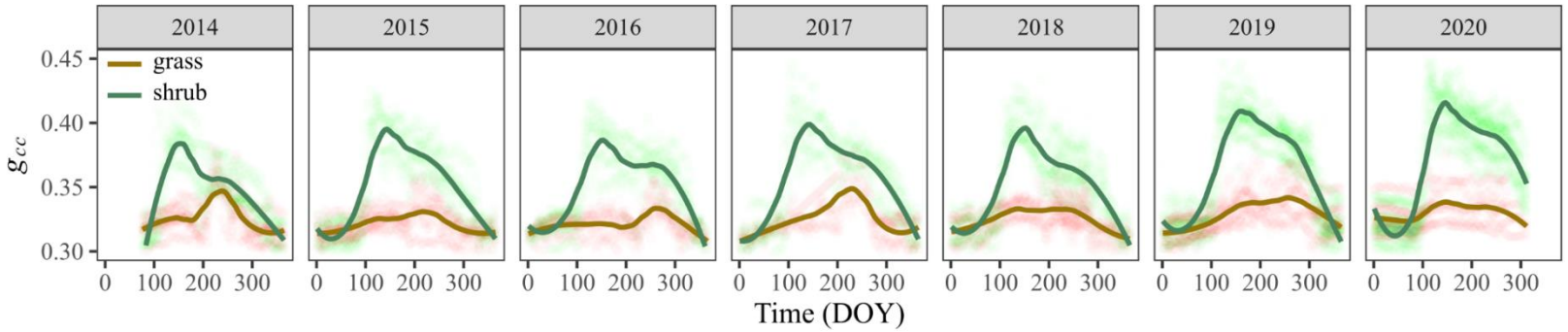

Figure 2.1. Annual greenness (as green chromatic coordinate, or g_{cc}) versus time (as Julian day of year) curves for grass (gold line) and shrub (green line) functional types at the Jornada Basin LTER.

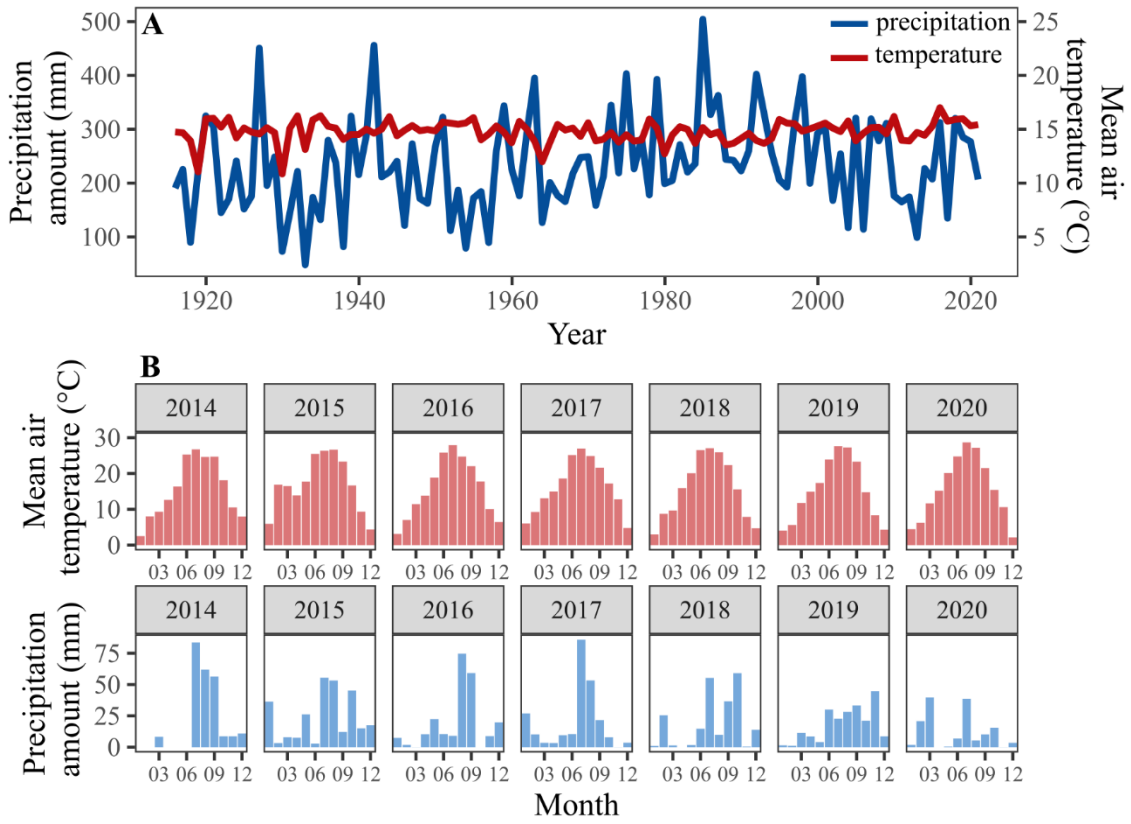

Figure 2.2. (A) Long-term (1915-2020) trends in annual precipitation amount and mean annual temperature at the Jornada; and (B) monthly mean air temperature (°C) and monthly precipitation sums (mm) over the study period (2014-2020) at the Jornada Basin LTER.

Table 2.1. Short-term (2014–2020) and long-term (1915–2020) climate means and coefficients of variation (CV) for temperature and precipitation at the Jornada Basin Long LTER.

	Study-period (2014–2020)		**Long-term (1915–2020)**	
	Mean	*Coefficient of Variation*	*Mean*	*Coefficient of Variation*
Temperature	289.7 K	0.26%	288.9 K	0.34%
Precipitation	242 mm	29%	232 mm	39%

Phenology Responses of Grasses and Shrubs

Grass and shrub greenup exhibited differential responses to environmental cues. Grass greenup responded significantly to winter precipitation (Fig. 2.3a, Table S2.3; fixed effect estimate: -1.8; CI: -2.60 – -1.01; $p < 0.05$; marginal $R^2 = 0.46$). Dry pre-season winter conditions resulted in delayed grass greenup, and wet conditions advanced grass greenup. The effect of winter precipitation on grass greenup resulted in extreme drought delaying this important phenological transition up to 110 days, from the earliest statistically estimated day-of-year (DOY) 95 to the latest DOY 205 (while holding temperature constant). The effect of winter temperature on grass greenup was also significant, indicating that warmer winter temperatures resulted in earlier grass greenup whereas cooler temperatures delayed grass greenup up to 98 days, from the earliest estimated DOY 75 to the latest DOY 173 (while holding precipitation constant) (Fig. 2.3b, Table S2.3; fixed effect estimate: -16.71; CI: -28.40 – -5.03; $p < 0.05$; marginal $R^2 = 0.46$). Shrub greenup, on the contrary, had a relatively constant date where the standard error of greenup around a mean DOY of 97 was only 0.27. Shrub greenup was ecologically insensitive to winter precipitation (Fig. 2.3c), and this fixed effect was not included in the best-selected explanatory model. Additionally, shrub greenup did not respond to winter temperature (Fig. 2.3d, Table S2.4; fixed effect estimate: -1.05; CI: -2.15 – 0.05; $p = 0.06$; marginal $R^2 = 0.036$).

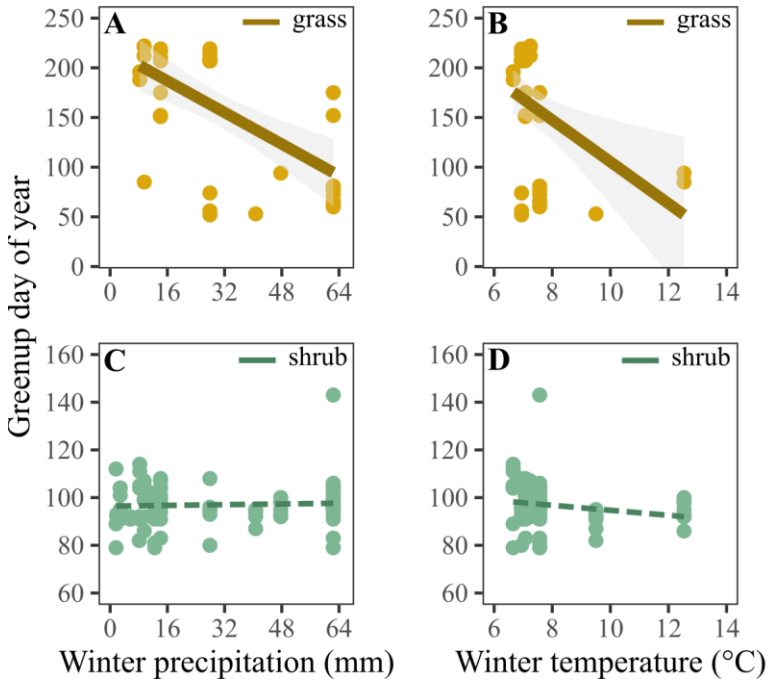

Figure 2.3. Winter temperature and winter precipitation effects on grass (A, B) and shrub (C, D) greenup, expressed as day of the year. Points represent plot-year replicates. Significant linear mixed model precipitation effects in (A), (B), and (C) are denoted by a solid line, which represents the predicted model fit ± 95% confidence interval, calculated as ± 2 x standard error around the effect size. In (A) and (B), grass greenup = 337.8 + (-1.8 x precipitation) + (-16.71 x mean air temperature). In (C) and (D), shrub greenup did not statistically respond to either winter precipitation or mean winter air temperature.

Grass senescence was significantly linked to cumulative spring and summer precipitation (Fig. 2.4a, Table S2.5; fixed effect estimate: 45.78; CI: 5.04 – 86.51; $p < 0.05$; marginal $R^2 = 0.15$). On the contrary, grass senescence did not depend on any changes in fall temperature (Fig. 2.4b), which was not included in the best-selected explanatory model. Growing-season drought corresponded with statistically estimated senescence as early as DOY 188. Higher accumulated precipitation over these seasons resulted in delayed senescence, which extended the growing season length. The selected logarithmic model indicates that delays in grass senescence date plateaued around DOY 300. Thus, sensitivity of grass senescence to precipitation appeared highest at low to

average rainfall amount and diminished during extremely wet years. Shrub senescence was insensitive to variability in both growing season precipitation (Fig. 2.4c, Table S2.6; fixed effect estimate: -0.05; CI: -0.16 – 0.06; p = 0.40; marginal R^2 = 0.007) and fall temperature (Fig. 2.4d).

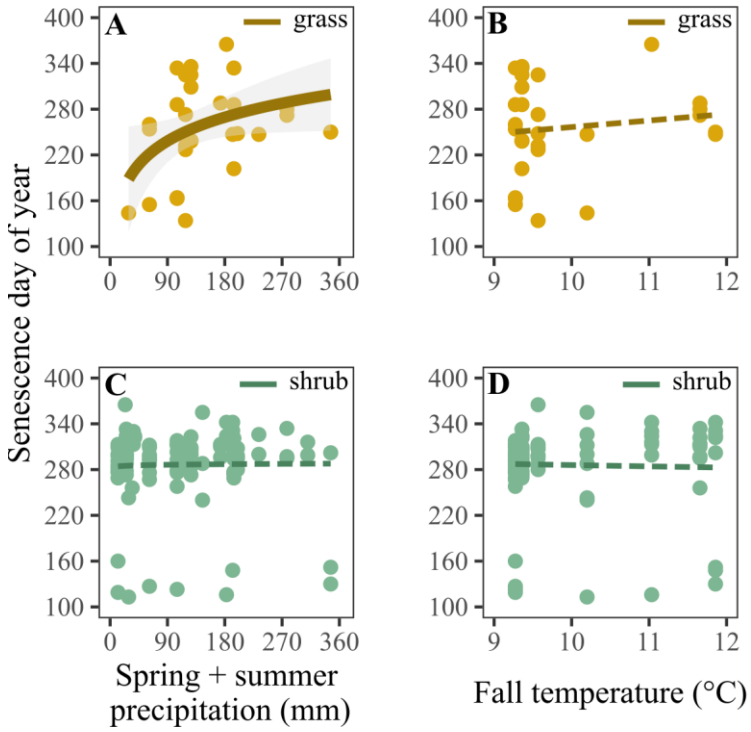

Figure 2.4. Fall temperature and spring + summer precipitation effects on grass (A, B) and shrub (C, D) senescence, expressed as day of the year. Points represent plot-year replicates. Significant linear mixed model precipitation effect in (A) is denoted by a solid line, which represents the predicted model fit ± 95% confidence interval, calculated as ± 2 x standard error around the effect size. In (A), grass senescence = 31.24 + (45.78 x log[precipitation + 2]), whereas temperature did not statistically explain grass senescence (B). In (C) and (D), shrub senescence did not statistically respond to either spring + summer precipitation or mean fall air temperature.

Discussion

Precipitation versus Temperature Controls of Phenology

Our study provides a unique lens to assess precipitation and temperature controls of phenology. We saw that precipitation had an effect on grass greenup and senescence, but temperature had an effect on just grass greenup. Shrubs, on the contrary, were insensitive to both environmental cues. To support our conclusion, we used the selected explanatory regressions (Table S2.2) to estimate the effects of long-term (>100 years, Fig. 2.2), historic precipitation and temperature on phenology for our study species at the Jornada. The results suggest that ambient precipitation variability from historic records had a potentially larger effect on phenology relative to temperature (Table 2.2). Precipitation at our site over 105 years explained 27% of the variability in grass greenup whereas historic temperature variability explained only 10% of the phenological variability. Precipitation also had a larger effect than temperature on grass senescence but the effects were smaller than observed for greenup (Table 2.2). This important conclusion of our work results from both higher sensitivity of our grass species to both precipitation and temperature at the start of season (Fig. 2.3) and higher interannual variability of precipitation relative to temperature (Table 2.1). Our results in conjunction with climate-change predictions suggests that, for dryland regions, changes in precipitation will be a more important driver in phenological shifts than temperature. While rising temperatures have already elicited phenological consequences and extended growing season length for mid and high-latitude ecosystems (Parmesan 2007, Cook et al. 2012, Richardson et al. 2018b), precipitation change will be the major driver of phenological change in drylands.

Table 2.2. Long-term (105 years) estimates and coefficients of variation (CV) of greenup and senescence in grasses and shrubs back-calculated from the selected explanatory models using historic, ambient precipitation and temperature as independent variables.

	Grass greenup		**Shrub greenup**	
	Range	*Coefficient of Variation*	*Range*	*Coefficient of Variation*
Winter precipitation **Winter temperature**	14–298 DOY	26%	92–105 DOY	3%
	Grass senescence		**Shrub senescence**	
	Range	*Coefficient of Variation*	*Range*	*Coefficient of Variation*
Spring + summer precipitation **Fall temperature**	153–300 DOY	9%	274–291 DOY	1%

Grasses and Shrubs Exhibit Contrasting Phenology Strategies

Phenological responses to the environment are reflective of a strategy that maximizes fitness and resource acquisition while reducing competition (Kikuzawa 1991, Jackson et al. 2001, Kraft et al. 2015, Römermann et al. 2016). Separation of phenological timing among species within a plant community reflects stabilization strategies that facilitate coexistence (Kraft et al. 2015, Cleland et al. 2012). Grass phenology strongly depended on shifts in precipitation more than changes in seasonal temperature. Additionally, grasses were more sensitive in their phenology at lower precipitation amounts; thus, drought has potentially higher and negative consequences for grass phenology over "deluge" by shortening growing season length by either delaying greenup, advancing senescence, or both. While there were deluge impacts on grass senescence in our study, these effects appear to plateau at precipitation totals over 200 mm. We interpreted the small response of senescence beyond 200 mm of precipitation to possible water saturation of the upper layers of the soil where most of the grass roots are concentrated (Jackson et al. 1996). When precipitation exceeds 200 mm, soil water may reach layers poorly explored by grasses and then absorbed by deep-rooted shrubs or lost via deep percolation. Satellite observations of West African savannah similarly found grasslands to be more sensitive to changes in precipitation than woody-dominated landscapes, which exhibited constant greenup dates (Ibrahim et al. 2021). Studies in a Mediterranean-type ecosystem, also reported that herbaceous species were more sensitive to changes in rainfall amount, especially drought, and exhibited delayed greenup (Esch et al. 2019). Because grasses account for 40% of the Jornada Basin aboveground net

primary productivity (Huenneke et al. 2002), and many other global drylands are grass-dominated, the ecological consequence of drought on grass phenology cannot be understated.

Grass response to short-term changes in the environment represents an ecological phenomena called phenological tracking (Cleland et al. 2012), which enables plants to adjust their growth to when favorable climatic conditions occur and maximizing growth for each year. This strategy allows grasses to maximize the use of water that otherwise would be lost via soil evaporation (Throop et al. 2012). Plants that exhibit this strategy may be more adaptive to variable precipitation predicted for future climate scenarios in drylands. The disadvantage is that coupling greenup to early precipitation pulses holds risk for plants during drought years. If no subsequent rain events occur thereafter, there is a possibility of invested carbon and nitrogen resources after a rain event for root (Lauenroth et al. 1987) or shoot growth that cannot be offset during a shortened growth period.

Shrub phenology is consistent among years and may reflect a strategy associated with access to a source of water with low interannual variance and a frost-avoidance strategy linked to predictable shifts in seasonal temperature (Medeiros and Pockman 2014). At any given latitude, photoperiod is another stable cue at annual time scales and is often synchronous with predictable patterns in seasonal temperature (Jackson 2009, Adole et al. 2019). Photoperiod is an indicator of very long-term adaptations over decadal/century time scales and represents a conservative phenological approach. A continental-scale study of Africa's terrestrial ecosystems found phenology to be

controlled by multiple drivers that were dominated by photoperiod (Adole et al. 2019). Early theories of phenology identified the strategy of tracking photoperiod and predictable temperature cues as favoring high-light environments where resources and water were available (Kikuzawa 1995, Jackson et al. 2001). Deep soil water has been shown to be a relatively stable source of water for shrubs (Duniway et al. 2018). If there are any precipitation effects on shrub phenology, we expect them to occur after high multi-year droughts or deluges (Fig. 2.5). If grass senescence responses plateau at high rainfall accumulation, this water becomes available to percolate to deeper soil layers that are more accessible by shrubs. It is also possible that shrub phenology responds to multi-year precipitation cycles that result in prolonged droughts or wet years. Increased frequency of climate anomalies, such as Pacific Decadal Oscillation (PDO) and El Nino-Southern Oscillation (ENSO), likely drive these multi-year cycles (Petrie et al. 2014, Felton et al. 2020). Thus, stable seasonal temperatures contrast the temperature- and water-insensitive shrubs at our site compared to temperature-sensitive trees in temperate systems that experience higher fluctuation of start-of-season temperatures (Zani et al. 2020).

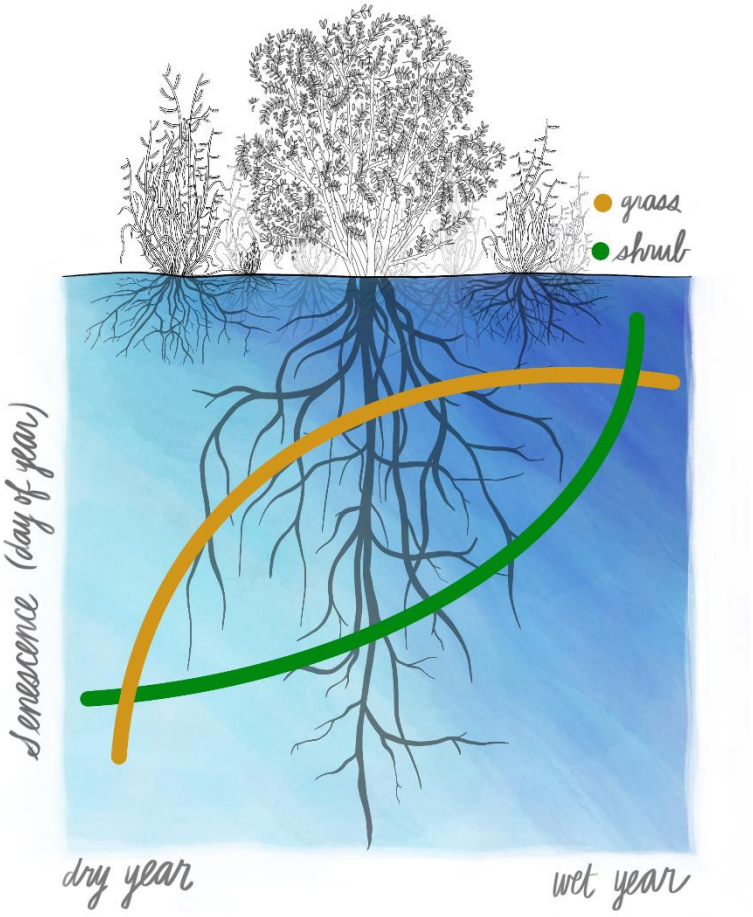

Figure 2.5. Hypothetical relationship between senescence day of year for grasses (gold line) and shrubs (green line) and annual precipitation amount. Saturation of surface soils at higher rainfall amounts results in percolation to deeper soil depths accessible by shrubs, eliciting a senescence response.

Implications for Future Climate Scenarios

While global temperature is rising and affecting temperate ecosystem phenology directly, temperature alone has a minimal effect on the phenology in drylands. Future climate simulations for the United States Southwest project a strong reduction in winter and spring precipitation under the ICPP RCP8.5 scenario (Wuebbles et al. 2014), which would drastically shorten grass growing season length through delayed greenup and

earlier senescence. Precipitation, particularly drought, affects grass phenology more than shrubs. Alteration of the length of growing season via changes to precipitation has important consequences for global carbon cycling since many drylands are comprised of grass-dominated systems. In terms of season length, how does this affect C fixation? Drought is altering the cycle of grass growth by shifting greenup and senescence, and thus shortening growing season length. Drought impacts to phenology may result in a reduction of grass cover, and therefore grass ANPP.

Our results suggest that warming winter temperatures could have a significant impact on grass phenology by advancing greenup dates. Nonetheless, temperature is not expected to increase as much in terms of variability or directionality in our semiarid system compared to mesic or temperate counterparts (Wuebbles et al. 2014). Future climate scenarios project a temperature increase under the RCP8.5 scenario of up to 3.2°C for southern New Mexico (Scott et al. 2016). This projected temperature increase is encompassed in the observed temperature range of our study (-8.65–33.35°C).

A reduction in plant cover through altered phenology will subsequently have larger impacts on energy and water balance. In an example driven by this study, decreased aboveground biomass of perennial grasses will result in increased bare ground exposure, and thus increased albedo and surface reflectance of incoming radiation. Furthermore, an increased percentage of bare ground will subsequently increase overland water flow, surface erosion, and water losses via evaporation (Okin et al. 2018), further increasing patchiness of desert landscapes and reinforcing mechanisms for woody-plant encroachment (Huenneke et al. 2002). Decreased plant transpiration will also decrease

latent heat loss during the growing season (Peñuelas et al. 2009), a mechanism that cools microclimates. Loss of herbaceous species, which have an open nutrient economy and high nutrient turnover (Sala et al. 2012b), will result in decreased litterfall inputs to these oligotrophic systems, thus further amplifying the openness of nutrient cycling under drought in these water-limited ecosystems.

This 7-year snapshot of the phenology of dominant grass and shrub species of the Chihuahuan semiarid ecosystem provides impetus for investigating temperature-precipitation controls on phenology at larger spatial and temporal scales across global drylands. Our experimental ranges of annual precipitation over the 7-year study period were 32–372 mm, mirroring historic precipitation extremes over the last century, while temperature showed a mean ambient range of 16.5–18.9°C that also represents long-term trends (Fig. 2.2a). The most complete vision of phenology responses to the interactive effects of water and temperature variability will depend on complimentary approaches (Cleland et al. 2007), such as combinations of existing long-term manipulative experiments, coordinated research networks (e.g., PhenoCam Network [Seyednasrollah et al. 2019] and the European Phenology Camera Network [Wingate et al. 2015]), and satellite observations that document large-scale change through time (Adole et al. 2019). Phenological studies will benefit from a greater understanding of how water-limited systems respond to extreme precipitation. Because temperature alone does not necessarily control phenology in all ecosystems, filling the research gap by including dryland responses to shifts in annual precipitation will be critical for our global understanding of controls on ANPP. This will ultimately be important to better understand the global

carbon cycle, the energy and water balance the capacity for dryland ecosystems to sequester carbon, and how the sensitivity of these systems to shifts in precipitation and temperature may affect the services they provide.

References

Adole, T., J. Dash, V. Rodriguez-Galiano, and P. M. Atkinson. 2019. "Photoperiod controls vegetation phenology across Africa." *Communications Biology* 2:391.

Atlas, U. 1992. *World Atlas of Desertification*, Vol. 80. Kent: UNEP and E. Arnold Ltd.

Ault, T. R. 2020. "On the essentials of drought in a changing climate." *Science* 368:256–260.

Bates, D., M. Maechler, B. Bolker, and S. Walker. 2014. "Lme4: Linear mixed-effects models using Eigen and S4." R Package Version 1:1–23.

Berg, A., and K. A. McColl. 2021. "No projected global drylands expansion under greenhouse warming." *Nature Climate Change* 11:1–7.

Bolker, B. M., M. E. Brooks, C. J. Clark, S. W. Geange, J. R. Poulsen, M. H. H. Stevens, and J.-S. S. White. 2009. "Generalized linear mixed models: a practical guide for ecology and evolution." *Trends in Ecology and Evolution* 24:127–135.

Browning, D. M., J. W. Karl, D. Morin, A. D. Richardson, and C. E. Tweedie. 2017. "Phenocams bridge the gap between field and satellite observations in an arid grassland ecosystem." *Remote Sensing* 9:1071.

Cleland, E., I. Chuine, A. Menzel, H. Mooney, and M. Schwartz. 2007. "Shifting plant phenology in response to global change." *Trends in Ecology and Evolution* 22:357–365.

Cleland, E. E., J. M. Allen, T. M. Crimmins, J. A. Dunne, S. Pau, S. E. Travers, E. S. Zavaleta, and E. M. Wolkovich. 2012. "Phenological tracking enables positive species responses to climate change." *Ecology* 93:1765–1771.

Collins, C. G., S. C. Elmendorf, R. D. Hollister, G. H. R. Henry, K. Clark, A. D. Bjorkman, I. H. Myers-Smith, J. S. Prevéy, I. W. Ashton, J. J. Assmann, J. M. Alatalo, M. Carbognani, C. Chisholm, E. J. Cooper, C. Forrester, I. S. Jónsdóttir, K. Klanderud, C. W. Kopp, C. Livensperger, M. Mauritz, J. L. May, U. Molau, S. F. Oberbauer, E. Ogburn, Z. A. Panchen, A. Petraglia, E. Post, C. Rixen, H. Rodenhizer, E. A. G. Schuur, P. Semenchuk, J. G. Smith, H. Steltzer, Ø. Totland, M. D. Walker, J. M. Welker, and K. N. Suding. 2021. "Experimental warming differentially affects vegetative and reproductive phenology of tundra plants." *Nature Communications* 12:3442.

Collins, S. L., S. R. Carpenter, S. M. Swinton, D. E. Orenstein, D. L. Childers, T. L. Gragson, N. B. Grimm, J. M. Grove, S. L. Harlan, J. P. Kaye, A. K. Knapp, G. P. Kofinas, J. J. Magnuson, W. H. McDowell, J. M. Melack, L. A. Ogden, G. P. Robertson, M. D. Smith, and A. C. Whitmer. 2011. "An integrated conceptual framework for long-term social–ecological research." *Frontiers in Ecology and the Environment* 9:351–357.

Cook, B. I., E. M. Wolkovich, T. J. Davies, T. R. Ault, J. L. Betancourt, J. M. Allen, K. Bolmgren, E. E. Cleland, T. M. Crimmins, N. J. B. Kraft, L. T. Lancaster, S. J. Mazer, G. J. McCabe, B. J. McGill, C. Parmesan, S. Pau, J. Regetz, N. Salamin, M. D. Schwartz, and S. E. Travers. 2012. "Sensitivity of spring phenology to warming across temporal and spatial climate gradients in two independent databases." *Ecosystems* 15:1283–1294.

Duniway, M. C., M. D. Petrie, D. P. C. Peters, J. P. Anderson, K. Crossland, and J. E. Herrick. 2018. "Soil water dynamics at 15 locations distributed across a desert landscape: insights from a 27-yr dataset." *Ecosphere* 9:e02335.

Esch, E. H., D. A. Lipson, and E. E. Cleland. 2019. "Invasion and drought alter phenological sensitivity and synergistically lower ecosystem production." *Ecology* 100:e02802.

Felton, A. J., A. K. Knapp, and M. D. Smith. 2020. "Precipitation-productivity relationships and the duration of precipitation anomalies: An underappreciated dimension of climate change." *Global Change Biology* 27:1127–1140.

Field, C. B., M. J. Behrenfeld, J. T. Randerson, and P. Falkowski. 1998. "Primary production of the biosphere: Integrating terrestrial and oceanic components." *Science* 281:237–240.

Filippa, G., E. Cremonese, M. Migliavacca, M. Galvagno, M. Forkel, L. Wingate, E. Tomelleri, U. Morra di Cella, and A. D. Richardson. 2016. "Phenopix: A R package for image-based vegetation phenology." *Agricultural and Forest Meteorology* 220:141–150.

Gherardi, L. A., and O. E. Sala. 2013. “Automated rainfall manipulation system: a reliable and inexpensive tool for ecologists.” *Ecosphere* 4:art18.

Gherardi, L. A., and O. E. Sala. 2019. “Effect of inter-annual precipitation variability on dryland productivity: A global synthesis.” *Global Change Biology* 25:269–276.

Gibbens, R. P., and J. M. Lenz. 2001. “Root systems of some Chihuahuan Desert plants.” *Journal of Arid Environments* 49:221–263.

Gile, L. H. 1981. “Soils and geomorphology in the basin and range area of southern New Mexico: Guidebook to the Desert Project, New Mexico.” *Bureau of Mines and Mineral Resources Memoir* 39:222.

Goulden, M. L., J. W. Munger, S.-M. Fan, B. C. Daube, and S. C. Wofsy. 1996. “Exchange of carbon dioxide by a deciduous forest: Response to interannual climate variability.” *Science* 271:1576–1578.

Gu, L., W. M. Post, D. D. Baldocchi, T. A. Black, A. E. Suyker, S. B. Verma, T. Vesala, and S. C. Wofsy. 2009. “Characterizing the seasonal dynamics of plant community photosynthesis across a range of vegetation types.” In *Phenology of Ecosystem Processes*, edited by A. Noormets, 35–58 . New York, NY: Springer.

Havstad, K. M., L. F. Huenneke, and W. H. Schlesinger, editors. 2006. *Structure and Function of a Chihuahuan Desert Ecosystem: The Jornada Basin Long-Term Ecological Research Site.* New York, NY: Oxford University Press.

Huenneke, L. F., J. P. Anderson, M. Remmenga, and W. H. Schlesinger. 2002. “Desertification alters patterns of aboveground net primary production in Chihuahuan ecosystems.” *Global Change Biology* 8:247–264.

Ibrahim, S., J. Kaduk, K. Tansey, H. Balzter, and U. M. Lawal. 2021. “Detecting phenological changes in plant functional types over West African savannah dominated landscape.” *International Journal Of Remote Sensing* 42:567–594.

Jackson, R. B., J. Canadell, J. R. Ehleringer, H. A. Mooney, O. E. Sala, and E. D. Schulze. 1996. “A global analysis of root distributions for terrestrial biomes.” *Oecologia* 108:389–411.

Jackson, R. B., M. J. Lechowicz, X. Li, and H. A. Mooney. 2001. “Phenology, growth, and allocation in global terrestrial productivity.” In *Terrestrial Global Productivity*, edited by B. Saugier, J. Roy, and H. A. Mooney, 61–82. San Diego, CA: Academic Press.

Jackson, S. D. 2009. “Plant responses to photoperiod.” *New Phytologist* 181:517–531.

Kikuzawa, K. 1991. “A cost-benefit analysis of leaf habit and leaf longevity of trees and their geographical pattern.” *The American Naturalist* 138:1250–1263.

Kikuzawa, K. 1995. “Leaf phenology as an optimal strategy for carbon gain in plants.” *Canadian Journal of Botany* 73:158–163.

Klosterman, S. T., K. Hufkens, J. M. Gray, E. Melaas, O. Sonnentag, I. Lavine, L. Mitchell, R. Norman, M. A. Friedl, and A. D. Richardson. 2014. “Evaluating remote sensing of deciduous forest phenology at multiple spatial scales using PhenoCam imagery.” *Biogeosciences* 11:4305–4320.

Kraft, N. J. B., O. Godoy, and J. M. Levine. 2015. “Plant functional traits and the multidimensional nature of species coexistence.” *Proceedings of the National Academy of Sciences* 112:797–802.

Kramer, K., I. Leinonen, and D. Loustau. 2000. “The importance of phenology for the evaluation of impact of climate change on growth of boreal, temperate and Mediterranean forests ecosystems: an overview.” *International Journal of Biometeorology* 44:67–75.

Lauenroth, W. K., O. E. Sala, D. G. Milchunas, and R. W. Lathrop. 1987. “Root dynamics of Bouteloua gracilis during short-term recovery from drought.” *Functional Ecology* 1:117–124.

Maestre, F. T., B. M. Benito, M. Berdugo, L. Concostrina-Zubiri, M. Delgado-Baquerizo, D. J. Eldridge, E. Guirado, N. Gross, S. Kéfi, and Y. Le Bagousse-Pinguet. 2021. “Biogeography of global drylands.” *New Phytologist* 231:540–558.

Medeiros, J. S., and W. T. Pockman. 2014. “Freezing regime and trade-offs with water transport efficiency generate variation in xylem structure across diploid populations of Larrea sp. (Zygophyllaceae).” *American Journal of Botany* 101:598–607.

Monger, H. C. 2006. “Soil development in the Jornada Basin.” In *Structure and Function of a Chihuahuan Desert Ecosystem: The Jornada Basin Long-Term Ecological Research Site*, edited by K. M. Havstad, L. F. Huenneke, and W. H. Schlesinger, 81–106. New York, NY: Oxford University Press.

Nemani, R. R., C. D. Keeling, H. Hashimoto, W. M. Jolly, S. C. Piper, C. J. Tucker, R. B. Myneni, and S. W. Running. 2003. “Climate-driven increases in global terrestrial net primary production from 1982 to 1999.” *Science* 300:1560–1563.

Occurrence records of Bouteloua eriopoda (Torr.) Torr. 2021. “GBIF Secretariat.” https://www.gbif.org/species/5289847.

Occurrence records of Bouteloua Lag. 2021. “GBIF Secretariat.” https://www.gbif.org/species/7557664.

Occurrence records of Prosopis glandulosa Torr. 2021. “GBIF Secretariat.” https://www.gbif.org/species/5358457.

Occurrence records of Prosopis L. 2021. “GBIF Secretariat.” https://www.gbif.org/species/2970763.

Okin, G. S., O. E. Sala, E. R. Vivoni, J. Zhang, and A. Bhattachan. 2018. “The interactive role of wind and water in functioning of drylands: What does the future hold?” *BioScience* 68:670–677.

Parmesan, C. 2007. “Influences of species, latitudes and methodologies on estimates of phenological response to global warming.” *Global Change Biology* 13:1860–1872.

Peñuelas, J., T. Rutishauser, and I. Filella. 2009. “Phenology Feedbacks on Climate Change.” *Science* 324:887–888.

Petrie, M. D., S. L. Collins, D. S. Gutzler, and D. M. Moore. 2014. “Regional trends and local variability in monsoon precipitation in the northern Chihuahuan Desert, USA.” *Journal of Arid Environments* 103:63–70.

Poulter, B., D. Frank, P. Ciais, R. B. Myneni, N. Andela, J. Bi, G. Broquet, J. G. Canadell, F. Chevallier, Y. Y. Liu, S. W. Running, S. Sitch, and G. R. van der Werf. 2014. “Contribution of semi-arid ecosystems to interannual variability of the global carbon cycle.” *Nature* 509:600–603.

Prăvălie, R. 2016. “Drylands extent and environmental issues. A global approach.” *Earth-Science Reviews* 161:259–278.

R Core Team. 2018. “R: A language and environment for statistical computing.” R Foundation for Statistical Computing, Vienna, Austria. https://www.R-project.org/.

Ramirez, G. A., G. Ramirez, and C. Tweedie. 2021. “Phenoanalyzer.” System Ecology Lab, University of Texas El Paso. https://selutep.squarespace.com/.

Reichmann, L. G., O. E. Sala, and D. P. C. Peters. 2013. “Precipitation legacies in desert grassland primary production occur through previous-year tiller density.” *Ecology* 94:435–443.

Richardson, A. D., K. Hufkens, T. Milliman, D. M. Aubrecht, M. Chen, J. M. Gray, M. R. Johnston, T. F. Keenan, S. T. Klosterman, M. Kosmala, E. K. Melaas, M. A. Friedl, and S. Frolking. 2018a. "Tracking vegetation phenology across diverse North American biomes using PhenoCam imagery." *Scientific Data* 5:180028.

Richardson, A. D., K. Hufkens, T. Milliman, D. M. Aubrecht, M. E. Furze, B. Seyednasrollah, M. B. Krassovski, J. M. Latimer, W. R. Nettles, R. R. Heiderman, J. M. Warren, and P. J. Hanson. 2018b. "Ecosystem warming extends vegetation activity but heightens vulnerability to cold temperatures." *Nature* 560:368–371.

Richardson, A. D., T. F. Keenan, M. Migliavacca, Y. Ryu, O. Sonnentag, and M. Toomey. 2013. "Climate change, phenology, and phenological control of vegetation feedbacks to the climate system." *Agricultural and Forest Meteorology* 169:156–173.

Römermann, C., S. F. Bucher, M. Hahn, and M. Bernhardt-Römermann. 2016. "Plant functional traits – fixed facts or variable depending on the season?" *Folia Geobotanica* 51:143–159.

Sakamoto, Y., M. Ishiguro, and G. Kitagawa. 1986. "Akaike information criterion statistics." *Dordrecht, The Netherlands: D. Reidel* 81:26853.

Sala, O. E., R. A. Golluscio, W. K. Lauenroth, and P. A. Roset. 2012. "Contrasting nutrient-capture strategies in shrubs and grasses of a Patagonian arid ecosystem." *Journal of Arid Environments* 82:130–135.

Schlesinger, W. H., editor. 2005. *Biogeochemistry*. Amsterdam: Elsevier.

Scott, J. D., M. A. Alexander, D. R. Murray, D. Swales, and J. Eischeid. 2016. "The climate change web portal: A system to access and display climate and Earth system model output from the CMIP5 archive." *Bulletin of the American Meteorological Society* 97:523–530.

Seyednasrollah, B., A. M. Young, K. Hufkens, T. Milliman, M. A. Friedl, S. Frolking, and A. D. Richardson. 2019. "Tracking vegetation phenology across diverse biomes using Version 2.0 of the PhenoCam Dataset." *Scientific Data* 6:222.

Shukla, J., C. Nobre, and P. Sellers. 1990. "Amazon deforestation and climate change." *Science* 247:1322–1325.

Sonnentag, O., K. Hufkens, C. Teshera-Sterne, A. M. Young, M. Friedl, B. H. Braswell, T. Milliman, J. O'Keefe, and A. D. Richardson. 2012. "Digital repeat photography for phenological research in forest ecosystems." *Agricultural and Forest Meteorology* 152:159–177.

Throop, H. L., L. G. Reichmann, O. E. Sala, and S. R. Archer. 2012. “Response of dominant grass and shrub species to water manipulation: an ecophysiological basis for shrub invasion in a Chihuahuan Desert grassland.” *Oecologia* 169:373–383.

Trenberth, K. E., A. Dai, R. M. Rasmussen, and D. B. Parsons. 2003. “The changing character of precipitation.” *Bulletin of the American Meteorological Society* 84:1205–1218.

Wingate, L., J. Ogée, E. Cremonese, G. Filippa, T. Mizunuma, M. Migliavacca, C. Moisy, M. Wilkinson, C. Moureaux, and G. Wohlfahrt. 2015. “Interpreting canopy development and physiology using a European phenology camera network at flux sites.” *Biogeosciences* 12:5995–6015.

Wuebbles, D., G. Meehl, K. Hayhoe, T. R. Karl, K. Kunkel, B. Santer, M. Wehner, B. Colle, E. M. Fischer, R. Fu, A. Goodman, E. Janssen, V. Kharin, H. Lee, W. Li, L. N. Long, S. C. Olsen, Z. Pan, A. Seth, J. Sheffield, and L. Sun. 2014. “CMIP5 climate model analyses: Climate extremes in the United States.” *Bulletin of the American Meteorological Society* 95:571–583.

Yahdjian, L., and O. E. Sala. 2002. “A rainout shelter design for intercepting different amounts of rainfall.” *Oecologia* 133:95–101.

Yao, J., J. J. Anderson, H. Savoy, and D. Peters. 2020. “Gap-filled daily precipitation at the 15 long-term NPP sites at Jornada Basin LTER, 1980-ongoing ver 75.” Environmental Data Initiative. https://doi.org/10.6073/pasta/cf3c45e5480551453f1f9041d664a28f.

Zani, D., T. W. Crowther, L. Mo, S. S. Renner, and C. M. Zohner. 2020. “Increased growing-season productivity drives earlier autumn leaf senescence in temperate trees.” *Science* 370:1066–1071.

Zhang, X., M. A. Friedl, C. B. Schaaf, A. H. Strahler, J. C. F. Hodges, F. Gao, B. C. Reed, and A. Huete. 2003. “Monitoring vegetation phenology using MODIS.” *Remote Sensing of the Environment* 84:471–475.

Supplementary Material to Chapter 2

Methods

Phenocamera Installation

Here, we provide an example of one phenocamera image (Figure S1), indicating the target grass and shrub patches within the plot area. On occasion, due to camera failure during key phenological phases or camera installation mid-season, images were missing and prevented adequate analyses following our image processing criteria. This information is recorded below (Table S2.1).

Model Selection

We used Akaike Information Criterion (AIC) to select the best model (Sakamoto et al. 1986). Models that met our criteria had the lowest AIC with $\Delta AIC > 2$, otherwise the most parsimonious model was selected (Table S2.2). Bolded AIC values in Table S2.2 indicate the selected model for all response variables.

Statistical Output

Mixed linear effects model output for grass greenup (Table S2.3), shrub greenup (Table S2.4), grass senescence (Table S2.5), and shrub senescence (Table S2.6) are provided below. All statistical analyses were performed in R version 4.0.3 (R Core Team 2018).

Table S2.1. Plot-year combinations that were removed due to insufficient image processing criteria, such as camera failure around the timing of greenup and senescence or plant mortality within the plot.

Plant	Year	No. plots removed
grass	2014	1
	2015	1
	2016	3
	2017	3
	2018	7
	2019	8
	2020	9
shrub	2017	1
	2018	6
	2019	1

Table S2.2. Akaike Information Criterion (AIC) for five compared models are presented below for grass and shrub greenup and senescence. Models that met our criteria had the lowest AIC with ΔAIC > 2, otherwise the most parsimonious model was selected. Selected models are indicated with a bold AIC value.

Plant	Model	df	AIC	ΔAIC
grass	greenup = precipitation + temperature + (1|year)	5	408.76	4.81
	greenup = temperature + (1|year)	4	414.69	10.75
	greenup = precipitation + (1|year)	4	418.58	14.64
	greenup = log(precipitation + 2) + temperature +	5	**403.94**	0.00
	greenup = log(precipitation + 2) + (1|year)	4	412.76	8.82
shrub	greenup = precipitation + temperature + (1|year)	5	693.91	7.80
	greenup = temperature + (1|year)	4	690.35	4.24
	greenup = precipitation + (1|year)	4	696.01	9.91
	greenup = log(precipitation + 2) + temperature +	5	**686.11**	0.00
	greenup = log(precipitation + 2) + (1|year)	4	688.48	2.38
grass	senescence = precipitation + temperature + (1|year)	5	315.66	11.66
	senescence = temperature + (1|year)	4	313.81	9.81
	senescence = precipitation + (1|year)	4	321.36	17.36
	senescence = log(precipitation + 2) + temperature +	5	**304.00**	0.00
	senescence = log(precipitation + 2) + (1|year)	4	309.41	5.41
shrub	senescence = precipitation + temperature + (1|year)	5	1185.17	8.26
	senescence = temperature + (1|year)	4	1180.14	3.24
	senescence = precipitation + (1|year)	4	1189.13	12.22
	senescence = log(precipitation + 2) + temperature +	5	**1176.91**	0.00
	senescence = log(precipitation + 2) + (1|year)	4	1180.87	3.96

Table S2.3. Output for mixed linear effects of winter precipitation amount and mean winter air temperature on grass greenup. Fixed effects estimates whose confidence intervals (CI) do not overlap with zero indicate a significant effect.

Predictors	**Estimates**	**Confidence Interval**	***p* -value**
(Intercept)	451.48	315.85 – 587.11	**<0.001**
log(Precipitation amount)	-50.41	-81.39 – -19.44	**0.001**
Mean air temperature	-17.26	-30.70 – -3.82	**0.012**
Random Effects			
σ^2	2393.43		
$\tau_{00\ year}$	186.09		
ICC	0.07		
$N_{\ year}$	7		
Observations	39		
Marginal R^2 / Conditional R^2	0.377 / 0.422		

Table S2.4. Output for mixed linear effects of mean winter air temperature on shrub greenup. Fixed effects estimates whose confidence intervals (CI) do not overlap with zero indicate a significant effect.

Predictors	**Estimates**	**Confidence Interval**	***p* -value**
(Intercept)	101.27	85.59 – 116.95	**<0.001**
log(Precipitation amount)	2.9	0.47 – 5.34	**0.019**
Mean air temperature	-1.59	-3.49 – 0.31	0.1
Random Effects			
σ^2	67.45		
$\tau_{00\ year}$	15.9		
ICC	0.19		
$N_{\ year}$	7		
Observations	96		
Marginal R^2 / Conditional R^2	0.101 / 0.272		

Table S2.5. Output for mixed linear effects of log(spring+summer precipitation amount) on grass senescence. Fixed effects estimates whose confidence intervals (CI) do not overlap with zero indicate a significant effect.

Predictors	**Estimates**	**Confidence Interval**	***p*-value**
(Intercept)	68.07	-186.14 – 322.27	0.6
log(Precipitation amount)	53.01	1.95 – 104.06	**0.042**
Mean air temperature	-7.3	-35.37 – 20.78	0.611
Random Effects			
σ^2	3480.73		
$\tau_{00\ year}$	0		
$N_{\ year}$	7		
Observations	29		
Marginal R^2 / Conditional R^2	0.142 / NA		

Table S2.6. Output for mixed linear effects of spring+summer precipitation amount on shrub senescence. Fixed effects estimates whose confidence intervals (CI) do not overlap with zero indicate a significant effect.

Predictors	**Estimates**	**Confidence Interval**	***p*-value**
(Intercept)	314.69	163.57 – 465.82	**<0.001**
log(Precipitation amount)	-0.86	-11.47 – 9.75	0.873
Mean air temperature	-2.44	-17.59 – 12.70	0.752
Random Effects			
σ^2	2454.85		
$\tau_{00\ year}$	203.7		
ICC	0.08		
$N_{\ year}$	7		
Observations	111		
Marginal R^2 / Conditional R^2	0.003 / 0.079		

Figure S2.1. Sample image captured from Wingscape TimeLapse Pro (WCT 00125) phenocamera containing grass and shrub patches within the plot.

References

R Core Team. 2018. "R: A language and environment for statistical computing." R Foundation for Statistical Computing, Vienna, Austria. https://R-project.org/.

Sakamoto, Y., M. Ishiguro, and G. Kitagawa. 1986. "Akaike information criterion statistics." *Dordrecht, The Netherlands: D. Reidel* 81:26853.

CHAPTER 3

DRYLANDS UNRESPONSIVE TO INCREASED NITROGEN AVAILABILITY: ACCESS TO ALTERNATIVE SOURCES?

Abstract

After water, nitrogen (N) availability is considered a widespread limiting factor of aboveground productivity in terrestrial systems. Yet after 14 years of supplemented water and N, the dominant grass in a semiarid grassland surprisingly did not increase aboveground net primary productivity. Within a long-term rainfall manipulation experiment crossed with N fertilization, we tested the hypothesis that dryland vegetation is accessing alternative sources of N, using mineral associated organic matter N (MAOM-N) under ambient conditions and sourcing bioavailable fertilizer N when available. We separated bulk soil into two density fractions and assessed changes in N content and isotopic ratios in relation to N and water availability. N dynamics in the soil revealed that plants likely use a combination of both particulate organic matter (POM) N and MAOM-N under low-N conditions, and foliar $\delta^{15}N$ values indicate that plants source fertilizer N under high-N conditions. Overall, N content increased in all soil pools when N was added, indicating increased capacity for dryland soil N sequestration. However, under high water and N availability, bulk soil N appears to decrease due to multiple possible loss mechanisms, such as microbially mediated gas emissions. N limitation in drylands remains a variable phenomenon, and we provide support for plant use of alternate N sources among soil density fractions.

Introduction

Nitrogen (N) is an essential and ubiquitous element required for nucleic acid, protein, and chlorophyll synthesis but is often deficient as bioavailable forms in terrestrial soils, limiting ecosystem productivity. In fact, the response of increased plant yield to added N is so highly repeatable and predictable that N limitation is considered a common ecosystem trait (Sterner and Elser 2002, LeBauer and Treseder 2008). However, aboveground net primary productivity (ANPP) response to N amendments increases with MAP; there is variable ANPP response to N fertilization in drylands, even under sufficient water availability (Hooper and Johnson 1999, Yahdjian et al. 2011, McHugh et al. 2017, Collins et al. 2017). After 14 years of experimental treatments, ANPP for the dominant grass species (*Bouteloua eriopoda*) in a Chihuahuan Desert semiarid grassland at the Jornada Basin Long Term Ecological Research Site (LTER; NM, USA) responded strongly and significantly to water availability (Fig. 3.1; Table S3.1; CI: 0.14 – 0.34, $p < 0.001$, marginal $R^2 = 0.42$), but not to increased N (Fig. 3.1; Table S3.1; CI: -21.65 – 12.62, $p = 0.60$, marginal $R^2 = 0.42$). These observations contrast the typical ecological paradigm with global implications for our understanding of the N cycle because drylands comprise over 45% of the terrestrial earth surface (Prăvălie 2016).

The leading explanation for the observed small N response in drylands is that these ecosystems are most frequently limited by soil-water availability and therefore do not respond to N amendments. However, when we removed water limitation by increasing rainfall by 80% (Fig. 3.1), we still did not observe a response to N fertilization. Thus, the central questions that guide this study are: 1) Why is there no

significant response to N fertilization under minimal water limitation? Because ANPP remained the same regardless of N availability, we expect plants to either alter N productivity (aboveground biomass produced per unit N absorbed), where N productivity must be higher in low N availability treatments, or switch N sources. As such, we asked: 2) Do plants alter N productivity in response to altered N and water availability? And 3) Do plants utilize N from alternate soil sources—such as mineral associated organic matter (MAOM)—to meet biological N demand? Finally, 4) how long can alternate N pools meet biological N demand?

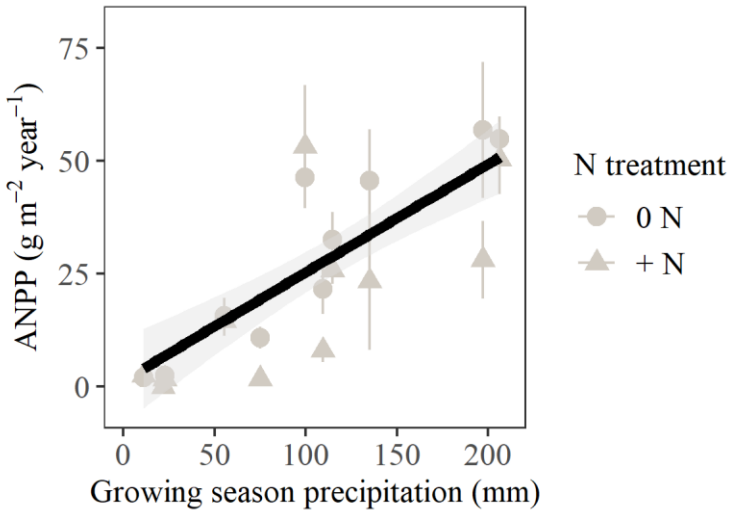

Figure 3.1. Effect of experimental precipitation and N treatments on aboveground net primary productivity (g m^{-2} year^{-1}) of the dominant grass species (*Bouteloua eriopoda*). Points represent annual means ± standard error. Because there was no statistical difference between N treatments, points are presented as the same color. Precipitation amount had a significantly positive effect, represented by the solid black line ± 95% confidence interval.

Inorganic N (IN; e.g., nitrate and ammonium ions) receives much ecological focus, as these constituents are deposited directly via anthropogenic inputs, are highly mobile in the soil pool given sufficient soil moisture, and are direct substrates for

microbial processes and plant uptake. The organic N (ON) pool is equally critical to ecological processes because ON acts as the primary supply to IN pools following depolymerization and may be directly immobilized by plants. Emerging frameworks hypothesize that plants exhibit dynamic, not passive, acquisition of N from multiple soil pools rather than exclusively from the inorganic N pool (Jilling et al. 2018, Daly et al. 2021). Recent studies using novel microdialysis techniques have shown plants to directly uptake ON, such as amino acids (Inselsbacher et al. 2014, Homyak et al. 2021). Thus, constituents within the bulk organic matter pool are highly dynamic, and turnover rates depend on complex interactions between substrates, microbial actors, and abiotic drivers (Kleber et al. 2011). Soil organic matter sources that contribute ON to the soil pool may be divided into two main, categorical pools: particulate organic matter (POM) and mineral associated organic matter (MAOM). MAOM has received increasing ecological attention over the past three decades because of its role as one of the main controls on C storage in soils (Kleber et al. 2015). MAOM also stores a lot of N (MAOM-N), but has been historically viewed as a recalcitrant source inaccessible by plants (Paul 2016). Given conditions that facilitate plant-rhizosphere mining (Jilling et al. 2018) and/or where N supply from POM is relatively balanced with the mineral sorption potential for MAOM (Fig. 1 in Daly et al. [2021]), MAOM-N is increasingly viewed as a potential ON source for biological sinks. The potential for MAOM destabilization, resulting in MAOM-N availability, may be especially relevant in dryland soils.

In dryland ecosystems, MAOM is stabilized through relatively weak Van der Waals forces held by Ca^{2+} cation bridges (Rowley et al. 2018). Because these

mechanisms of stabilization are energetically weaker than their humic and acidic environmental counterparts, dryland ecosystems are expected to be more vulnerable to disturbance and destabilization (Kleber et al. 2015). A major determinant of MAOM destabilization is microbial activity; directional increases in soil moisture stimulate microbial activity and MAOM mining, whereas prolonged droughts desiccate soils and inhibit biological activity, facilitating stabilization (Torn et al. 2009). Increasing precipitation variability would also destabilize MAOM soil fractions by increasing the frequency of large rainfall pulses, which maintain elevated soil moisture longer during prolonged dry periods. Drylands are experiencing extreme rainfall and drought events of novel magnitude and frequency with projected increases in precipitation variability (Gherardi and Sala 2019, Pörtner et al. 2022). Combined with the many observations that xeric vegetation does not exhibit effects of N limitation, a critical need to understand precipitation controls on N cycling in dryland ecosystems underpins this study.

Here, we present the results from a long-term rainfall manipulation experiment in the Jornada Basin Long Term Ecological Research (LTER) site (NM, USA), which is located in the northern Chihuahuan Desert. The Jornada Basin LTER is an excellent study system for dryland processes due to its closed basin topography, monsoonal precipitation regime, calcareous soils, and plant genera that are generally representative of dryland characteristics globally. We tested the hypotheses: 1) plants shift N productivity under altered N and water availability and 2) plants use N from different soil sources, such as mineral organic matter (MAOM) to meet biological demand. We

conclude with remarks about how long alternate N sources may sustain plant grow in low N environments.

Methods

Study Site Description

This research took place at the Jornada Basin LTER site, located at 32.56 latitude and -106.78 longitude (Las Cruces, NM, USA). Long-term mean annual temperature is 16°C, and long-term mean annual precipitation is 250 mm, most of which falls as monsoonal rainfall during the summer growing season. The herbaceous vegetation community is dominated by the perennial C_4 grass, *Bouteloua eriopoda* (black grama), which comprises 39% of the aboveground net primary productivity of the site (Huenneke et al. 2002, Reichmann et al. 2013a). Soils are classified as Cacique loamy fine sand with weakly developed textural B (argillic) horizons overlaying semi-indurated to indurated caliche at approximately 60 cm in depth (Gile 1981, Monger 2006).

Precipitation Sums

Monthly precipitation sums were obtained from the Jornada YUCCA meteorological station (32.57 latitude, -106.769 longitude; approximately 2.25 km northeast from experimental plots), available on the Environmental Data Initiative (EDI) (Thatcher and Bestelmeyer 2021). Growing season precipitation is defined as the precipitation amount summed over the months of June through September. Precipitation values were then adjusted according to rainfall manipulation treatments defined below.

Experimental Design

Rainfall manipulation and nitrogen fertilization treatments were started in 2006 along with control plots that received ambient rainfall (replicates n = 6, total sample size N = 32; 2.5 x 2.5 m plots; Reichmann *et al.* 2013b). Rainfall treatments were achieved using passive rainout shelters that intercepted incoming precipitation by 80% but allowed > 92% of photosynthetically active radiation to reach the plot. Rainout shelters were coupled with automated irrigation systems that simultaneously applied 80% of incoming precipitation during rain events through PVC-pipe and aboveground sprinklers using a solar-powered battery pumping system (Gherardi and Sala 2013). Manipulation intensities were based on extremes of historical precipitation data for the region. These automated rainfall manipulation systems were deployed during the summer growing season. Our rainfall treatments were also crossed factorially with a nitrogen fertilization treatment, where granular ammonium nitrate (NH_4NO_3) was applied to whole plots twice during each growing season and equated a total of 10 g N m^{-2} yr^{-1}. Fertilizer was dissolved in water equivalent to a 2 mm rain event to reduce volatilization or loss via wind, and the same amount of water was applied to all non-fertilized plots.

Aboveground Net Primary Productivity Measurements

Aboveground net primary productivity (ANPP) was measured in each plot using the point-intercept method. Plants were identified to species every cm along three 2.5 m transects. Plant cover was not estimated within a 20 cm buffer at both transect ends to

account for potential edge effects of our rainfall manipulation treatments. Plant cover was then composited across the three sub-plot transects and converted to biomass based on plant functional type to provide an estimate of ANPP (g m^{-2} yr^{-1}). ANPP data for the years 2011, 2012, 2018, and 2020 are included in this manuscript as they correspond to years where plants were also biogeochemically analyzed. We derived plant N productivity (g C g N^{-1} m^{-2} $year^{-1}$) as:

$$A = \frac{ANPP}{N} \qquad \textit{eq. 3.1}$$

Where A = nitrogen productivity, ANPP = aboveground net primary productivity, and N = the total N estimated in aboveground biomass (foliar %N x ANPP, where %N was determined analytically, methods below).

Field Sampling

Field collection of leaves for chemical analyses took place during peak biomass months following the summer monsoon: August 2011, September 2012, September 2018, and September 2020. A total of four to five sun leaves were collected from three *Bouteloua* patches (when possible; some drought plots had zero *Bouteloua* cover), from the four cardinal directions and the center. Surface soil samples (0–10 cm) were collected in 2020 using 2.54 cm diameter soil corer and composited from five sub-plot samples that were representative of the general ground cover of the plot, ranging from bare ground to underneath dominant plant patches. Soil samples were passed through a 2 mm sieve to remove large particulates and roots. A soil sub-sample was set aside and air-dried for further soil density fractionation analyses.

Soil Density Separation

To explore N dynamics among different soil density fractions, a subset of the 2020 soils were set aside prior to oven-drying and separated into two density fractions using the sodium polytungstate (SPT) flotation method (Sollins et al. 2006). Following the procedures of Sollins *et al.* (2006) and Throop *et al.* (2013), We dissolved 1,051 g of SPT-O POLY GEE brand sodium polytungstate powder—a low-C and low-N formula for soil analyses—in 799 mL nanopure water to achieve a 1 L solution with a density of 1.85 g cm^{-3}. Through a seven-density fractionation procedure, Throop *et al.* (2013) previously determined that a density of 1.85 cm^{-3} effectively separated soil particles at the Jornada Basin LTER into light density organic matter (hereafter "particulate organic matter" [POM]) and mineral-bound heavy density (hereafter "mineral associated organic matter" [MAOM]) fractions. We weighed 40 g of soil into 250 mL wide-mouth bottles with 200 mL of SPT solution, and subsequently shook the samples for 3 h on a benchtop shaker table (Eberback 6010). Samples were then centrifuged at 1,285 RPM for 30 minutes. The floating material (light density POM fraction) was aspirated using a vacuum and collected in a vacuum flask. Based on studies in other grasslands and prior trial runs that we conducted, repeating the steps above (SPT addition through aspiration steps) did not improve recovery of the POM light fraction.

Each separated fraction was collected onto four 150 mm GF/F filters (Whatman brand) using a Buchner funnel and vacuum filtration system and rinsed with 500 mL of nanopure water. Filters were dried at 60°C for 48 h, and the collected soils were then carefully brushed away from the filters. The separated and dried soils were then weighed

to calculate mass proportions relative to bulk soil mass. We acknowledge the potential for mass loss at this step because filters were not pre-weighed. Moreover, dissolved organic matter was not recovered during the SPT rinsing step and was assumed lost. Rates of soluble organic C loss during this stage may range from 8% (Kramer et al. 2009) to 20% (Crow et al. 2007). Rates of soluble organic N loss may be estimated between 0.07%, derived from N content (0.7 g N kg^{-1} bulk) measured in the light POM fraction of a subtropical mixed grassland-woodland (Liao et al. 2006), to 16%, based on one study conducted in a temperate forest (Schulze et al. 2009). In addition, POM light fraction recovery during the filtration step was minimal and did not provide sufficient material for subsequent chemical and isotopic analyses.

Isotopic and Chemical Analyses

To prepare for chemical analyses of total N and stable N isotopes, foliar and soil samples were dried at 70°C for 48 h. Foliar samples were ground into a fine powder using a Desktop High Energy Vibratory Ball Mill (VQ-N ball mill Thomas Scientific), and soil samples were ground using a mortar and pestle. The grinding components were carefully cleaned with ethanol between each sample. Samples were then weighed to the nearest one-hundreth of a milligram using a Sartorius microbalance. Approximately 2 mg of ground foliar tissue was weighed into 4 x 6 mm tin capsules, whereas approximately 95 mg of bulk soil was weighed into 5 x 9 mm tins. Due to expected low-N values based on Throop *et al.* (2013), approximately 150 mg of 2020 density-separated soil was

weighed into 9 x 10 mm tins. All tins were carefully folded and stored in a desiccator to prevent water absorption prior to analyses.

Plant and soil samples were analyzed for total N and stable N isotopes. The 2011 and 2012 foliar samples were run on a GVI IsoPrime and an Elementar Cube elemental analyzer at the Boston University Stable Isotope Laboratory. One analytical replicate was run per 10 samples. In-house standards of peptone and glycine calibrated to USGS 40 and 41 were alternately analyzed after every 15 unknown samples. All 2018 and 2020 samples were run in analytical triplicates and flash combusted with a coupled continuous-flow elemental analyzer-isotope ratio mass spectrometer system consisting of a Costech EA interfaced to a Delta Advantage peripheral at the METAL Core Laboratory of Arizona State University. Calibration curves for 2018 and 2020 plant samples were built using tomato leaves (NIST 1573a) and for 2020 soils using low-nitrogen Montana soil (NIST 2711). In-house glycine standards calibrated to USGS 40 and 41 were analyzed after every third unknown sample and at the beginning and end of each run.

Nitrogen content output from the elemental analyzer was presented as %N of the sample. For soils, we then converted this value to N content relative to the mass of bulk soil (mg N g^{-1} bulk soil) using the dry mass proportions calculated earlier. Because the POM fraction was not recovered, total N and $\delta^{15}N$ for the POM fraction presented in this manuscript were calculated using a mass balance approach from the measured bulk and MAOM fraction variables (c.f., Keller et al. 2021). We recognize, due to potential mass loss described above, that the POM fraction results should be interpreted with caution, and the focus on this paper will be on bulk and MAOM pool results.

Standards and unknowns were corrected for linearity, and unknowns were normalized to isotopic values of standard reference materials using a two-point calibration curve of in-house standards calibrated to USGS 40 and 41 standard reference materials. Stable isotope nitrogen ratios are standardized to atmospheric air and expressed in permil (‰) as:

$$\delta = \frac{R_{sa}}{R_{std}} - 1 \qquad \textit{eq. 3.2}$$

Where R_{sa} is the molar $^{15}N/^{14}N$ isotopic ratio of the sample and R_{std} is the molar isotopic ratio of atmospheric air (0.0036765).

All standards and unknown samples presented in this manuscript underwent quality assessment and quality control. Acceptable accuracy of tomato leaf standards and in-house glycine or peptone standards was defined as having a residual error of ≤ 0.2‰. Acceptable accuracy of the low-N Montana soil standard was defined as having a residual error of ≤ 0.3‰. Acceptable precision for all standards was defined as having a standard deviation of ≤ 0.2‰. A blank (empty tin cup) was included at the beginning of each analytical run for all 2011, 2012, and 2018 plants, and after every 5-8 unknown samples for 2020 bulk soils. Due to the large sample weights of the 2020 density-separated samples, a blank was also included after every unknown sample and an O_2 macro pulse was used during combustion to affirm that full combustion occurred.

Unknown samples adhered to QA/QC when samples fell within the standard calibration range and exhibited a standard deviation among analytical replicates of ≤ 0.2‰. If unknowns had a standard deviation > 0.2‰, an attempt to meet QA/QC requirements was first conducted by removing one outlier replicate, reducing the number

of analytical replicates to 2. If this did not resolve the precision measurement, the sample was flagged, re-ground, and re-run on the IRMS. Any data that remained flagged after re-running were discarded from the final data set.

Statistical Analyses

All statistical analyses were performed in R version 4.2.2 (R Core Team 2018). The multi-year plant response variables—ANPP, foliar %N, N productivity, and foliar $\delta^{15}N$ —were regressed using linear mixed-effects models in the lme4 package of R (Bates et al. 2014) against growing season precipitation amount (mm) and N fertilization treatment with the year collected as the random effect:

$$Y_{sij} = \beta_0 + S_{0s} + \beta_1 X_i + \beta_2 X_j + \beta_1 X_i \beta_2 X_j + e_{sij} \qquad \textit{eq. 3.3}$$

$$S_{0s} \sim N(0, \tau_{00}^2\ ),$$

$$e_{sij} \sim N(0, \sigma^2)$$

Where Y_{sij} = response (ANPP, foliar %N, N productivity, foliar $\delta^{15}N$), β_0 = intercept, S_{0s} = random effect (year sampled), $\beta_1 X_i$ = fixed effect 1 (precipitation amount), $\beta_2 X_j$ = fixed effect 2 (N treatment), e_{sij} = residuals.

The 2020 bulk soil and density fraction total N and $\delta^{15}N$ responses were regressed against growing season amount (mm), N fertilization treatment, and soil pH using multiple linear regressions:

$$Y_{ij} = \beta_0 + \beta_1 X_i + \beta_2 X_j + \beta_1 X_i \beta_2 X_j + e_{ij} \qquad \textit{eq. 3.4}$$

$$e_{ij} \sim N(0, \sigma^2)$$

Where Y_{ij} = response (bulk soil, POM, or MAOM %N), β_0 = intercept, $\beta_1 X_i$ = independent variable 1 (precipitation amount), $\beta_2 X_j$ = independent variable 2 (N treatment), e_{ij} = residuals. Regression assumptions were tested and met for all response variables, and residuals for all explanatory models were tested for and exhibited normality.

Results

Treatment Effects

Experimental rainfall amounts achieved through the automated rainfall manipulation systems consisted of an overall range of 11–201 mm for the four sampling years presented in this study (Table S3.2). An N treatment effect was achieved via fertilizer application, effectively elevating bulk %N at the surface (0–10 cm) by 0.01% compared to unfertilized plots (Table S3.2; Reichmann *et al.* 2013a). The mean $\delta^{15}N$ of the applied fertilizer (granular NO_3NH_4) was 3.87 ± 0.72 ‰ (mean ± standard error) over the experimental period. Soil in fertilized plots also exhibited higher mean $\delta^{15}N$ by 2.94‰ compared to unfertilized plots (Tables S3.2).

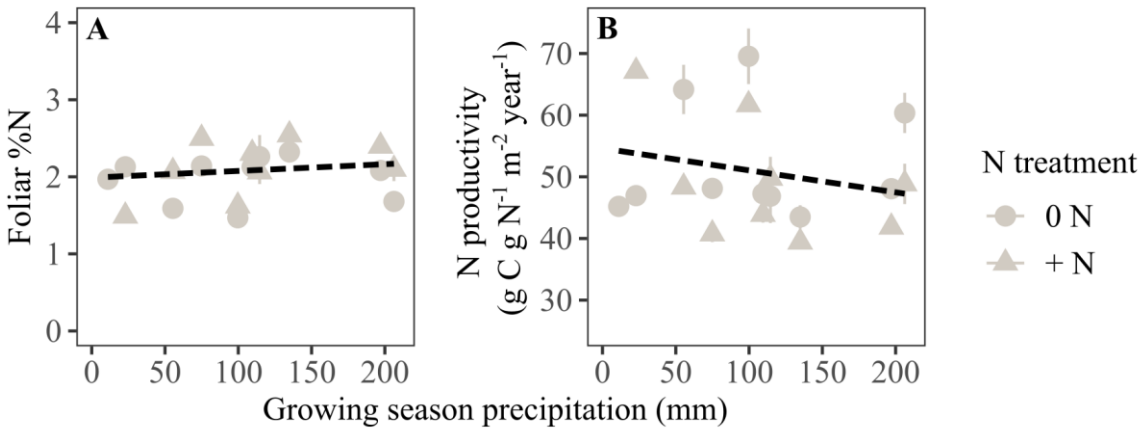

Figure 3.2. Effect of experimental precipitation and nitrogen treatments on (A) foliar %N and (B) N productivity of the dominant grass species (*Bouteloua eriopod*a). Points represent annual means ± standard error. Because there was no statistical difference between N treatments, points are presented as the same color. Significant effects of precipitation are represented by a solid line ± 95% confidence interval.

Plant Responses

We previously established that the dominant grass did not increase ANPP to N amendments even after water limitation was reduced. Furthermore, the dominant grass did not change foliar %N in response to either N treatment (Fig. 3.2a; Table S3.3; CI: -0.24 – 0.46, p = 0.53, marginal R^2 = 0.08) or precipitation amount (Fig. 3.2a; Table S3.3; CI: -1.42 x 10^{-3} – 2.70 x 10^{-3}, p = 0.53, marginal R^2 = 0.08). Plant N productivity also did not respond to N treatment (Fig. 3.2b; Table S3.4; CI: -12.82 – 6.13, p = 0.48, marginal R^2 = 0.07) or precipitation amount (Fig. 3.2b; Table S3.4; CI: 0.07 – 0.03, p = 0.47, marginal R^2 = 0.07).

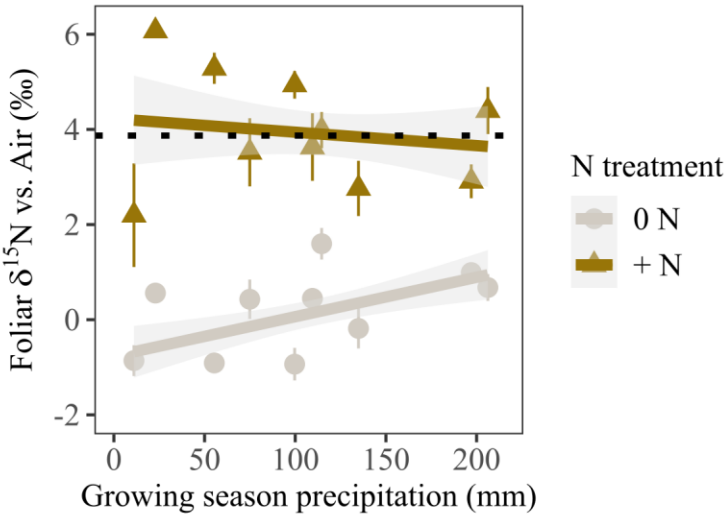

Figure 3.3. Effect of experimental precipitation and nitrogen treatments on foliar $\delta^{15}N$ of the dominant grass species (*Bouteloua eriopod*a). Points represent annual means ± standard error. A significant statistical difference between N treatment is represented by differences in point color. Precipitation amount significantly interacted with N treatment and is represented by separate solid lines ± 95% confidence intervals that correspond with N treatment color.

Foliar $\delta^{15}N$ ratios differed significantly for the dominant grass between fertilized and unfertilized plots (Fig. 3.3; Table S3.5; CI: -6.07 – -3.93, $p < 0.001$, marginal $R^2 = 0.69$). Vegetation in fertilized plots had mean $\delta^{15}N$ values closer to the applied fertilizer (Fig. 4.3, dotted line) compared to vegetation in unfertilized plots. Furthermore, precipitation interacted with N treatment for foliar $\delta^{15}N$ (Fig. 3.3; Table S3.5; CI: 2.73×10^{-3} – 0.02, $p < 0.05$, marginal $R^2 = 0.69$). Grass in unfertilized plots exhibited a significant increase in foliar $\delta^{15}N$ with precipitation amount. Conversely, grass in fertilized plots exhibited a significant decrease in foliar $\delta^{15}N$ with precipitation amount.

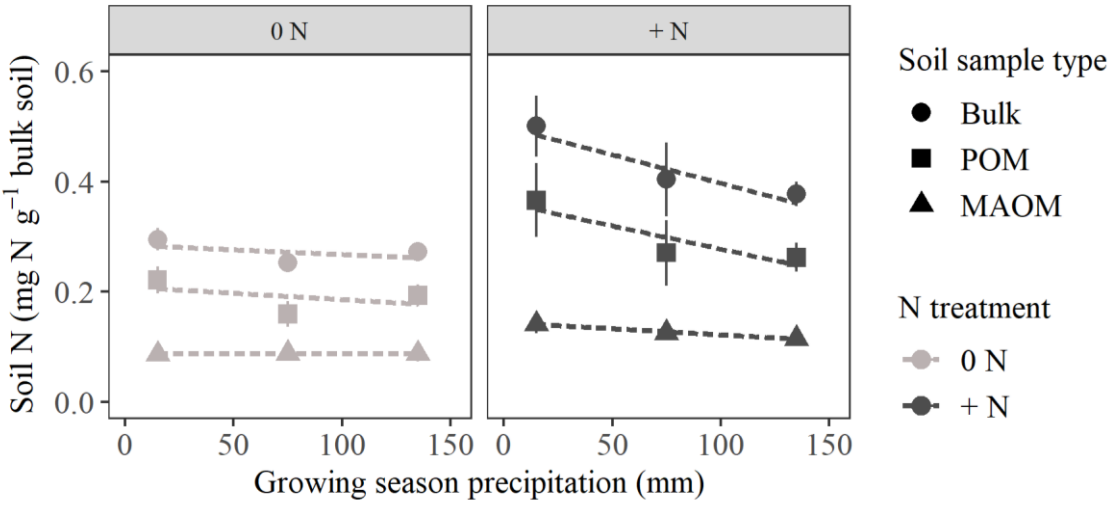

Figure 3.4. Effect of experimental precipitation and N treatments on N content (mg N g^{-1} bulk soil) of the (A) unfertilized and (B) fertilized bulk, particulate organic matter (POM), and mineral associated organic matter (MAOM) soil pools. Points represent annual means ± standard error. A significant statistical difference between N treatment is represented by differences in point color. There was no effect of precipitation on the bulk soil, POM, or MAOM soil pools.

Soil Responses

We performed chemical analyses on soil density fractions from 2020, the culmination of 14 years of experimental rainfall and N manipulation. N fertilization resulted in higher N content for the bulk soil (Fig. 3.4; Table S3.6; $F_{3,43} = 11.53$, $p < 0.001$, adjusted $R^2 = 0.41$), POM fraction (Fig. 3.4; Table S3.6; $F_{3,28} = 3.79$, $p < 0.05$, adjusted $R^2 = 0.21$), and MAOM fraction (Fig. 3.4; Table S3.6; $F_{3,30} = 6.11$, $p < 0.001$, adjusted $R^2 = 0.32$). Precipitation did not have an effect on soil N content in either unfertilized or fertilized treatments. In unfertilized treatments, N content remained constant across precipitation amount for bulk soil (Fig. 3.4a; Table S3.6; precipitation $p = 0.68$, interaction $p = 0.17$, adjusted $R^2 = 0.41$), the POM fraction (Fig. 3.4a; Table S3.6; precipitation $p = 0.67$, interaction $p = 0.42$, adjusted $R^2 = 0.21$), and the MAOM fraction

(Fig. 3.4a; Table S3.6; precipitation p = 0.96, interaction p = 0.27, adjusted R^2 = 0.32). Similarly, precipitation did not modify N content in fertilized bulk soil (Fig. 3.4b; Table S3.6), the fertilized POM fraction (Fig. 3.4b; Table S3.6), or the fertilized MAOM fraction (Fig. 3.4b; Table S3.6). However, N content trends across all soil pools appear decreasing in fertilized treatments.

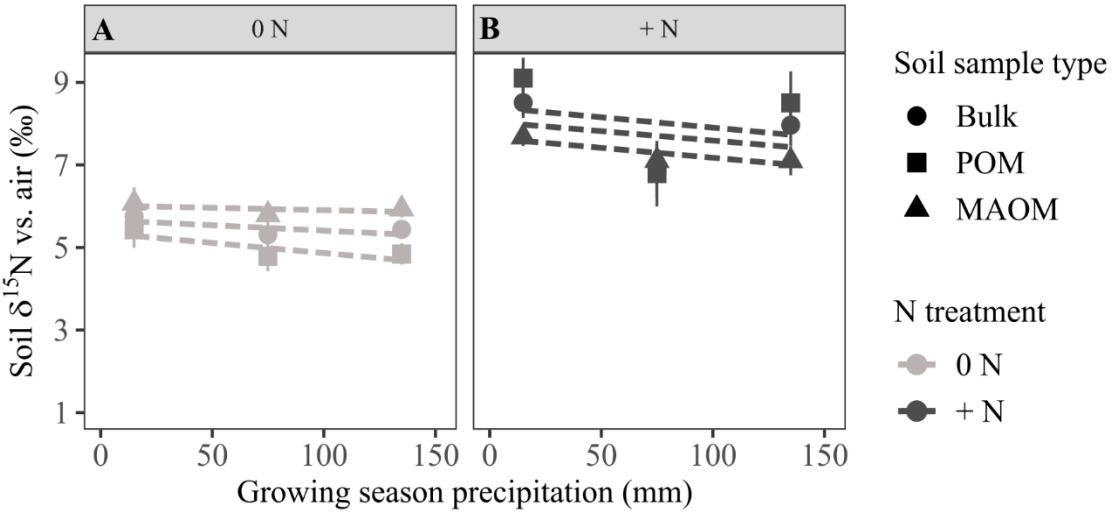

Figure 3.5. Effect of experimental precipitation and N treatments on $\delta^{15}N$ of the (A) unfertilized and (B) fertilized bulk, particulate organic matter (POM), and mineral associated organic matter (MAOM) soil pools. Points represent annual means ± standard error. A significant statistical difference between N treatments is represented by differences in point color. There was no effect of precipitation on bulk, POM, or MAOM $\delta^{15}N$.

MAOM from unfertilized plots, averaged across precipitation treatments had a higher $\delta^{15}N$ of 5.93 ± 0.28‰ (mean ± standard error) compared to unfertilized bulk soil (5.47 ± 0.20‰) and the unfertilized POM fraction (5.61 ± 0.34 ‰). When comparing across N treatments, stable N isotope ratios were lower in unfertilized treatments (Fig. 3.5a) compared fertilized treatments for bulk soil (Fig. 3.5b; Table S3.7; $F_{3,23}$ = 10.10, p < 0.01, adjusted R^2 = 0.51), POM (Fig. 3.5b; Table S3.7; $F_{3,22}$ = 8.57, p = 0.01,

adjusted R^2 = 0.48), and MAOM (Fig. 3.5b; Table S3.7; $F_{3,32}$ = 10.31, p < 0.01, adjusted R^2 = 0.44) fractions. Precipitation amount did not modify these values in either N treatment for bulk soil (Fig. 3.5; Table S3.7; precipitation p = 0.68, interaction p = 0.83), POM (Fig. 3.5; Table S3.7; precipitation p = 0.65, interaction p = 0.95), or MAOM fractions (Fig. 3.5; Table S3.7; precipitation p = 0.75, interaction p = 0.48).

Discussion

Plant Adjustments to Altered N and Water Availability

Four years of ANPP and isotopic analyses comparing $\delta^{15}N$ of leaves and fertilizer led us to conclude that the dominant grass species (*B. eriopoda*) did uptake ammonium nitrate fertilizer (Fig. 3.3, gold line). We conclude from this result that our experimental N amendments were able to reach plant tissues. However, the increased N availability did not increase ANPP further, even with reduced water limitation.

Increased microbial and plant competition under high water availability conditions may limit access to the bioavailable soil N pool. As a result, organisms in N-limited environments typically improve N sequestration (Sterner and Elser 2002, Mason et al. 2022). We recognize that nutrient use efficiency could be more accurately quantified not just as the inverse of foliar N concentration (c.f., Chapin 1980), but as the inverse of nutrient concentration aboveground litterfall, root turnover, and the organic matter increment of the vegetation (Vitousek 1982) or with additional metrics, such as mean residence time (Berendse and Aerts 1987). Nonetheless, we did not see any difference in N productivity between N treatments or across precipitation amounts. While

fertilized treatments sourced bioavailable N to plants, supported by our foliar isotopic data, we conclude that plants in unfertilized treatments likely access multiple soil N pools.

Alternative N Sources under Low-N Conditions

We summarize our findings and new hypotheses in conceptual Figure 3.6. The assessment of POM and MAOM under different N availability regimes indicates that plant N demand in low N conditions, regardless of water availability, is met by a combination of both POM and MAOM (Fig. 3.6a). First, because plant ANPP increased with precipitation amount, POM supply also increased. We did not observe any significant change in bulk or POM-N for two hypothetical reasons. First, in addition to creating POM, plants derive N from POM-N and maintain mass balance. Plant-N derivation from POM fits the ecological paradigm that after depolymerization of ON derived by POM, N is mineralized to inorganic forms by microbes and immobilized by plants. Second, POM readily undergoes microbial decomposition and exchange with MAOM binding sites, resulting in MAOM formation (Daly et al. 2021). This process may occur fast. For example, one study found that about 60% of N was stored in MAOM just 112 days after ^{15}N-labeled N compounds were applied to soils (Bosshard et al. 2008). Thus, under low-N and high-water availability conditions, the ecosystem maintains a relatively stable state between N supply (via aboveground plant biomass) and N demand, with potentially small N losses, after 14 years of directional increases in soil moisture.

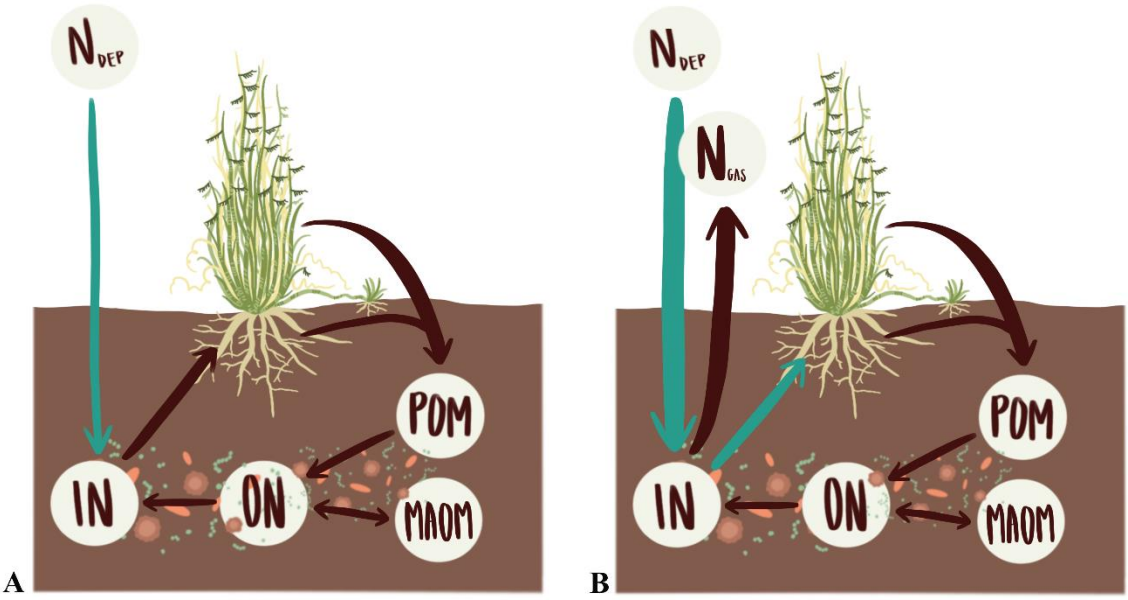

Figure 3.6. Conceptual diagram of simplified soil N dynamics under (A) low N availability and (B) high N availability. Brown arrows represent N fluxes between natural N sources and sinks, whereas blue arrows represent N fluxes derived from fertilizer N inputs.

If the dominant grass derived some N from MAOM under low-N conditions, the rate of MAOM-N uptake by plants was equal to the rate of MAOM-N formation by microbes because we did not see a detectable change in MAOM-N pool. MAOM-N mining and uptake was likely possible because foliar $\delta^{15}N$ was higher under directionally wet conditions over four sampling years compared to ambient or drought conditions. An increase in foliar $\delta^{15}N$ under low N and high-water availability indicates that the N source under wet conditions was also isotopically enriched. MAOM-N stable isotope signatures are typically enriched compared to background soil due to formation via microbial processes (Kleber et al. 2015), highlighting a potential N source for plants under consistently moist soil conditions. Indeed, we also observed unfertilized MAOM-N having higher $\delta^{15}N$ than bulk or POM-N. Thus, plants in unfertilized treatments may derive isotopically-enriched N from MAOM under high water availability conditions

(Fig. 3.3, gray line). Moreover, the statistically lower amounts of N in all soil pools in unfertilized compared to fertilized treatments indicates possible drawdown of N from the all soil pools, including the mineral fraction, compared to plants in fertilized plots that likely source most N from the fertilizer rather than the native soil N pool.

Potential N Sequestration versus Loss under High-N Conditions

N additions in the literature have varying effects on the mineral soil fraction, ranging from no effect on MAOM-C or MAOM-N (Keller et al. 2022) to significant destabilization of MAOM-C (Neff et al. 2002, Mack et al. 2004, Püspök et al. 2022). Contrary to the N draw-down hypothesis posed above, the increase in N content for all soil pools in fertilized treatments for our study may instead indicate that chronic fertilization increased N in all pools. This would indicate a potential for the soil at our study site to sequester excessive N inputs. This has global change implications by highlighting dryland ecosystem capability to directly offset greenhouse gas emissions or indirectly buffer negative effects of nutrient runoff and pollution by storing N in soil pools. The ability for soils to store nutrients long-term depends on the system's critical load (Bingham and Cotrufo 2016). If OM absorption sites reach capacity, then excess N may be lost via gaseous or leaching pathways (Fig. 3.6b). Dryland soils, for example, are responsible for 30% of global N gas emissions (Bowden 1986, Hu et al. 2017), mostly as products from microbial processes that include NO, an air pollutant at high concentrations, and N_2O, a powerful greenhouse gas.

In our study, under high N and high-water availability, bulk soil N appeared to decrease with increased precipitation amount, although this relationship was not statistically significant. We hypothesize this potential loss may have occurred for to two reasons. First, soil structure may have destabilized due to soil acidification in fertilized plots (Fig. S3.1; $F_{3,32} = 5.85$, $p < 0.05$, adjusted $R^2 = 0.29$). Soil acidification is a common consequence of chronic N enrichment because mineralization and oxidation of N compounds generate H^+ ions faster than the uptake of NO_3^--N by plants and microbes can offset this release (Bolan et al. 1991). Decreased pH promotes the leaching of Ca^{2+} from soil cation exchange sites, which deconstructs cation bridges that stabilize soil organic matter, and protons can bind to cation exchange sites that OM could otherwise use. Thus, soil acidification—by way of chronic N inputs—may alter the availability and stability of organic N.

Furthermore, by significantly increasing soil N through fertilization, conditions may select for a microbial community that shifted towards bacterial dominance (Moore et al. 2003), which would stimulate decomposition of MAOM and result in N loss. Simultaneously, massive inputs of inorganic N over our study period could have also concurrently increased microbial N gas loss through processes such as denitrification or nitrification, using native N as the substrates for these losses. A long-term study conducted in the arctic tundra also found a decreases in MAOM-C and MAOM-N after 20 years (Mack et al. 2004) with microbial activity as the primary explanation.

Ultimately, N in destabilized soil pools that cannot further sequester N has the potential to be lost via erosion or leaching. This has important implications for the long-

term availability of N for biological uptake, balance of the N cycle in drylands, soil C and N stabilization, and global carbon cycling overall. Ultimately, the balance between the rate of soil organic matter formation and destabilization is dependent on numerous factors, such as soil type, microbial mineralization rates, and climate change (Kleber et al. 2015).

Conclusion

The typical N limitation paradigm posits that ecosystems receiving excess N increase productivity until a threshold is reached, and N is subsequently lost via leaching or gas emissions (Aber et al. 1998). Drylands' role in N cycling, however, may follow an alternative model that distinguishes between the overall capacity of an ecosystem to retain N and its kinetic—or temporary—N saturation. Kinetic N saturation occurs when the N input rate temporarily exceeds the uptake rate of N sinks, resulting in temporal asynchrony between N cycle linkages (Lovett and Goodale 2011, Homyak et al. 2014). Better predictors of kinetic N saturation are needed to identify when systems lose or retain N since this transition is not always successional. Kinetic N saturation is one possible explanation for the variability of dryland vegetation responses to increased N availability. We captured no plant response to increased N availability due to possible drawdown from multiple soil pools. Moreover, soils in the semiarid grassland we studied demonstrated potential to sequester N. Targeted isotope tracer studies that examine N turnover times within multiple sinks under variable water and N availability conditions would disentangle the exact fate of N inputs and losses. Undoubtedly, N limitation in

drylands does not follow the typical paradigm of their mesic counterparts (Osborne et al. 2022), which poses an exciting research dimension in ecology.

References

Aber, J., W. McDowell, K. Nadelhoffer, A. Magill, G. Berntson, M. Kamakea, S. McNulty, W. Currie, L. Rustad, and I. Fernandez. 1998. "Nitrogen saturation in temperate forest ecosystems." *BioScience* 48:921–934.

Bates, D., M. Maechler, B. Bolker, and S. Walker. 2014. "Lme4: Linear mixed-effects models using Eigen and S4." R Package Version 1:1–23.

Berendse, F., and R. Aerts. 1987. "Nitrogen-use-efficiency: A biologically meaningful definition?" *Functional Ecology* 1:293–296.

Bingham, A. H., and M. F. Cotrufo. 2016. "Organic nitrogen storage in mineral soil: Implications for policy and management." *Science of the Total Environment* 551–552:116–126.

Bolan, N. S., M. J. Hedley, and R. E. White. 1991. "Processes of soil acidification during nitrogen cycling with emphasis on legume based pastures." *Plant and Soil* 134:53–63.

Bosshard, C., E. Frossard, D. Dubois, P. Mäder, I. Manolov, and A. Oberson. 2008. "Incorporation of nitrogen-15-labeled amendments into physically separated soil organic matter fractions." *Soil Science Society of America Journal* 72:949–959.

Bowden, W. B. 1986. "Gaseous nitrogen emmissions from undisturbed terrestrial ecosystems: An assessment of their impacts on local and global nitrogen budgets." *Biogeochemistry* 2:249–279.

Chapin, F. S. 1980. "The mineral nutrition of wild plants." *Annual Review of Ecology and Systematics* 11:233–260.

Collins, S. L., L. M. Ladwig, M. D. Petrie, S. K. Jones, J. M. Mulhouse, J. R. Thibault, and W. T. Pockman. 2017. "Press-pulse interactions: Effects of warming, N deposition, altered winter precipitation, and fire on desert grassland community structure and dynamics." *Global Change Biology* 23:1095–1108.

Crow, S. E., C. W. Swanston, K. Lajtha, J. R. Brooks, and H. Keirstead. 2007. "Density fractionation of forest soils: methodological questions and interpretation of incubation results and turnover time in an ecosystem context." *Biogeochemistry* 85:69–90.

Daly, A. B., A. Jilling, T. M. Bowles, R. W. Buchkowski, S. D. Frey, C. M. Kallenbach, M. Keiluweit, M. Mooshammer, J. P. Schimel, and A. S. Grandy. 2021. "A holistic framework integrating plant-microbe-mineral regulation of soil bioavailable nitrogen." *Biogeochemistry* 154:211–229.

Gherardi, L. A., and O. E. Sala. 2013. "Automated rainfall manipulation system: a reliable and inexpensive tool for ecologists." *Ecosphere* 4:art18.

Gherardi, L. A., and O. E. Sala. 2019. "Effect of inter-annual precipitation variability on dryland productivity: A global synthesis." *Global Change Biology* 25:269–276.

Gile, L. H. 1981. "Soils and geomorphology in the basin and range area of southern New Mexico: Guidebook to the Desert Project, New Mexico." *Bureau of Mines and Mineral Resources Memoir* 39:222.

Homyak, P. M., J. O. Sickman, A. E. Miller, J. M. Melack, T. Meixner, and J. P. Schimel. 2014. "Assessing nitrogen-saturation in a seasonally dry chaparral watershed: Limitations of traditional indicators of N-saturation." *Ecosystems* 17:1286–1305.

Homyak, P. M., E. W. Slessarev, S. Hagerty, A. C. Greene, K. Marchus, K. Dowdy, S. Iverson, and J. P. Schimel. 2021. "Amino acids dominate diffusive nitrogen fluxes across soil depths in acidic tussock tundra." *New Phytologist* 231:2162–2173.

Hooper, D. U., and L. Johnson. 1999. "Nitrogen limitation in dryland ecosystems: Responses to geographical and temporal variation in precipitation." *Biogeochemistry* 46:47.

Hu, H.-W., P. Trivedi, J.-Z. He, and B. K. Singh. 2017. "Microbial nitrous oxide emissions in dryland ecosystems: mechanisms, microbiome and mitigation." *Environmental Microbiology* 19:4808–4828.

Huenneke, L. F., J. P. Anderson, M. Remmenga, and W. H. Schlesinger. 2002. "Desertification alters patterns of aboveground net primary production in Chihuahuan ecosystems." *Global Change Biology* 8:247–264.

Inselsbacher, E., O. A. Oyewole, and T. Näsholm. 2014. "Early season dynamics of soil nitrogen fluxes in fertilized and unfertilized boreal forests." *Soil Biology and Biochemistry* 74:167–176.

Jilling, A., M. Keiluweit, A. R. Contosta, S. Frey, J. Schimel, J. Schnecker, R. G. Smith, L. Tiemann, and A. S. Grandy. 2018. "Minerals in the rhizosphere: Overlooked mediators of soil nitrogen availability to plants and microbes." *Biogeochemistry* 139:103–122.

Keller, A. B., E. T. Borer, S. L. Collins, L. C. DeLancey, P. A. Fay, K. S. Hofmockel, A. D. B. Leakey, M. A. Mayes, E. W. Seabloom, C. A. Walter, Y. Wang, Q. Zhao, and S. E. Hobbie. 2022. "Soil carbon stocks in temperate grasslands differ strongly across sites but are insensitive to decade-long fertilization." *Global Change Biology* 28:1659–1677.

Kleber, M., P. S. Nico, A. Plante, T. Filley, M. Kramer, C. Swanston, and P. Sollins. 2011. "Old and stable soil organic matter is not necessarily chemically recalcitrant: Implications for modeling concepts and temperature sensitivity." *Global Change Biology* 17:1097–1107.

Kleber, M., K. Eusterhues, M. Keiluweit, C. Mikutta, R. Mikutta, and P. S. Nico. 2015. "Mineral–organic associations: Formation, properties, and relevance in soil environments." In *Advances in Agronomy*, edited by D. L. Sparks, 1–140. San Diego, CA: Elsevier.

Kramer, M. G., K. Lajtha, G. Thomas, and P. Sollins. 2009. "Contamination effects on soil density fractions from high N or C content sodium polytungstate." *Biogeochemistry* 92:177–181.

LeBauer, D. S., and K. K. Treseder. 2008. "Nitrogen limitation of net primary productivity in terrestrial ecosystems is globally distributed." *Ecology* 89:371–379.

Liao, J. D., T. W. Boutton, and J. D. Jastrow. 2006. "Storage and dynamics of carbon and nitrogen in soil physical fractions following woody plant invasion of grassland." *Soil Biology and Biochemistry* 38:3184–3196.

Lovett, G. M., and C. L. Goodale. 2011. "A new conceptual model of nitrogen saturation based on experimental nitrogen addition to an oak forest." *Ecosystems* 14:615–631.

Mack, M. C., E. A. G. Schuur, M. S. Bret-Harte, G. R. Shaver, and F. S. Chapin. 2004. "Ecosystem carbon storage in arctic tundra reduced by long-term nutrient fertilization." *Nature* 431:440–443.

Mason, R. E., J. M. Craine, N. K. Lany, M. Jonard, S. V. Ollinger, P. M. Groffman, R. W. Fulweiler, J. Angerer, Q. D. Read, P. B. Reich, P. H. Templer, and A. J. Elmore. 2022. "Evidence, causes, and consequences of declining nitrogen availability in terrestrial ecosystems." *Science* 376:eabh3767.

McHugh, T. A., E. M. Morrissey, R. C. Mueller, L. V. Gallegos-Graves, C. R. Kuske, and S. C. Reed. 2017. "Bacterial, fungal, and plant communities exhibit no biomass or compositional response to two years of simulated nitrogen deposition in a semiarid grassland." *Environmental Microbiology* 19:1600–1611.

Monger, H. C. 2006. “Soil development in the Jornada Basin.” In *Structure and Function of a Chihuahuan Desert Ecosystem: The Jornada Basin Long-Term Ecological Research Site*, edited by K. M. Havstad, L. F. Huenneke, and W. H. Schlesinger, 81–106. New York, NY: Oxford University Press.

Moore, J. C., K. McCann, H. Setälä, and P. C. De Ruiter. 2003. “Top-down is bottom-up: Does predation in the rhizosphere regulate aboveground dynamics?” *Ecology* 84:846–857.

Neff, J. C., A. R. Townsend, G. Gleixner, S. J. Lehman, J. Turnbull, and W. D. Bowman. 2002. “Variable effects of nitrogen additions on the stability and turnover of soil carbon.” *Nature* 419:915–917.

Osborne, B. B., B. T. Bestelmeyer, C. M. Currier, P. M. Homyak, H. L. Throop, K. Young, and S. C. Reed. 2022. “The consequences of climate change for dryland biogeochemistry.” *New Phytologist* 236:15–20.

Paul, E. A. 2016. “The nature and dynamics of soil organic matter: Plant inputs, microbial transformations, and organic matter stabilization.” *Soil Biology and Biochemistry* 98:109–126.

Prăvălie, R. 2016. “Drylands extent and environmental issues. A global approach.” *Earth-Science Reviews* 161:259–278.

Püspök, J. F., S. Zhao, A. D. Calma, G. L. Vourlitis, S. D. Allison, E. L. Aronson, J. P. Schimel, E. J. Hanan, and P. M. Homyak. 2022. “Effects of experimental nitrogen deposition on soil organic carbon storage in Southern California drylands.” *Global Change Biology* 00:1–20.

R Core Team. 2018. “R: A language and environment for statistical computing.” R Foundation for Statistical Computing, Vienna, Austria. https://www.R-project.org/.

Reichmann, L. G., O. E. Sala, and D. P. Peters. 2013a. “Water controls on nitrogen transformations and stocks in an arid ecosystem.” *Ecosphere* 4:1–17.

Reichmann, L. G., O. E. Sala, and D. P. C. Peters. 2013b. “Precipitation legacies in desert grassland primary production occur through previous-year tiller density.” *Ecology* 94:435–443.

Rowley, M. C., S. Grand, and É. P. Verrecchia. 2018. “Calcium-mediated stabilisation of soil organic carbon.” *Biogeochemistry* 137:27–49.

Schulze, K., W. Borken, J. Muhr, and E. Matzner. 2009. “Stock, turnover time and accumulation of organic matter in bulk and density fractions of a Podzol soil.” *European Journal Of Soil Science* 60:567–577.

Sollins, P., C. Swanston, M. Kleber, T. Filley, M. Kramer, S. Crow, B. A. Caldwell, K. Lajtha, and R. Bowden. 2006. “Organic C and N stabilization in a forest soil: Evidence from sequential density fractionation.” *Soil Biology and Biochemistry* 38:3313–3324.

Sterner, R. W., and J. J. Elser. 2002. *Ecological Stoichiometry: The Biology of Elements from Molecules to the Biosphere*. Princeton, NJ: Princeton University Press.

Thatcher, D. and Bestelmeyer, B. 2021. “Monthly precipitation data from a network of standard gauges at the Jornada Experimental Range (Jornada Basin LTER) in southern New Mexico, January 1916 - ongoing ver 739.” Environmental Data Initiative.https://doi.org/10.6073/pasta/3086f4fa60f1e0ec807c269490d47ed3.

Throop, H. L., K. Lajtha, and M. Kramer. 2013. “Density fractionation and ^{13}C reveal changes in soil carbon following woody encroachment in a desert ecosystem.” *Biogeochemistry* 112:409–422.

Torn, M. S., C. W. Swanston, C. Castanha, and S. E. Trumbore. 2009. “Storage and turnover of organic matter in soil.” In *Biophysico-Chemical Processes Involving Natural Nonliving Organic Matter in Environmental Systems*, edited by N. Senesi, B. Xing, and P. M. Huang, 219–272. Hoboken, NJ: John Wiley & Sons, Inc.

Vitousek, P. 1982. “Nutrient cycling and nutrient use efficiency.” *The American Naturalist* 119:553–572.

Yahdjian, L., L. Gherardi, and O. E. Sala. 2011. “Nitrogen limitation in arid-subhumid ecosystems: A meta-analysis of fertilization studies.” *Journal of Arid Environments* 75:675–680.

Supplementary Material to Chapter 3

Table S3.1. Effect of experimental precipitation and nitrogen treatments on the dominant grass aboveground net primary productivity (ANPP) over four sampling years (2011, 2012, 2018, and 2020). Output for mixed linear effects of precipitation and N availability on *Bouteloua eriopoda* ANPP (g m^{-2} $year^{-1}$). Fixed effects estimates whose confidence intervals (CI) do not overlap with zero indicate a significant effect.

Predictors	**Estimates**	**Confidence Interval**	***p*-value**
(Intercept)	-3.50	-18.70 – 11.70	0.648
Precipitation amount	0.24	0.14 – 0.34	**<0.001**
N treatment	-4.51	-21.65 – 12.62	0.601
Precipitation*N treatment	0.11	-0.02 – 0.24	0.102
Random Effects			
σ^2	389.99		
$\tau_{00\ year\ sampled}$	67.24		
ICC	0.15		
$N_{year\ sampled}$	4		
Observations	101		
Marginal R^2 / Conditional R^2	0.424 / 0.508		

Table S3.2. Experimental rainfall and nitrogen treatments at a 14-year-old rainfall manipulation experiment at the Jornada Basin LTER. Values for rainfall represent sums over the growing season (June – September) in millimeters (mm), for the years 2011, 2012, 2018, and 2020. Values for soil nitrogen are presented as mean percent ± standard error (SE) for the year 2020.

Year sampled	Ambient growing season rainfall (mm)	Manipulated rainfall range (mm)	Ambient soil N (%)	+N treatment soil N(%)	Ambient soil $\delta^{15}N$	+N treatment soil $\delta^{15}N$
2011	114.55	22.91 – 206.19	0.035 ± 0.0023	0.041 ± 0.0030	7.71 ± 0.65	9.59 ± 0.80
2012	55.37	11.07 – 99.67	0.040 ± 0.0031	0.039 ± 0.0022	7.21 ± 0.49	11.06 ± 1.23
2018	109.47	21.89 – 197.05	0.034 ± 0.0024	0.049 ± 0.0043	5.41 ± 0.11	8.90 ± 0.42
2020	74.93	14.99 – 134.87	0.027 ± 0.0012	0.042 ± 0.0040	5.47 ± 0.14	7.71 ± 0.41

Table S3.3. Effect of experimental precipitation and nitrogen treatments on the dominant grass %N over four sampling years (2011, 2012, 2018, and 2020). Output for mixed linear effects of precipitation and N availability on *Bouteloua eriopoda* foliar %N. Fixed effects estimates whose confidence intervals (CI) do not overlap with zero indicate a significant effect.

Predictors	**Estimates**	**Confidence Interval**	***p* -value**
(Intercept)	2.09	1.70 – 2.48	<0.001
Precipitation amount	0.00	-0.00 – 0.00	0.534
N treatment	0.11	-0.24 – 0.46	0.528
Precipitation*N treatment	0.00	-0.00 – 0.00	0.057
Random Effects			
σ^2	0.09		
$\tau_{00\ year\ sampled}$	0.07		
ICC	0.44		
$N_{year\ sampled}$	4		
Observations	95		
Marginal R^2 / Conditional R^2	0.082 / 0.484		

Table S3.4. Effect of experimental precipitation and nitrogen treatments on the dominant grass N productivity over four sampling years (2011, 2012, 2018, and 2020). Output for mixed linear effects of precipitation and N availability on *Bouteloua eriopoda* N productivity. Fixed effects estimates whose confidence intervals (CI) do not overlap with zero indicate a significant effect.

Predictors	**Estimates**	**Confidence Interval**	***p* -value**
(Intercept)	51.05	39.92 – 62.18	<0.001
Precipitation amount	-0.02	0.07 – 0.03	0.465
N treatment	-3.35	-12.82 – 6.13	0.484
Precipitation*N treatment	0.06	-0.00 – 0.13	0.064
Random Effects			
σ^2	54.07		
$\tau_{00\ year\ sampled}$	64.66		
ICC	0.54		
$N_{year\ sampled}$	4		
Observations	86		
Marginal R^2 / Conditional R^2	0.066 / 0.575		

Table S3.5. Effect of experimental precipitation and nitrogen treatments on the dominant grass $\delta^{15}N$ over four sampling years (2011, 2012, 2018, and 2020). Output for mixed linear effects of precipitation and N availability on *Bouteloua eriopoda* foliar $\delta^{15}N$. Fixed effects estimates whose confidence intervals (CI) do not overlap with zero indicate a significant effect.

Predictors	**Estimates**	**Confidence Interval**	***p* -value**
(Intercept)	4.42	3.50 – 5.33	<0.001
Precipitation amount	0.00	-0.01 – 0.00	0.185
N treatment	-5.00	-6.07 – -3.93	**<0.001**
Precipitation*N treatment	0.01	0.00 – 0.02	**0.01**
Random Effects			
σ^2	1.54		
$\tau_{00\ year\ sampled}$	0.09		
ICC	0.06		
$N_{year\ sampled}$	4		
Observations	102		
Marginal R^2 / Conditional R^2	0.689 / 0.707		

Table S3.6. Effects of experimental precipitation and N treatments on N content (mg N g^{-1} bulk soil) of bulk soil and two soil fractions from one sampling year (2020), after 14 years of rainfall manipulation. Output for linear regressions of precipitation and N availability on bulk soil, particulate organic matter (POM) soil fraction, and mineral associated organic matter (MAOM) soil fraction N content. Significant regressions are indicated by model fits with $p < 0.05$.

Sample type	Variable	Slope	F-statistic	Degrees of Freedom	*p* -value	Adjusted R^2
Bulk soil	Precipitation amount	-1.7×10^{-4}	11.53	43	0.68	0.41
	N treatment	0.22			**< 0.001**	
	Precipitation*N treatment	-8.6×10^{-4}			0.17	
Particulate organic matter (POM) fraction	Precipitation amount	-2.33×10^{-4}	3.79	28	0.67	0.21
	N treatment	0.15			**0.03**	
	Precipitation*N treatment	-6.09×10^{-4}			0.42	
Mineral associated organic matter (MAOM) fraction	Precipitation amount	6.92×10^{-6}	6.11	30	0.96	0.32
	N treatment	5.70×10^{-2}			**< 0.01**	
	Precipitation*N treatment	-2.29×10^{-4}			0.27	

Table S3.7. Effects of experimental precipitation and N treatments on $\delta^{15}N$ of bulk soil and two soil fractions from one sampling year (2020). Output for linear regressions of precipitation and N availability on bulk soil, particulate organic matter (POM) soil fraction, and mineral associated organic matter (MAOM) soil fraction $\delta^{15}N$. Significant regressions are indicated by model fits with $p < 0.05$.

Sample type	Variable	Slope	F-statistic	Degrees of Freedom	*p* -value	Adjusted R^2
Bulk soil	Precipitation amount	-2.61×10^{-3}	10.10	23	0.68	0.51
	N treatment	2.38			**<0.01**	
	Precipitation*N treatment	-1.94×10^{-3}			0.83	
Particulate organic matter (POM) fraction	Precipitation amount	-3.89×10^{-3}	8.57	22	0.65	0.48
	N treatment	2.83			**0.01**	
	Precipitation*N treatment	-6.91×10^{-4}			0.95	
Mineral associated organic matter (MAOM) fraction	Precipitation amount	-1.15×10^{-3}	10.31	32	0.75	0.44
	N treatment	1.64			**<0.01**	
	Precipitation*N treatment	-3.66×10^{-3}			0.48	

Figure S3.1. Effect of experimental precipitation and N treatments on bulk soil pH. Oven-dried bulk soil from 2020 was used to assess soil pH using a benchtop pH meter (Fischer Scientific Accumet AB150). Points represent annual means ± standard error. A significant statistical difference between N treatment is represented by differences in point color. Precipitation amount was not a significant factor.

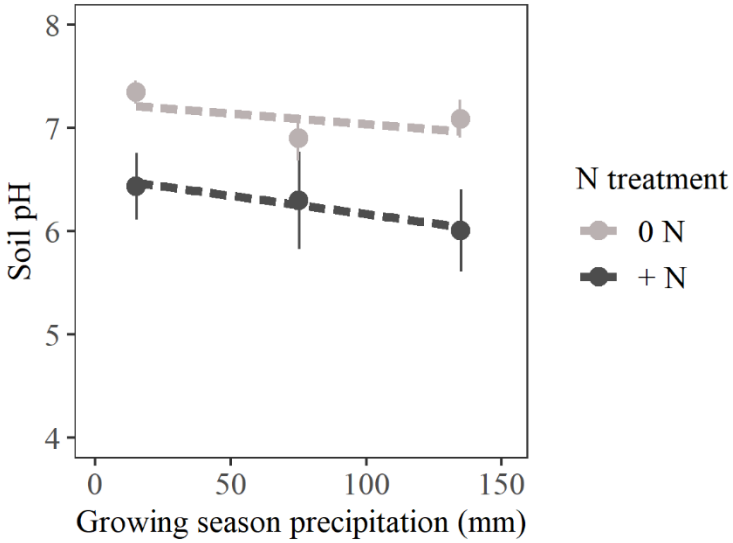

CHAPTER 4

ACCLIMATION OF THE NITROGEN CYCLE TO CHANGES IN PRECIPITATION

Abstract

As precipitation is expected to shift under climate change, we asked how the acclimation of the N cycle to changes in water availability occur and how long does this acclimation take. We found that site-averaged foliar $\delta^{15}N$ decreases with annual precipitation across continents. However, within a desert grassland, interannual foliar and soil $\delta^{15}N$ increased with precipitation amount. Using rainfall manipulation field experiments, we then assessed trends in foliar and soil $\delta^{15}N$ as duration of the rainfall manipulation increased, from 5 to 14 years. When parsed temporally, the $\delta^{15}N$-precipitation slope showed initially increasing trends that decreased after 14 years of rainfall manipulation. When compared to the global explanatory model of $\delta^{15}N$ vs. MAP, we estimated rates of acclimation at one site to range from 10 to 27 years. Stable isotopes may be a reasonable proxy to assess ecosystem N availability, which we conclude is changing through time in relation to precipitation extremes at rates that conflict with spatial trends. We hypothesize that response lags to changes in precipitation between plants and microorganisms control acclimation. Ignoring acclimation by predicting future N availability using spatial models alone would have inaccurately estimated the directionality and rates of N availability under climate change.

Introduction

Understanding the consequences of climate change on ecosystem functioning is the most important objective of current ecology. Near term (2021–2040) and long-term (beyond 2040) global warming up to 1.5°C is projected with high confidence to lead to unavoidable increases in multiple climate hazards to ecosystems and humans (Pörtner et al. 2022). Ecological systems autonomously change and match novel environmental conditions, a phenomenon known as acclimation that operates at different time scales and levels of organization. Acclimation occurs at the organismic level, as individuals show phenotypic plasticity (Wilson and Franklin 2002). It also occurs at the level of community organization, as the relative abundance of species is driven by the different strategies of organisms (Garcia-Pichel and Sala 2022). Different mechanisms for acclimation also occur at different time scales (Smith et al. 2009). Physiological changes are first to occur when environmental conditions change. If conditions remain altered, then acclimation progresses to changes in species abundance and species composition first because of local extinctions, followed by new species establishment or invasion (Shea and Chesson 2002). Acclimation at multiple levels and time scales collectively affect ecosystem functioning. The focus of this work is to understand acclimation rates of nutrient cycling as a result of directional change in climate, specifically water availability. Here, we focus on the ecosystem nitrogen (N) cycle and address the issue of acclimation through a long-term field manipulative experiment and continental-scale data synthesis.

The concept of lags in ecosystem responses to changes in the environment is intrinsically associated with the concept of acclimation (Monger et al. 2015). For example, aboveground net primary productivity (ANPP) shows small responses to a change in precipitation from one year to the next, relative to the difference in average production between two sites with the same difference in mean precipitation (Sala et al. 2012). Lags from dry or wet years account for the ameliorated response from year to year (Reichmann et al. 2013b). The variability of ANPP is strongly associated with mean annual precipitation across space whereas this relationship is much weaker within sites through time (Lauenroth and Sala 1992, Sala et al. 2012). Lags that result from legacies of wet and dry years (Sala et al. 2012) explain this spatiotemporal disparity. The physiological and ecological phenomena that account for weaker temporal relationships highlight how individual ecosystems acclimate to changes in precipitation amount. Thus, using either spatial or temporal data has enormous consequences for projections of the effects of climate change on ecosystem functioning (Felton et al. 2022). Models using spatially distributed data of climate effects on ecosystem functioning have steeper slopes than temporal models because they reflect perfect acclimation with biotic components of the ecosystem in equilibrium with abiotic conditions.

Nitrogen (N) availability, defined as the N supply relative to the N demand for growth (Mason et al. 2022), underlies major aspects of ecosystem structure and functioning. An essential nutrient for protein synthesis in all living taxa, N often constrains the growth of plants and subsequent food web dependents. Increased N deposition derived from anthropogenic activities in the last decades is pushing many

regions of the planet across a threshold with consequences for ecosystems and human health (Rockström et al. 2009). In other regions and due to the accelerated rise in atmospheric carbon dioxide, however, depletion of the N supply is increasing rapidly, potentially constraining plant growth (Mason et al. 2022). In dryland ecosystems, the dominant control on ecosystem functioning is soil-water availability (Yahdjian et al. 2011). Plant N uptake and subsequent assimilation is highly dependent on the soil-leaf water potential difference that drives water uptake. Drylands are pulsed ecosystems characterized by dry quiescent periods interrupted by rainfall events that trigger a burst of microbial and plant activity (Noy-Meir 1973, Collins et al. 2014). However, the lags in the response to pulses varies between microorganisms, responsible for N mineralization, and plants, responsible for a large fraction of N immobilization (Austin et al. 2004). Therefore, dryland soils tend to accumulate N during periods of drought (Reichmann *et al.* 2013a; Homyak *et al.* 2017; Finger-Higgens *et al.* 2023) and lose excess N during periods of sufficient soil moisture (Yahdjian and Sala 2010, Homyak et al. 2017). Moreover, abiotic N loss may occur during periods of both dry and wet soil conditions (McCalley and Sparks 2009). Thus, the supply of N in drylands is typically high relative to plant demand for growth compared to other ecosystems. Because drylands cover nearly 45% of the terrestrial earth surface (Prăvălie 2016), changes in the precipitation regime have major implications for dryland vegetation N uptake, growth, and subsequent carbon and biogeochemical cycling globally (Poulter et al. 2014, Ahlström et al. 2015, MacBean et al. 2021).

To understand acclimation of the N cycle to changes in climate, we focused on the spatial versus temporal relationships between N availability and precipitation. Four questions guide this study's framework: 1) Are responses of N availability to changes in precipitation amount through time at one site similar to responses across space? 2) Is there evidence of acclimation in the N cycle as a response to climate change? 3) If so, what are the rates of acclimation through time, and can we estimate convergence with observations across space? 4) Finally, what are the ecological mechanisms behind the potential acclimation of the N cycle? Here, we present results from unique short- and long-term field experiments that simulated precipitation extremes over 5–14 years and compared the effects on N availability with new and previous continental-scale spatial observations.

We addressed our acclimation of the N cycle questions using two complementary approaches: 1) global and long-term $\delta^{15}N$ data from Craine et al. (Craine et al. 2018, 2019) and the National Ecological Observatory Network (NEON; 2022) and 2) foliar and soil stable isotopes of N ($\delta^{15}N$) from long-term rainfall manipulation experiments at the Jornada Basin Long Term Ecological Research (LTER) site, a semiarid grassland located in the northern Chihuahuan Desert. We used $\delta^{15}N$ as a metric to assess N availability and ecosystem acclimation in response to precipitation, following the rationale presented in Mason *et al.* (2022). A foliar $\delta^{15}N$ ratio close to zero could indicate high rates of biological N fixation, a process with near-zero discrimination for the heavier isotope. Transformations, especially loss pathways such as microbial nitrate reduction or ammonia volatilization (McCalley and Sparks 2009), result in fractionation that leaves

heavier isotope ratios in the soil substrate, which are also reflected in foliar values. Relatively high soil N availability compared to N demand by biological sinks is typically associated with isotopic values enriched in ^{15}N because N loss pathways of inorganic N are amplified (Mason et al. 2022).

Methods

Data overview

To elucidate differences between patterns in $\delta^{15}N$ across space versus one site through time, we used two complementary approaches. To build our spatial explanatory regressions, global foliar $\delta^{15}N$ were obtained from the dataset available from (Craine et al. 2018, 2019), consisting of over 43,000 samples spanning all continents except Antarctica and acquired from 258 datasets over 128 unique years (between 1876-2017). The temporal component of this study was conducted at the Jornada Basin Long Term Ecological Research (LTER) site (32.56 latitude, -106.78 longitude; Las Cruces, NM, USA). Rainfall manipulation treatments commenced in multiple years and spanned a range of experimental durations at the time of field sampling, from 4 years to 14 years (Table S4.1). We note that only some of these experiments were sampled repeatedly while others were sampled once in time. Nevertheless, because we present multiple years and time durations of rainfall manipulations within one site, we categorize this portion of our analyses as "temporal" as a means to distinguish the nature of these data compared to the single-time point samples in the global, spatial dataset.

Synthesis of spatial relationships

All spatial isotope data were pooled, regardless of plant functional type. Craine et al. assigned mean annual precipitation (MAP) and mean annual temperature (MAT) to each data point based on geographic location from (New et al. 2002). In addition, we included foliar isotope data made available from the National Ecological Observatory Network (NEON; data product ID DP1.10026.001) (NEON [National Ecological Observatory Network] 2022) across North America over 6 years (2016–2021). Climate data were obtained from the NEON field site metadata (NEON [National Ecological Observatory Network] 2022), available on the Field Sites webpage. Isotopic data were then site-averaged according to the latitude and longitude rounded to the nearest tenth decimal place.

Site-averaged foliar $\delta^{15}N$ for the global spatial dataset were then regressed against mean annual precipitation and mean annual temperature using multiple linear regression:

$$Y_{si} = \beta_0 + \beta_1 X_i + e_i \qquad \textit{eq. 4.1}$$

$$Y_{sj} = \beta_0 + \beta_2 X_j + e_j \qquad \textit{eq. 4.2}$$

$$Y_{sij} = \beta_0 + \beta_1 X_i + \beta_2 X_j + e_{ij} \qquad \textit{eq. 4.3}$$

$$Y_{sij} = \beta_0 + \beta_1 X_i + \beta_2 X_j + \beta_1 X_i \beta_2 X_j + e_{ij} \qquad \textit{eq. 4.4}$$

$$e_{ij} \sim N(0, \sigma^2)$$

Where Y_{ij} = site-averaged foliar $\delta^{15}N$, β_0 = intercept, $\beta_1 X_i$ = fixed effect 1 (precipitation amount), $\beta_2 X_j$ = fixed effect 2 (temperature), e_{ij} = residuals. Some continents exhibited mean annual precipitation values that were not normally distributed (i.e., Australia). Thus, the above regressions were also conducted using ln(precipitation):

$$Y_i = \beta_0 + \ln(\beta_1 X_i) + e_i \qquad \textit{eq. 4.5}$$

$$Y_{ij} = \beta_0 + \ln(\beta_1 X_i) + \beta_2 X_j + e_{ij} \qquad \textit{eq. 4.6}$$

$$Y_{ij} = \beta_0 + \ln(\beta_1 X_i) + \beta_2 X_j + \ln(\beta_1 X_i)\,\beta_2 X_j + e_{ij} \qquad \textit{eq. 4.7}$$

$$e_{ij} \sim N(0, \sigma^2)$$

The best global model was then selected using Akaike Information Criteria (Sakamoto et al. 1986); models that met our criteria had the lowest AIC with ΔAIC > 2, otherwise the most parsimonious model was selected. The two models with the lowest AIC for global spatial analyses were then compared for continental-level analyses (eqs. 4 and 7). Additionally, we chose these models for comparison as they provided the most comprehensive climatic explanation for potential changes in $\delta^{15}N$. All spatial statistical analyses were performed in R version 4.2.2 (Team 2013). Regression assumptions were tested and met for all analyses.

Study site description

The Jornada Basin LTER receives a mean precipitation amount of 250 mm annually. Seventy six percent of this mean annual precipitation comes in the form of summer monsoonal storms derived from the Gulf of Mexico (44). The dominant plant species include the C3 perennial shrub, *Prosopis glandulosa* (honey mesquite) and the C4 perennial grass, *Bouteloua eriopoda* (black grama), which together comprise 67% of the aboveground net primary productivity at our study site (8, 45). Soils are classified as Cacique loamy fine sand with weakly developed textural B (argillic) horizons overlaying

semi-indurated to indurated caliche at approximately 30–60 cm in depth (Gile 1981, Monger 2006).

Experimental design

Descriptions of experiments that were sampled at the Jornada Basin LTER can be found in Table S4.1. Plot size depended on the experiment, either 2.5 x 2.5 m or 2.5 x 5.0 m. All experimental plots had control plots that received ambient rainfall with no rainout shelter or irrigation system. Water treatments were achieved using rainout shelters that decreased incoming precipitation by 50% or 80% and automated irrigation systems that simultaneously applied 50% or 80% of incoming precipitation (Yahdjian and Sala 2002, Gherardi and Sala 2013). During precipitation events, shelters intercepted and redirected incoming rainfall to a PVC irrigation system connected to sprinklers surrounding +50% or +80% treatment plots by means of a solar-powered pump. Manipulation intensities were based on extremes of historical precipitation data for the region.

Monthly precipitation sums were obtained from Jornada Basin LTER meteorological stations, available on the Environmental Data Initiative, nearest to the experimental plots (Thatcher, D. and Bestelmeyer, B. 2021), summed over the growing season (June-September), and then adjusted according to the rainfall manipulation treatment. The range of growing season precipitation amount achieved experimentally was 11–206 mm over the experimental years (Table S4.1). We present precipitation amount as a continuous variable for our results due to the multi-year, multi-treatment nature of our study design. Some years were considerably drier than others, and the

rainfall amount received is more biologically meaningful to consider as a variable than categorical treatments.

Field sampling and stable isotope analyses

Field collection of leaves and soils for isotopic analyses took place during peak biomass months following the summer monsoon: August 2011, September 2012, September 2018, and September 2020. Replication and sample sizes can be found in Table S4.1. Four to five leaves were collected from three *Bouteloua* patches (when possible; some drought plots had zero *Bouteloua* cover) and the central *Prosopis* shrub (if present). Specifically, the leaves were collected from the four cardinal directions and the center (Cook *et al.* 2017). Surface soil samples (0–10 cm) were collected using 2.54 cm diameter soil corer and composited from five sub-plot samples that were representative of the general ground cover of the plot, ranging from bare ground to underneath dominant plant patches. Soil samples were then passed through a 2 mm sieve. Foliar and soil samples were subsequently dried at 70°C for 48 h and ground into a fine powder using a Desktop High Energy Vibratory Ball Mill (VQ-N ball mill Thomas Scientific) for foliar samples and a mortar and pestle for soil samples. The stainless grinding tools were carefully cleaned with ethanol between each sample.

Foliar and soil samples were analyzed for percent N content and stable nitrogen isotope ratios ($\delta^{15}N$). Foliar samples were encapsulated in 4 x 6 mm tins while soil samples were encapsulated in 5 x 9 mm tins. All 2011 and 2012 samples were run on a GVI IsoPrime and an Elementar Cube elemental analyzer at the Boston University Stable

Isotope Laboratory. One analytical replicate was run per 10 samples, and any anomalous results were rerun. In-house standards of peptone and glycine calibrated to USGS 40 and 41 were alternately analyzed after every 15 unknown samples. All 2018 and 2020 samples were run in analytical triplicates and flash combusted with a coupled continuous-flow elemental analyzer-isotope ratio mass spectrometer system consisting of a Costech EA interfaced to a Delta Advantage peripheral at the METAL Core Laboratory of Arizona State University. Calibration curves for 2018 and 2020 plant samples were built using tomato leaves (NIST 1573a) and for 2018 and 2020 soils using low-nitrogen Montana soil (NIST 2711). In-house glycine standards calibrated to USGS 40 and 41 were analyzed after every third unknown sample and at the beginning and end of each run.

Standards and unknowns were corrected for linearity, and unknowns were normalized to isotopic values of standard reference materials using a two-point calibration curve of in-house standards calibrated to USGS 40 and 41 standard reference materials. Acceptable accuracy of tomato leaf standards and in-house glycine or peptone standards was defined as having a residual error of $\leq 0.2‰$. Acceptable accuracy of the low-nitrogen Montana soil standard was defined as having a residual error of $\leq 0.3‰$. Acceptable precision for all standards was defined as having a standard deviation of $\leq 0.2‰$. A blank (empty tin cup) was included at the beginning of each analytical run for all 2011, 2012, and 2018 plants and soils, and after every 5-8 unknown samples for 2020 soils. Stable isotope nitrogen ratios are standardized to atmospheric air and expressed in permil (‰) as:

$$\delta = \frac{R_{sa}}{R_{std}} - 1 \qquad \textit{eq. 4.8}$$

Where R_{sa} is the molar $^{15}N/^{14}N$ ratio of the sample and R_{std} is the molar isotopic ratio of atmospheric air (0.0036765). All data presented in this manuscript underwent quality assessment and quality control. QA/QC was successful met when standards met accuracy and precision requirements defined above and when unknowns fell within the standard calibration range and exhibited a standard deviation among analytical replicates of ≤ 0.2‰. If unknowns had a standard deviation > 0.2‰, an attempt to meet QA/QC requirements was first conducted by removing one outlier replicate, reducing the number of analytical replicates to 2. If this did not resolve the precision measurement, the sample was flagged, re-ground, and re-run on the IRMS. Any data that remained flagged after re-running were discarded from the final data set.

Statistical analyses of temporal data

For the temporal analyses within the Jornada Basin LTER data set, we analyzed site-level control plots across our study site that were not parsed temporally using a linear mixed effects model in the lme4 package (Bates et al. 2014):

$$Y_{si} = \beta_0 + S_{1s} + S_{2s} + \beta_1 X_i + e_{si} \qquad \textit{eq. 4.9}$$

$$S_{1s} \sim N(0, \tau_{00}^2),$$

$$S_{2s} \sim N(0, \tau_{00}^2)$$

$$e_{si} \sim N(0, \sigma^2)$$

Where Y_{si} = foliar or soil $\delta^{15}N$, β_0 = intercept, S_{1s} = random effect 1 (year sampled), S_{1s} = random effect 2 (experiment | plot), $\beta_1 X_i$ = fixed effect (precipitation amount), e_{si} =

residuals. For temporally parsed statistics with the Jornada Basin LTER dataset, which included rainfall treatments, and for the spatial analyses we used simple linear regressions with precipitation alone as the explanatory variable (eq. 4.2). We did not include temperature because MAT is a relatively constant climate variable at our study site (Currier and Sala 2022).

Finally, rates of acclimation for changes in $\delta^{15}N$ versus precipitation through time at the Jornada Basin LTER were calculated by estimating the amount of time each temporal slope would match the global and individual continental slopes of $\delta^{15}N$ versus precipitation (derived from equations 4.5 and 4.8):

$$slope_{spatial} \sim slope_{JRN} * time_{years} + intercept_{JRN} \quad \textit{eq. 4.10}$$

All temporal statistical analyses were performed in R version 4.2.2 (Team 2013). Regression assumptions were tested for all analyses. In the case for the temporal soil analyses, the dependent variable ($\delta^{15}N$) exhibited some non-normality, which was not rectified through transformation. Nevertheless, the residuals of all soil models were tested for and exhibited normality.

Results

At the continental scale, the model containing ln(precipitation) and temperature, and their interaction (eq. 7), best explained patterns in $\delta^{15}N$. Site-averaged foliar $\delta^{15}N$ decreased significantly with mean annual precipitation (Table S4.2). Globally, the slope of $\delta^{15}N$ versus the natural log of mean annual precipitation was negative (Fig. 4.1, black line; Table S3.3; $F_{3,2542} = 301.90$, $p < 0.001$, $R^2 = 0.27$) with a significant interaction

effect with temperature (Table S4.3; $p < 0.05$). The untransformed value of this slope ($m = -0.0045$) is discussed further in this manuscript to provide ecological meaning and context for the results. Across six continents, arid sites had higher N availability than mesic sites, resulting in a negative relationship between site-averaged foliar $\delta^{15}N$ and mean annual precipitation (Fig. 4.1). The strength of MAP on $\delta^{15}N$ depended on the continent and possible interactions with temperature (Table S4.3). The effect of MAP on $\delta^{15}N$ was strongest in Australia (Fig. 4.1, green line; Table S4.3; $F_{3,224} = 73.56$, ln(precip) $p < 0.001$, ln(precip)*temp interaction $p = 0.37$, $R^2 = 0.49$) and weakest in Europe (Fig. 4.1, teal line; Table S4.3; $F_{3,96} = 5.13$, precip $p = 0.13$, precip*temp interaction $p < 0.05$, $R^2 = 0.11$). Full statistical output for all continents can be found in Table S4.3.

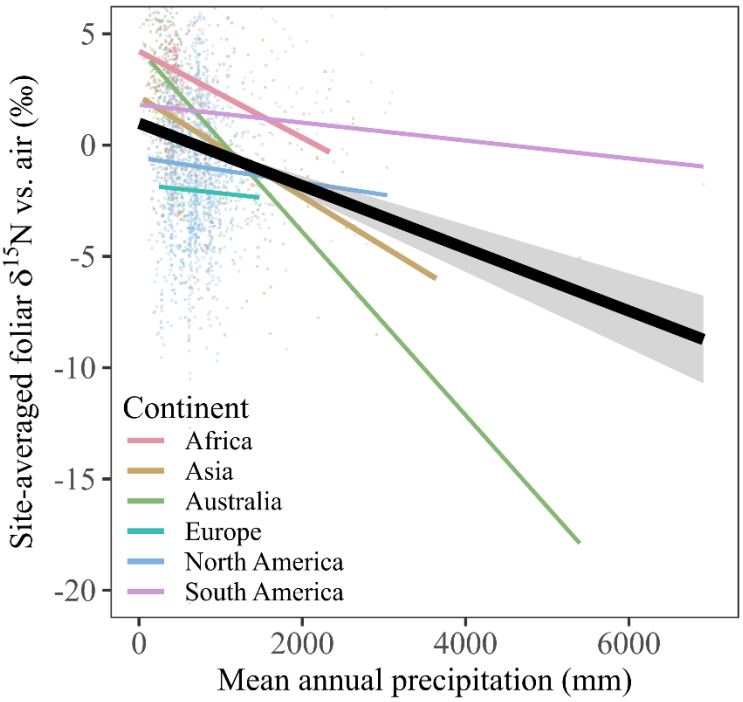

Figure 4.1. Site-averaged foliar $\delta^{15}N$ related to MAP at the continental scale. Data are untransformed for viewing purposes, but the supplementary material details which regressions included a natural log transformation of the independent variable (precipitation). Black line indicates global explanatory model with 95% confidence intervals. Solid lines indicate significant explanatory regressions ($p < 0.05$).

In the multi-year and multi-experiment observations from the Jornada Basin LTER, $\delta^{15}N$ increased significantly with ambient precipitation amount for the dominant plant community, consisting of pooled dominant grass plus shrub data (Fig. 4.2a; Table S4.4; CI: 0.01 – 0.04, $p < 0.01$, marginal $R^2 = 0.18$), and the dominant grass (Fig. 4.2b; Table S4.5; CI: 0.004 – 0.05, $p < 0.05$, marginal $R^2 = 0.42$). $\delta^{15}N$ also increased with precipitation amount for the dominant shrub (Fig. 4.2c; Table S4.6; CI: -0.003 – 0.02, $p = 0.13$, marginal $R^2 = 0.09$) and in surface soils (Fig. 4.2d; Table S4.7; -0.02 – 0.07, $p = 0.24$, marginal $R^2 = 0.43$), although these patterns were not statistically significant. It is worthy to note that the random effect variances were estimated as zero for these analyses. Nonetheless, we felt that it was important to retain the random effect terms (year and

plots within each experiment) to reflect the semi-repeated sampling and blocked nature of our experimental design. (Bolker et al. 2009) affirm that in cases like this, the results remain unchanged and the random effect parameters may be retained.

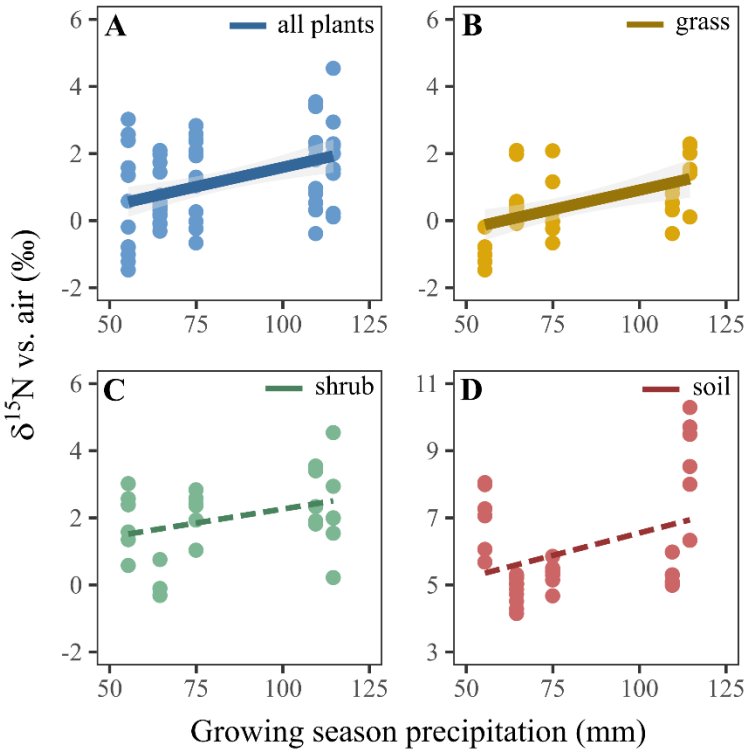

Figure 4.2. Foliar and soil $\delta^{15}N$ as it relates to ambient growing season precipitation at the Jornada Basin LTER (NM, USA) for: A) the plant community (pooled dominant grass plus dominant shrub data), B) *Bouteloua eriopoda*, the dominant grass, C) *Prosopis glandulosa*, the dominant shrub, and D) surface soil (0–10 cm). Points represent individual plot-year samples, and solid lines indicate significant explanatory regressions with 95% confidence intervals.

Further temporal analyses under directional precipitation extremes at the Jornada Basin LTER revealed potential ecosystem acclimation of the N cycle (Fig. 4.3; Tables S4.8 and S4.9). As time since onset of directional precipitation extremes increased (from 5 to 14 years), the slope of $\delta^{15}N$ versus precipitation decreased for the plant community (Fig. 4.3a), dominant plant species (Fig. 4.3b and 4.3c), and surface soil (Fig. 4.3d). The

overall pattern is that the relationship between $\delta^{15}N$ and precipitation amount was positive after 5 years of directional precipitation shift and decreased to slopes with zero or negative values after 14 years of directional precipitation shift. Within the plant community level (Fig. 4.3a), slopes for *B. eriopoda*, the dominant grass species, also followed this decreasing pattern (Fig. 4.3b. Slopes for the dominant shrub species, *P. glandulosa*, increased between years 5 and 6 and then decreased by year 14 (Fig. 4.3c). Surface soil (0–10 cm; Fig. 4.3d) also exhibited decreasing slopes through time that mirrored the aboveground observations. Statistical output for regressions within each time period can be found in Table S4.8 and across time periods in Table S4.9.

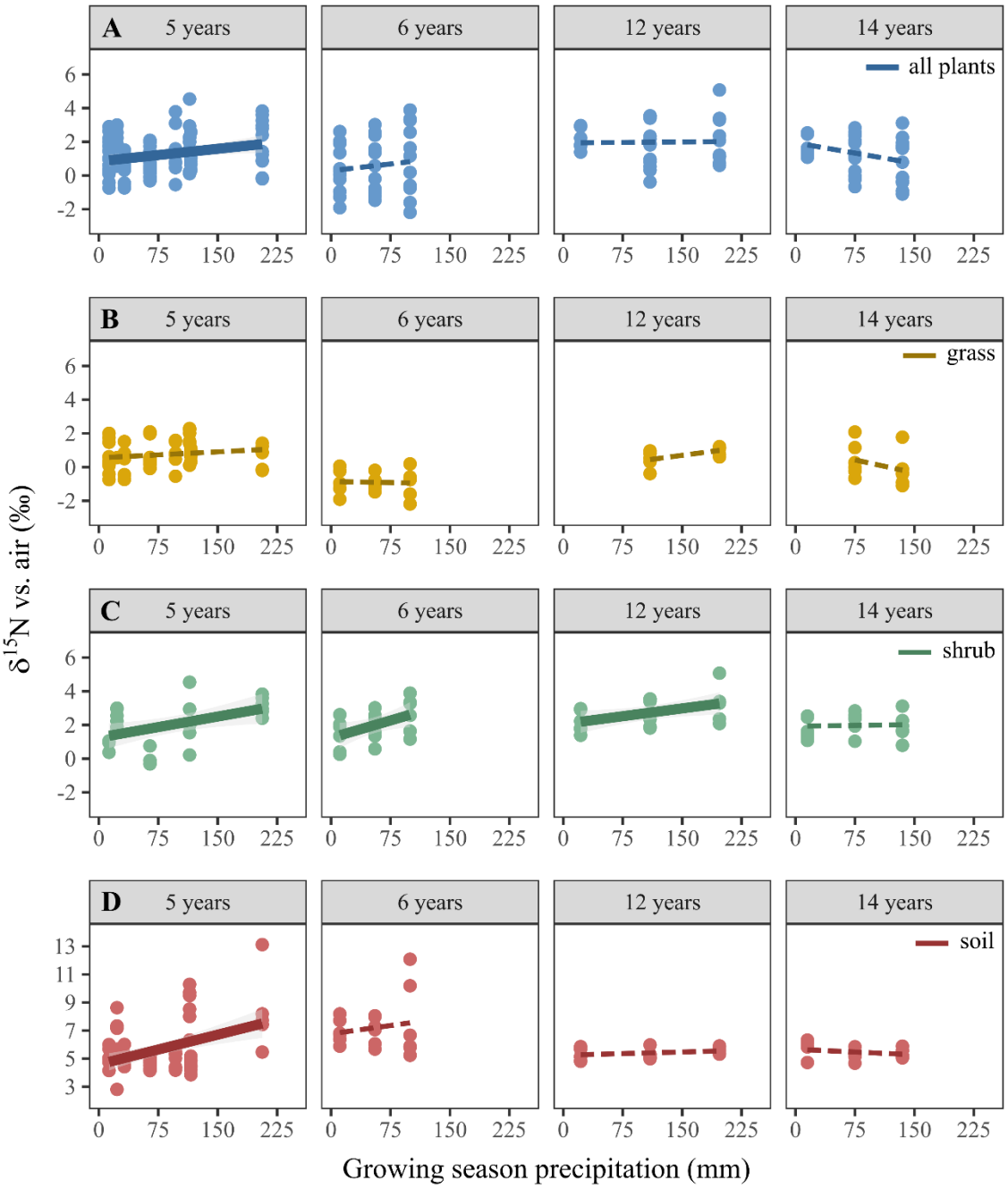

Figure 4.3. Temporal dynamics of foliar and soil $\delta^{15}N$ vs. air (‰). Time (in years) since onset of the directional rainfall manipulation is displayed at the top of each panel for: A) the plant community, B) *Bouteloua eriopoda*, the dominant grass, C) *Prosopis glandulosa*, the dominant shrub, and D) surface soil (0–10 cm). Points represent individual plot-year samples, and solid lines indicate significant explanatory regressions with 95% confidence intervals.

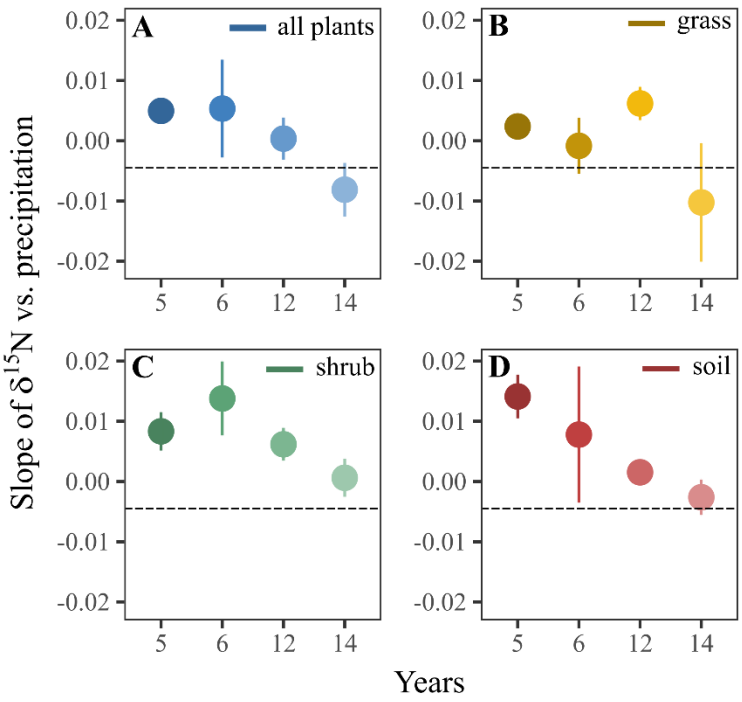

Figure 4.4. Slopes of $\delta^{15}N$ versus time (in years) since the onset of the directional rainfall manipulation. The black dashed line represents the global slope (Fig. 4.1) of $\delta^{15}N$ versus mean annual precipitation. Points represent slopes ± standard error of N availability versus precipitation amount for A) the plant community (Fig. 4.3a), B) the dominant grass (*Bouteloua eriopoda*; Fig. 4.3b), C) the dominant shrub (*Prosopis glandulosa*; Fig. 4.3c), and D) surface soil (Fig. 4.3d).

We then predicted the approximate rates of N cycle acclimation relative to the global- and continental-scale relationships between $\delta^{15}N$ and MAP at the Jornada for the two dominant plant species and surface soils. Overall rate of acclimation to the global slope for plants and soils was estimated to be approximately 16 years (Fig. 4.4; dotted black line denotes slope of the global spatial trend in Fig. 4.1). Specifically, the N cycle at the plant community level acclimated to the global explanatory slope in 13 years (Fig. 4.4a). The dominant grass acclimated at 15 years (Fig. 4.4b), and the dominant shrub acclimated slower at 21 years (Fig. 4.4c). Finally, the temporal relationship for soil converged with the spatial rate after 15 years (Fig. 4.4d). We also considered the possible

range of acclimation rates compared to individual continental slopes of $\delta^{15}N$ vs. MAP (Table 4.1). We found the range of acclimation to be 11–18 years for the plant community, 10–24 years for the dominant grass, 17–27 years for the dominant shrub, and 13–19 years for soils.

Table 4.1. Estimated time of convergence (years) between temporal slopes of $\delta^{15}N$ versus precipitation at the Jornada Basin LTER and the global- and continental-scale spatial slopes of $\delta^{15}N$ versus precipitation

Group	Continent	Estimated Convergence Time (years)
Plant community	Global (all)	13.21
	Africa	17.90
	Asia	17.27
	Australia	10.65
	Europe	11.19
	N. America	11.73
	S. America	12.55
Dominant grass (*Bouteloua eriopoda*)	Global (all)	15.06
	Africa	24.21
	Asia	23.00
	Australia	10.09
	Europe	11.14
	N. America	12.18
	S. America	13.79
Dominant shrub (*Prosopis glandulosa*)	Global (all)	20.66
	Africa	26.58
	Asia	25.79
	Australia	17.44
	Europe	18.12
	N. America	18.80
	S. America	19.84
Soil (0-10 cm)	Global (all)	15.34
	Africa	19.15
	Asia	18.65
	Australia	13.26
	Europe	13.70
	N. America	14.14
	S. America	14.81

Discussion

The isotopic-precipitation relationships we found at the continental scale are typical; arid sites tend to have higher $\delta^{15}N$ ratios than mesic sites (Handley et al. 1999, Amundson et al. 2003). The ecological explanation is that accumulated losses of N relative to ecosystem N pools are greater in drier sites. This relationship demonstrates that dryland ecosystems compared to wetter ecosystems tend to have relatively higher N supply compared to demand. Temporal relationships between N availability and environmental drivers have received less attention than spatial patterns, until recently (Craine et al. 2018, Caldararu et al. 2022, Mason et al. 2022). Within a long-term rainfall manipulation experiment at one site, we expected temporal relationship between N availability and precipitation to be negative given the global observations built from over 43,000 data points. However, we observed a positive relationship between N availability and precipitation. The positive temporal relationship between $\delta^{15}N$ and precipitation has also been observed by studies conducted in other arid and semiarid systems (Wang et al. 2014, Sperber et al. 2017, Liu et al. 2017). We concluded that responses of N availability as measured by soil and foliar $\delta^{15}N$ to changes in precipitation amount through time are different from responses across space.

The mechanisms between the temporal and spatial model differences are central to understand acclimation of the N cycle. First, the positive relationship between N availability and annual precipitation in systems subjected to normal sequences of wet and dry years would be explained by differential lags of plants and microbial communities.

Second, we suggest that the observed decreases through time in the slope of the temporal model relating N availability with precipitation (Fig. 4.3) was the result of two phenomena: 1) An increase in N availability with time in treatments that experienced prolonged drought; and 2) A decrease in N availability with time in treatments that experienced directional increases in precipitation. In other words, N availability increased through time in drought treatments and decreased in irrigated treatments, jointly reducing the slope of N availability-precipitation relationship.

The initial positive slope between N availability and precipitation amount is likely explained by net N mineralization rates that respond faster than net immobilization to precipitation pulses (Austin et al. 2004, Sperber et al. 2017). Initial experimental treatments and ambient conditions experienced more frequent wet–dry cycles compared to the 14-year irrigated treatments. The cyclical wet–dry process allows inorganic and organic N to accumulate during dry periods. Wet periods stimulate microbial activity, and subsequent drying results in increases in microbial cell lysis and further supply of labile organic matter. After a precipitation pulse, microbes and the mineralization process respond rapidly, increasing available N. In addition to increases in N mineralization, microbial gas production with high isotopic fractionation also occurs. However, plant response is slower because plant growth is limited by existing infrastructure of roots, tillers and leaves that take time to deploy. And, if pulses are too short, deployment cost may not be offset by growth during the wet pulse (Lauenroth et al. 1987).

The positive relationship between N availability and precipitation reversed through time. This change in the slope can be explained by examining mechanisms that

increased N availability under drought treatments and decreased N availability under wet treatments. First, drought treatments experienced significant dominant grass (*B. eriopoda*) mortality, eliminating an important N sink and resulting in significant accumulation of inorganic N during dry periods (Reichmann *et al.* 2013a; Homyak *et al.* 2017; Finger-Higgens *et al.* 2023). N mineralization apparently continued operating at a rate higher than immobilization due to possible microbial mining of older, mineral-associated organic matter (MAOM) sources (Daly et al. 2021). Variable wet–dry cycles and soil alkalinity characteristic of desert soils can also facilitate MAOM destabilization in long-term drought treatments (Torn et al. 2009). Mineralized MAOM-N that may become increasingly available through time is enriched with ^{15}N since initial formation and stabilization is typically due to microbial activity. We did not observe accumulation in bulk %N across precipitation or years (Figs. S4.1, S4.2), presumably because accumulation of inorganic N may be balanced by microbially-mediated or abiotic loss. Directional increases in precipitation increased the duration of wet periods and eventually reduced N leakiness between sources and biological sinks, which decreased N availability. In addition, N loss via leaching is a phenomena considered intrinsic to dryland ecosystems (Lovett and Goodale 2011) and may induce N limitation throughout the remainder of the growing season, further coupling the source–sink connection.

Understanding acclimation of ecosystem functioning to climate change is essential to predicting the future of ecosystems under a novel climate. Predictions based on spatial models would yield faster and larger responses than predictions based on temporal models. Therefore, one must use caution when predicting ecosystem changes

and need to consider acclimation rates. In the case of the N cycle, ignoring acclimation and utilizing spatial models instead of a temporal model to predict the future of the N cycle under climate change predictions of increased aridity would have grossly overestimated N availability. Differences between realized N availability and overestimates derived from spatial models have implications for the C cycle. For example, N limitation of plant productivity directly affects how much C can be sequestered and stored above- and belowground. Following this logic, the use of spatial models could have hidden N limitation of the C cycle in drylands that occupy 45% of the global terrestrial surface (Prăvălie 2016) with predicted expansion under future climate scenarios (Huang et al. 2016).

We estimated the fastest rates of N cycle acclimation because we manipulated changes in rainfall amount to be directional and extreme. Climate change will bring directional changes and increased variability in precipitation with extreme droughts and floods of novel frequency and magnitude (Gherardi and Sala 2019). We expect that enhanced interannual precipitation variability may slow down acclimation. Thus, rates of acclimation under combined directional changes in precipitation and enhanced variability may be slower than those reported here. We recognize that foliar $\delta^{15}N$ provides limited interpretation compared to whole-plant $\delta^{15}N$ values, given that differential fractionation may occur within plant stems and roots during assimilation. Nevertheless, the results presented here are generalizable and provide the basis for future directions and targeted isotope-tracer studies. We further expect that the broad results of this study will be generalizable across global ecosystems, but the rate of acclimation would depend on

intrinsic ecosystem characteristics. We hypothesize that the rate of acclimation would decrease or time to convergence would increase with the life span of dominant vegetation. Based on the results from this study, grasslands would be the fastest to acclimate and ecosystems dominated by long-lived woody vegetation would be the slowest. Conversely, sandy soils that experience frequent wet-dry cycles may be more likely to increase N availability via MAOM destabilization and microbial mining, increasing acclimation rates. Long-term effects of interacting components of the N cycle, however, remain unclear as some mechanisms that increase N availability will eventually reach disequilibrium and potentially lead to overall reduced N availability. Nonetheless, the concepts presented here identify critical assumptions of assessing global trends based on temporally versus spatially explicit approaches.

References

Ahlström, A., M. R. Raupach, G. Schurgers, B. Smith, A. Arneth, M. Jung, M. Reichstein, J. G. Canadell, P. Friedlingstein, A. K. Jain, E. Kato, B. Poulter, S. Sitch, B. D. Stocker, N. Viovy, Y. P. Wang, A. Wiltshire, S. Zaehle, and N. Zeng. 2015. "The dominant role of semi-arid ecosystems in the trend and variability of the land CO_2 sink." *Science* 348:895–899.

Amundson, R., A. T. Austin, E. a. G. Schuur, K. Yoo, V. Matzek, C. Kendall, A. Uebersax, D. Brenner, and W. T. Baisden. 2003. "Global patterns of the isotopic composition of soil and plant nitrogen." *Global Biogeochemical Cycles* 17.

Austin, A. T., L. Yahdjian, J. M. Stark, J. Belnap, A. Porporato, U. Norton, D. A. Ravetta, and S. M. Schaeffer. 2004. "Water pulses and biogeochemical cycles in arid and semiarid ecosystems." *Oecologia* 141:221–235.

Bates, D., M. Maechler, B. Bolker, and S. Walker. 2014. "Lme4: Linear mixed-effects models using Eigen and S4." *R Package Version* 1:1–23.

Bolker, B. M., M. E. Brooks, C. J. Clark, S. W. Geange, J. R. Poulsen, M. H. H. Stevens, and J.-S. S. White. 2009. "Generalized linear mixed models: a practical guide for ecology and evolution." *Trends in Ecology and Evolution* 24:127–135.

Caldararu, S., T. Thum, L. Yu, M. Kern, R. Nair, and S. Zaehle. 2022. "Long-term ecosystem nitrogen limitation from foliar $\delta^{15}N$ data and a land surface model." *Global Change Biology* 28:493–508.

Collins, S. L., J. Belnap, N. B. Grimm, J. A. Rudgers, C. N. Dahm, P. D'Odorico, M. Litvak, D. O. Natvig, D. C. Peters, W. T. Pockman, R. L. Sinsabaugh, and B. O. Wolf. 2014. "A multiscale, hierarchical model of pulse dynamics in arid-land ecosystems." *Annual Review of Ecology, Evolution, and Systematics* 45:397–419.

Cook, C. S., B. R. Erkkila, S. Chakraborty, B. J. Tipple, T. E. Cerling, and J. R. Ehleringer. 2017. *Stable Isotope Biogeochemistry and Ecology: Laboratory Manual*. University of Utah.

Craine, J. M., A. J. Elmore, L. Wang, J. Aranibar, M. Bauters, P. Boeckx, B. E. Crowley, M. A. Dawes, S. Delzon, A. Fajardo, Y. Fang, L. Fujiyoshi, A. Gray, R. Guerrieri, M. J. Gundale, D. J. Hawke, P. Hietz, M. Jonard, E. Kearsley, T. Kenzo, M. Makarov, S. Marañón-Jiménez, T. P. McGlynn, B. E. McNeil, S. G. Mosher, D. M. Nelson, P. L. Peri, J. C. Roggy, R. Sanders-DeMott, M. Song, P. Szpak, P. H. Templer, D. Van der Colff, C. Werner, X. Xu, Y. Yang, G. Yu, and K. Zmudczyńska-Skarbek. 2018. "Isotopic evidence for oligotrophication of terrestrial ecosystems." *Nature Ecology and Evolution* 2:1735–1744.

Craine, J. M., A. J. Elmore, L. Wang, J. Aranibar, M. Bauters, P. Boeckx, B. E. Crowley, M. A. Dawes, S. Delzon, A. Fajardo, Y. Fang, L. Fujiyoshi, A. Gray, R. Guerrieri, M. J. Gundale, D. J. Hawke, P. Hietz, M. Jonard, E. Kearsley, T. Kenzo, M. Makarov, S. Marañón-Jiménez, T. P. McGlynn, B. E. McNeil, S. G. Mosher, D. M. Nelson, P. L. Peri, J. C. Roggy, R. Sanders-DeMott, M. Song, P. Szpak, P. H. Templer, D. Van Der Colff, C. Werner, X. Xu, Y. Yang, G. Yu, and K. Zmudczyńska-Skarbek. 2019. "Data from: Isotopic evidence for oligotrophication of terrestrial ecosystems." Dryad. https://doi.org/10.5061/dryad.v2k2607.

Currier, C. M., and O. E. Sala. 2022. "Precipitation versus temperature as phenology controls in drylands." *Ecology*:e3793.

Daly, A. B., A. Jilling, T. M. Bowles, R. W. Buchkowski, S. D. Frey, C. M. Kallenbach, M. Keiluweit, M. Mooshammer, J. P. Schimel, and A. S. Grandy. 2021. "A holistic framework integrating plant-microbe-mineral regulation of soil bioavailable nitrogen." *Biogeochemistry* 154:211–229.

Felton, A. J., R. K. Shriver, M. Stemkovski, J. B. Bradford, K. N. Suding, and P. B. Adler. 2022. "Climate disequilibrium dominates uncertainty in long-term projections of primary productivity." *Ecology Letters* 25:2688–2698.

Finger-Higgens, R., T. B. B. Bishop, J. Belnap, E. L. Geiger, E. E. Grote, D. L. Hoover, S. Reed, and M. C. Duniway. 2023. “Droughting a megadrought: Ecological consequences of a decade of experimental drought atop aridification on the Colorado Plateau.” *Global Change Biology* n/a.

Garcia-Pichel, F., and O. E. Sala. 2022. “Expanding the pulse-reserve paradigm to microorganisms on the basis of differential reserve management strategies.” *BioScience* 72:638–650.

Gherardi, L. A., and O. E. Sala. 2013. “Automated rainfall manipulation system: a reliable and inexpensive tool for ecologists.” *Ecosphere* 4:art18.

Gherardi, L. A., and O. E. Sala. 2019. “Effect of inter-annual precipitation variability on dryland productivity: A global synthesis.” *Global Change Biology* 25:269–276.

Gile, L. H. 1981. “Soils and geomorphology in the Basin and Range area of southern New Mexico: Guidebook to the Desert Project, New Mexico.” *Bureau of Mines and Mineral Resources Memoir* 39:222.

Handley, L. L., A. T. Austin, G. R. Stewart, D. Robinson, C. M. Scrimgeour, J. A. Raven, T. H. E. Heaton, and S. Schmidt. 1999. “The ^{15}N natural abundance ($\delta 15N$) of ecosystem samples reflects measures of water availability.” *Functional Plant Biology* 26:185.

Havstad, K. M., L. F. Huenneke, and W. H. Schlesinger, editors. 2006. *Structure and Function of a Chihuahuan Desert Ecosystem: The Jornada Basin Long-Term Ecological Research Site*. New York, NY: Oxford University Press.

Homyak, P. M., S. D. Allison, T. E. Huxman, M. L. Goulden, and K. K. Treseder. 2017. “Effects of drought manipulation on soil nitrogen cycling: A meta-analysis.” *Journal of Geophysical Research: Biogeosciences* 122:3260–3272.

Huang, J., H. Yu, X. Guan, G. Wang, and R. Guo. 2016. “Accelerated dryland expansion under climate change.” *Nature Climate Change* 6:166–171.

Huenneke, L. F., J. P. Anderson, M. Remmenga, and W. H. Schlesinger. 2002. “Desertification alters patterns of aboveground net primary production in Chihuahuan ecosystems.” *Global Change Biology* 8:247–264.

Lauenroth, W. K., O. E. Sala, D. G. Milchunas, and R. W. Lathrop. 1987. “Root dynamics of Bouteloua gracilis during short-term recovery from drought.” *Functional Ecology* 1:117–124.

Lauenroth, W. K., and O. E. Sala. 1992. “Long-term forage production of North American shortgrass steppe.” *Ecological Applications* 2:397–403.

Liu, D., W. Zhu, X. Wang, Y. Pan, C. Wang, D. Xi, E. Bai, Y. Wang, X. Han, and Y. Fang. 2017. “Abiotic versus biotic controls on soil nitrogen cycling in drylands along a 3200 km transect.” *Biogeosciences* 14:989–1001.

Lovett, G. M., and C. L. Goodale. 2011. “A new conceptual model of nitrogen saturation based on experimental nitrogen addition to an oak forest.” *Ecosystems* 14:615–631.

MacBean, N., R. L. Scott, J. A. Biederman, P. Peylin, T. Kolb, M. E. Litvak, P. Krishnan, T. P. Meyers, V. K. Arora, V. Bastrikov, D. Goll, D. L. Lombardozzi, J. E. M. S. Nabel, J. Pongratz, S. Sitch, A. P. Walker, S. Zaehle, and D. J. P. Moore. 2021. “Dynamic global vegetation models underestimate net CO_2 flux mean and inter-annual variability in dryland ecosystems.” *Environmental Research Letters* 16:094023.

Mason, R. E., J. M. Craine, N. K. Lany, M. Jonard, S. V. Ollinger, P. M. Groffman, R. W. Fulweiler, J. Angerer, Q. D. Read, P. B. Reich, P. H. Templer, and A. J. Elmore. 2022. “Evidence, causes, and consequences of declining nitrogen availability in terrestrial ecosystems.” *Science* 376:eabh3767.

McCalley, C. K., and J. P. Sparks. 2009. “Abiotic gas formation drives nitrogen loss from a desert ecosystem.” *Science* 326:837–840.

Monger, H. C. 2006. “Soil development in the Jornada Basin.” In *Structure and Function of a Chihuahuan Desert Ecosystem: The Jornada Basin Long-Term Ecological Research Site*, edited by K. M. Havstad, L. F. Huenneke, and W. H. Schlesinger, 81–106. New York, NY: Oxford University Press.

Monger, C., O. E. Sala, M. C. Duniway, H. Goldfus, I. A. Meir, R. M. Poch, H. L. Throop, and E. R. Vivoni. 2015. “Legacy effects in linked ecological–soil–geomorphic systems of drylands.” *Frontiers in Ecology and the Environment* 13:13–19.

NEON (National Ecological Observatory Network). 2022. “Plant foliar traits (DP1.10026.001).” https://doi.org/10.48443/kmc7-8g05.

NEON (National Ecological Observatory Network). 2022. “Explore field sites.” https://www.neonscience.org/field-sites/explore-field-sites.

New, M., D. Lister, M. Hulme, and I. Makin. 2002. “A high-resolution data set of surface climate over global land areas.” *Climate Research* 21:1–25.

Noy-Meir, I. 1973. “Desert ecosystems: Environment and producers.” *Annual Review of Ecology and Systematics*:25–51.

Pörtner, H. O., D. C. Roberts, H. Adams, C. Adler, P. Aldunce, E. Ali, R. A. Begum, R. Betts, R. B. Kerr, and R. Biesbroek, editors. 2022. *Climate Change 2022: Impacts, Adaptation and Vulnerability. Contribution of Working Group II to the Sixth Assessment Report of the Intergovernmental Panel on Climate Change*. Geneva, Switzerland: IPCC.

Poulter, B., D. Frank, P. Ciais, R. B. Myneni, N. Andela, J. Bi, G. Broquet, J. G. Canadell, F. Chevallier, Y. Y. Liu, S. W. Running, S. Sitch, and G. R. van der Werf. 2014. "Contribution of semi-arid ecosystems to interannual variability of the global carbon cycle." *Nature* 509:600–603.

Prăvălie, R. 2016. "Drylands extent and environmental issues. A global approach." *Earth-Science Reviews* 161:259–278.

R Core Team. 2018. "R: A language and environment for statistical computing." R Foundation for Statistical Computing, Vienna, Austria. https://www.R-project.org/.

Reichmann, L. G., O. E. Sala, and D. P. Peters. 2013a. "Water controls on nitrogen transformations and stocks in an arid ecosystem." *Ecosphere* 4:1–17.

Reichmann, L. G., O. E. Sala, and D. P. C. Peters. 2013b. "Precipitation legacies in desert grassland primary production occur through previous-year tiller density." *Ecology* 94:435–443.

Rockström, J., W. Steffen, K. Noone, Å. Persson, F. S. Chapin, E. F. Lambin, T. M. Lenton, M. Scheffer, C. Folke, H. J. Schellnhuber, B. Nykvist, C. A. de Wit, T. Hughes, S. van der Leeuw, H. Rodhe, S. Sörlin, P. K. Snyder, R. Costanza, U. Svedin, M. Falkenmark, L. Karlberg, R. W. Corell, V. J. Fabry, J. Hansen, B. Walker, D. Liverman, K. Richardson, P. Crutzen, and J. A. Foley. 2009. "A safe operating space for humanity." *Nature* 461:472–475.

Sakamoto, Y., M. Ishiguro, and G. Kitagawa. 1986. "Akaike information criterion statistics." *Dordrecht, The Netherlands: D. Reidel* 81:26853.

Sala, O. E., L. A. Gherardi, L. Reichmann, E. Jobbagy, and D. Peters. 2012. "Legacies of precipitation fluctuations on primary production: theory and data synthesis." *Philosophical Transactions Of The Royal Society B: Biological Sciences* 367:3135–3144.

Shea, K., and P. Chesson. 2002. "Community ecology theory as a framework for biological invasions." *Trends in Ecology and Evolution* 17:170–176.

Smith, M. D., A. K. Knapp, and S. L. Collins. 2009. "A framework for assessing ecosystem dynamics in response to chronic resource alterations induced by global change." *Ecology* 90:3279–3289.

Sperber, C. von, O. A. Chadwick, K. L. Casciotti, K. G. Peay, C. A. Francis, A. E. Kim, and P. M. Vitousek. 2017. “Controls of nitrogen cycling evaluated along a well-characterized climate gradient.” *Ecology* 98:1117–1129.

Thatcher, D. and Bestelmeyer, B. 2021. “Monthly precipitation data from a network of standard gauges at the Jornada Experimental Range (Jornada Basin LTER) in southern New Mexico, January 1916 - ongoing ver 739.” Environmental Data Initiative. https://doi.org/10.6073/pasta/3086f4fa60f1e0ec807c269490d47ed3.

Torn, M. S., C. W. Swanston, C. Castanha, and S. E. Trumbore. 2009. “Storage and Turnover of Organic Matter in Soil.” In *Biophysico-Chemical Processes Involving Natural Nonliving Organic Matter In Environmental Systems*, edited by N. Senesi, B. Xing, and P. M. Huang, 219–272. Hoboken, NJ: John Wiley & Sons, Inc.

Wang, C., X. Wang, D. Liu, H. Wu, X. Lü, Y. Fang, W. Cheng, W. Luo, P. Jiang, J. Shi, H. Yin, J. Zhou, X. Han, and E. Bai. 2014. “Aridity threshold in controlling ecosystem nitrogen cycling in arid and semi-arid grasslands.” *Nature Communications* 5:4799.

Wilson, R. S., and C. E. Franklin. 2002. “Testing the beneficial acclimation hypothesis.” *Trends in Ecology and Evolution* 17:66–70.

Yahdjian, L., and O. E. Sala. 2002. “A rainout shelter design for intercepting different amounts of rainfall.” *Oecologia* 133:95–101.

Yahdjian, L., and O. E. Sala. 2010. “Size of precipitation pulses controls nitrogen transformation and losses in an arid Patagonian ecosystem.” *Ecosystems* 13:575–585.

Yahdjian, L., L. Gherardi, and O. E. Sala. 2011. “Nitrogen limitation in arid-subhumid ecosystems: A meta-analysis of fertilization studies.” *Journal of Arid Environments* 75:675–680.

Supplementary Material to Chapter 4

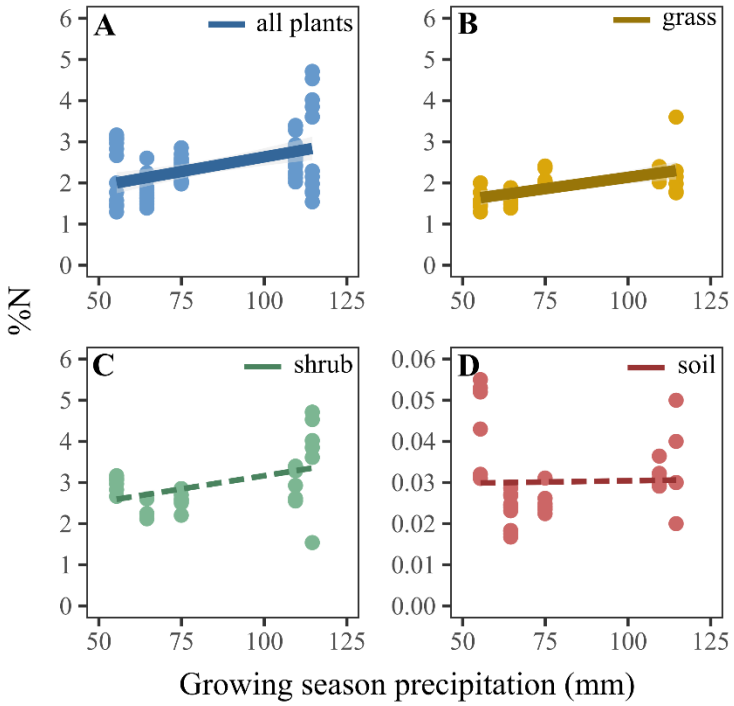

Figure S4.1. Foliar and soil %N as it relates to growing season precipitation at the Jornada Basin LTER (NM, USA) for: A) the plant community, B) *Bouteloua eriopoda*, the dominant grass, C) *Prosopis glandulosa*, the dominant shrub, and D) surface soil (0–10 cm). Solid lines indicate significant explanatory regressions with 95% confidence intervals.

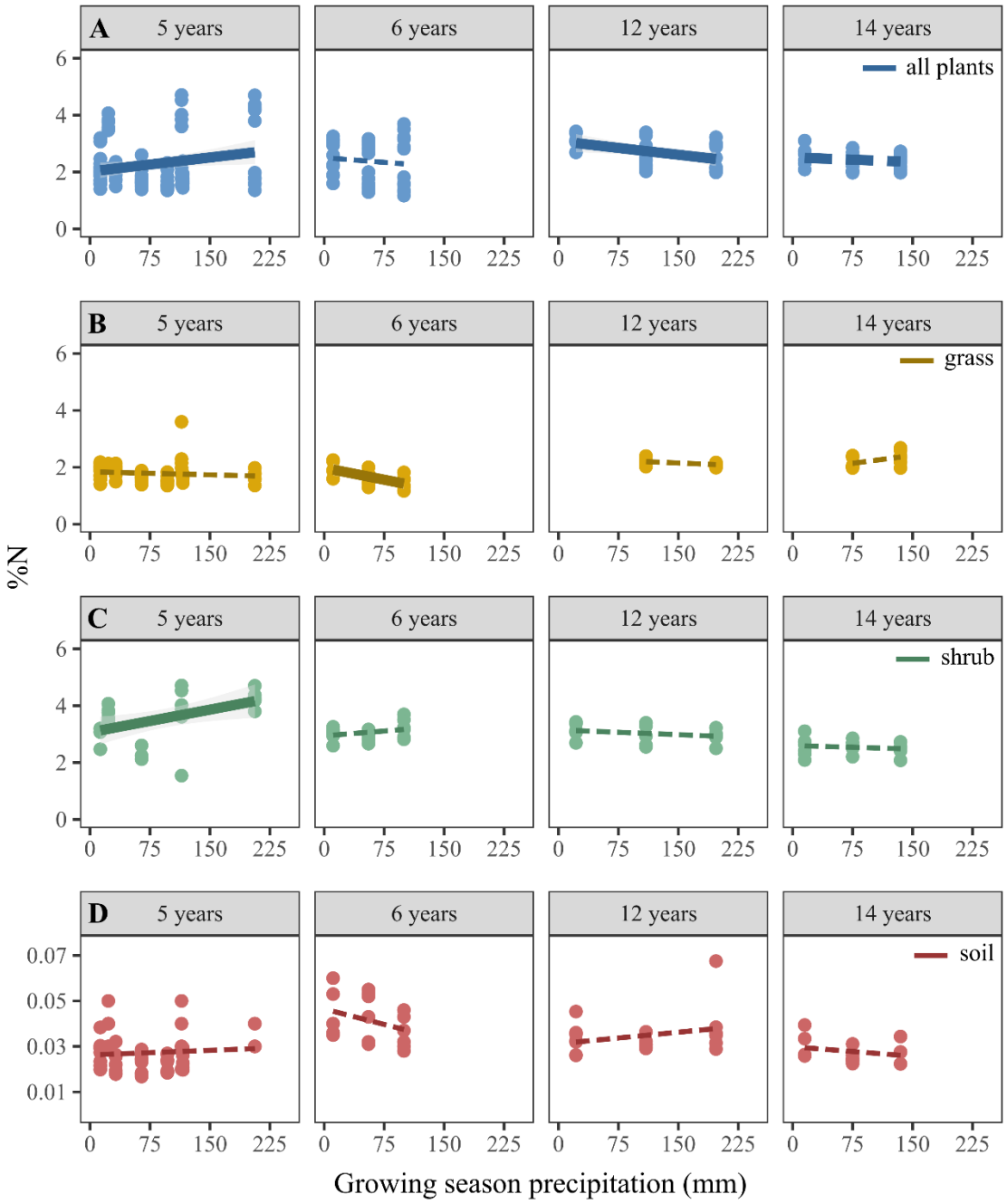

Figure S4.2. Temporal dynamics of foliar and soil %N and directional shifts in precipitation amount. Time (in years) since onset of the directional rainfall manipulation is displayed at the top of each panel for: A) the plant community, B) *Bouteloua eriopoda*, the dominant grass, C) *Prosopis glandulosa*, the dominant shrub, and D) surface soil (0–10 cm). Solid lines indicate significant explanatory regressions with 95% confidence intervals.

Table S4.1. Rainfall manipulation experiment details at the Jornada Basin LTER. Relevant information about the rainfall manipulation experiments utilized in the temporal analyses of this study are below. The closest meteorological stations, represented by "Rain gauge ID," were utilized to calculate growing season rainfall annually at each experiment.

Experiment name	Rainfall Treatments	Replication (n)	Sample size (N)	Plot size	Rain gauge ID	Plants sampled	Year started	Year sampled	Ambient growing season rainfall (mm)*	Manipulated rainfall range (mm)
LTREB 1	-80% ambient +80%	6	18	2.5 x 2.5 m	YUCCA	*Bouteloua eriopoda, Prosopis glandulosa*	2006	2011	114.55	22.91–206.19
								2012	55.37	11.07–99.67
								2018	109.47	21.89–197.05
								2020	74.93	14.99–134.87
LTREB 2	-80% -50% ambient +50% +80%	8	40	2.5 x 5.0 m	RABBIT	*Bouteloua eriopoda*	2015	2020	64.52	12.90–116.14
DroughtNet	-80% ambient	3	6	2.5 x 2.5 m	RABBIT	*Bouteloua eriopoda, Prosopis glandulosa*	2015	2020	64.52	12.90–64.52

*Precipitation data are available on the Environmental Data Initiative (EDI data package ID knb-lter-jrn.210380001.740)

Table S4.2. Akaike Information Criterion (AIC) for regression comparisons are presented below for all and individual continents. Models that met our criteria had the lowest AIC with ΔAIC > 2, otherwise the most parsimonious model was selected. Selected models are indicated with a bold AIC value.

Continent	Model	Degrees of Freedom	AIC	ΔAIC
All (global)	$\delta^{15}N$ ~ preciptation + temperature + precipitation*temperature	5	12758.21	140.56
	$\delta^{15}N$ ~ preciptation + temperature	4	12821.05	203.4
	$\delta^{15}N$ ~ preciptation	3	13310.46	692.81
	$\delta^{15}N$ ~ temperature	3	13073.22	455.57
	$\delta^{15}N$ ~ ln(preciptation) + temperature + ln(precipitation)*temperature	5	12617.65	0
	$\delta^{15}N$ ~ ln(preciptation) + temperature	4	12625.11	7.46
	$\delta^{15}N$ ~ ln(preciptation)	3	13165.22	547.57
Africa	$\delta^{15}N$ ~ preciptation + temperature + precipitation*temperature	5	1277.546	53.33
	$\delta^{15}N$ ~ ln(preciptation) + temperature + ln(precipitation)*temperature	5	1224.217	0.00
Asia	**$\delta^{15}N$ ~ preciptation + temperature + precipitation*temperature**	5	1312.641	0.00
	$\delta^{15}N$ ~ ln(preciptation) + temperature + ln(precipitation)*temperature	5	1317.93	5.29
Australia	$\delta^{15}N$ ~ preciptation + temperature + precipitation*temperature	5	1146.811	44.49
	$\delta^{15}N$ ~ ln(preciptation) + temperature + ln(precipitation)*temperature	5	1102.318	0.00
Europe	**$\delta^{15}N$ ~ preciptation + temperature + precipitation*temperature**	5	497.0469	0.00
	$\delta^{15}N$ ~ ln(preciptation) + temperature + ln(precipitation)*temperature	5	498.5546	1.51
N. America	$\delta^{15}N$ ~ preciptation + temperature + precipitation*temperature	5	7478.869	12.37
	$\delta^{15}N$ ~ ln(preciptation) + temperature + ln(precipitation)*temperature	5	7466.496	0.00
S. America	**$\delta^{15}N$ ~ preciptation + temperature + precipitation*temperature**	5	701.493	0.00
	$\delta^{15}N$ ~ ln(preciptation) + temperature + ln(precipitation)*temperature	5	703.1994	1.71

Table S4.3. Relationship between mean annual precipitation and foliar $\delta^{15}N$ across six continents. The table details output for multiple linear regressions, selected using AIC. Significant regressions are indicated by model fits with $p < 0.05$.

Continent	Intercept	Variable	Slope	*p*-value	F-statistic	Degrees of Freedom	Adjusted R^2
All (global)	14.74	ln(Preciptiation)	-2.59	< **0.001**	301.90	2452	0.27
		Temperature	0.0047	0.94			
		log(Precip)*Temp	0.028	**0.0021**			
Africa	36.86	ln(Precipitation)	-6.06	< **0.001**	35.14	256	0.28
		Temperature	-1.14	**0.028**			
		ln(Precip)*Temp	0.21	**0.0083**			
Asia	44.78	Precipitation	-0.0098	< **0.001**	47.11	262	0.34
		Temperature	-0.19	< **0.001**			
		Precip*Temp	0.00040	< **0.001**			
Australia	28.50	ln(Precipitation)	-4.49	< **0.001**	73.56	224	0.49
		Temperature	-0.20	0.52			
		ln(Precip)*Temp	0.041	0.37			
Europe	-0.24	Precipitation	-0.0019	0.13	5.13	96	0.11
		Temperature	-0.36	< **0.001**			
		Precip*Temp	0.00043	**0.026**			
N. America	7.62	ln(Precipitation)	-1.55	< **0.001**	95.92	1454	0.16
		Temperature	0.63	< **0.001**			
		ln(Precip)*Temp	-0.056	**0.004**			
S. America	15.71	Precipitation	-0.0036	<**0.001**	14.7	140	0.22
		Temperature	-0.10	0.054			
		Precip*Temp	0.0001	**0.017**			

Table S4.4. Effect of ambient precipitation on plant community N availability. Output for mixed linear effects of precipitation on plant community foliar $\delta^{15}N$. Fixed effects estimates whose confidence intervals (CI) do not overlap with zero indicate a significant effect.

Predictors	**Estimates**	**Confidence Interval**	***p*-value**
(Intercept)	-0.72	-1.77 – 0.34	0.18
Precipitation	0.02	0.01 – 0.04	**<0.001**
Random Effects			
σ^2	1.37		
$\tau_{00\ plot:experiment}$	0		
$\tau_{00\ year\ collected}$	0		
$\tau_{00\ experiment}$	0		
N_{plot}	17		
$N_{experiment}$	3		
$N_{year\ collected}$	4		
Observations	66		
Marginal R^2 / Conditional R^2	0.18 / NA		

Table S4.5. Effect of ambient precipitation on dominant grass N availability. Output for mixed linear effects of precipitation on dominant grass (*Bouteloua eriopoda*) foliar $\delta^{15}N$. Fixed effects estimates whose confidence intervals (CI) do not overlap with zero indicate a significant effect.

Predictors	**Estimates**	**Confidence Interval**	***p*-value**
(Intercept)	-1.65	-3.52 – 0.23	0.08
Precipitation	0.02	0.00 – 0.05	**0.02**
Random Effects			
σ^2	0.46		
$\tau_{00\ plot:experiment}$	0.1		
$\tau_{00\ year\ collected}$	0.22		
$\tau_{00\ experiment}$	0		
N_{plot}	17		
$N_{experiment}$	3		
$N_{year\ collected}$	4		
Observations	34		
Marginal R^2 / Conditional R^2	0.42 / NA		

Table S4.6. Effect of ambient precipitation on dominant shrub N availability. Output for mixed linear effects of precipitation on dominant shrub (*Prosopis glandulosa*) foliar $\delta^{15}N$. Fixed effects estimates whose confidence intervals (CI) do not overlap with zero indicate a significant effect.

Predictors	**Estimates**	**Confidence Interval**	***p*-value**
(Intercept)	0.55	-1.18 – 2.27	0.52
Precipitation	0.01	0.00 – 0.02	0.13
Random Effects			
σ^2	0.59		
$\tau_{00\ plot:experiment}$	0.31		
$\tau_{00\ year\ collected}$	0		
$\tau_{00\ experiment}$	0.72		
N_{plot}	9		
$N_{experiment}$	2		
$N_{year\ collected}$	4		
Observations	27		
Marginal R^2 / Conditional R^2	0.09 / NA		

Table S4.7. Effects of ambient precipitation on soil N availability. Output for mixed linear effects of precipitation on surface soil (0-10 cm) $\delta^{15}N$. Fixed effects estimates whose confidence intervals (CI) do not overlap with zero indicate a significant effect.

Predictors	**Estimates**	**Confidence Interval**	***p* -value**
(Intercept)	4.14	-0.10 – 8.39	0.06
Precipitation	0.03	-0.02 – 0.07	0.24
Random Effects			
σ^2	0.54		
$\tau_{00\ plot:experiment}$	0.04		
$\tau_{00\ year\ collected}$	1.99		
$\tau_{00\ experiment}$	0		
N_{plot}	17		
$N_{experiment}$	3		
$N_{year\ collected}$	4		
Observations	35		
Marginal R^2 / Conditional R^2	0.43 / NA		

Table S4.8. Effects of precipitation extremes on ecosystem N availability through time. Output for linear regressions of precipitation on plant community, dominant grass (*Bouteloua eriopoda*), dominant shrub (*Prosopis glandulosa*), and surface soil (0-10 cm) $\delta^{15}N$. The primary result of focus is the change in slope through time. Significant regressions are indicated by model fits with $p < 0.05$.

Group	Time (years)	Intercept	Slope	F-statistic	Degrees of Freedom	*p*-value	Adjusted R^2
Plant community	5	0.65	0.0056	9.41	87	**<0.05**	0.09
	6	0.29	0.0054	0.0007	33	0.52	-0.02
	12	1.85	0.0000	0.0007	32	0.98	-0.03
	14	2.00	-0.0100	5.31	37	**<0.05**	0.10
Dominant grass (*Bouteloua eriopoda*)	5	0.60	0.0022	1.44	63	0.24	0.01
	6	-0.86	-0.0008	0.03	15	0.86	-0.06
	12	-0.58	0.0080	9.39	12	**<0.05**	0.39
	14	1.24	-0.0117	2.52	14	0.14	0.09
Dominant shrub (*Prosopis glandulosa*)	5	1.29	0.0081	6.76	22	**<0.05**	0.20
	6	1.23	0.0138	5.03	16	**<0.05**	0.19
	12	2.06	0.0061	5.88	18	**<0.05**	0.20
	14	1.87	0.0012	0.13	21	0.72	-0.04
Soil (0–10 cm)	5	4.58	0.0131	13.55	65	**<0.05**	0.16
	6	6.77	0.0078	0.48	16	0.50	-0.03
	12	5.72	-0.0020	1.04	24	0.32	0.00
	14	5.60	-0.0053	4.84	23	**<0.05**	0.14

Table S4.9. Output for linear regressions relating the change in temporal slopes of $\delta^{15}N$ versus precipitation to duration of rainfall manipulation experiments for the plant community, the dominant grass (*Bouteloua eriopoda*), dominant shrub (*Prosopis glandulosa*), and surface soil (0-10 cm). Significant regressions are indicated by $p < 0.05$.

Group	Intercept	Slope	F-statistic	Degrees of Freedom	*p* -value	Adjusted R^2
Plant community	0.013	-0.0013	10.21	2	0.09	0.75
Dominant grass (*Bouteloua eriopoda*)	0.0055	-0.00066	0.42	2	0.58	0.58
Dominant shrub (*Prosopis glandulosa*)	0.017	-0.0010	4.56	2	0.17	0.54
Soil (0–10 cm)	0.020	-0.0016	25.04	2	**0.038**	0.89

CHAPTER 5

CONCLUSIONS

Research objective 1 of my dissertation was to determine the relative contribution of precipitation versus temperature on plant functional type phenology, which I addressed in Chapter 2. I analyzed phenological patterns of two plant functional types at the Jornada Basin LTER, the dominant grass and the dominant shrub, over 7 years at the plot-scale within a long-term rainfall manipulation experiment. I found that *Bouteloua eriopoda,* the dominant grass, was more sensitive to changes in precipitation compared to temperature, especially at the start of the season. Directional decreases in precipitation resulted in delayed grass greenup and accelerated senescence, shortening growing season length significantly. Deep-rooted *Prosopis glandulosa*, on the other hand, was insensitive to either precipitation or temperature variability. This 7-year snapshot of the phenology of dominant grass and shrub species of the Chihuahuan semiarid ecosystem provides impetus for investigating temperature-precipitation controls on phenology at larger spatial and temporal scales across global drylands. Shortening of herbaceous growing season length will lead to decreases in ANPP in grass-dominated ecosystems, with feedbacks that will affect C and water balances. Because drylands are so ubiquitous, phenological studies will benefit from a greater understanding of how water-limited systems respond to precipitation.

Research objective 2 was to determine how long-term, directional changes to precipitation amount and N availability affect soil N stocks within bulk soil and among two density soil fractions, which I addressed in Chapter 3. Further, I aimed to elucidate

how these N stock dynamics may explain the lack of ANPP response to high N and high-water availability at the Jornada. I found that the *B. eriopoda* ANPP did not respond to N amendments even when water limitation was reduced. When I examined the foliar stable N isotope signature, I confirmed that plants from N amendment plots appear to uptake the fertilizer, but they do not alter N productivity under any N or precipitation conditions. To investigate if plants switch N sources between soil fractions under low and high N availability, I assessed bulk soil N, POM-N, and MAOM N content. In bulk soil and both density fractions, N amendments increased overall %N. When I considered the effects of precipitation, bulk soil N and POM-N dynamics remained surprisingly stable under directional precipitation changes under both low and high N conditions. I concluded that N is not yet limiting at our study site because plants derive N from multiple soil pools, and N leakiness is low when water availability is high. Conversely, plants in high-N conditions likely derive a majority of their N from N fertilizer, and N originating from the soil pools may be lost under high water availability in gaseous forms.

Research objective 3 was to assess the long-term patterns in ecosystem acclimation of the N cycle to directional changes in precipitation amount, which was addressed in Chapter 4. I integrated above and belowground processes using natural abundances of stable nitrogen isotopes for plants and soils; I found that N availability decreased with annual precipitation in space across continents, but it posed initially increasing trends in response to rainfall amount at the Jornada that eventually decreased after 14 years. I concluded that mechanisms for the acclimation process are associated with differential lags to changes in precipitation between plants and microorganisms.

Furthermore, I estimated the fastest rates of N cycle acclimation because rainfall was manipulated to be a directional and extreme climate driver. Climate change will bring directional changes and increased variability in precipitation with extreme droughts and deluges of novel frequency and magnitude. Enhanced inter annual precipitation variability may slow down acclimation. Thus, rates of acclimation under combined directional changes in precipitation and enhanced variability may be slower than those reported in this dissertation. Nonetheless, the concepts presented here identify critical assumptions of assessing global trends based on temporally versus spatially explicit approaches. Ignoring acclimation by predicting future N availability using spatial models would have overestimated N availability and C sequestration under climate change.

This dissertation represents a multi-faceted approach to understanding long-term extremes on dryland ecosystem processes, ranging from plant phenology to nutrient cycling. Chapter 2 unravels causal mechanisms between environmental drivers and plant phenology responses at a unique spatiotemporal scale. Implementation of phenocams within long-term climate change experiments will continue to refine our understanding of climate relationships to plant growth, which the potential to improve climate models that rely on accurate climate–process relationships and outcomes. Chapter 3 took another approach to understand the effects of precipitation on ecosystem functioning by examining soil density fraction N dynamics. As ecosystem C sequestration becomes an increasingly important and interesting topic, my research contributes another perspective on mechanisms that may stabilize or destabilize N associated with the soil mineral fraction, which will feedback to C dynamics undoubtedly. Fine-scale isotope tracing

between soil fractions and plant tissues would help elucidate precisely what N sources plant utilize under different water availability conditions. Finally, I integrated above and belowground ecosystem responses to precipitation extremes in Chapter 4. This paper uniquely approaches the concept of acclimation through the lens of N cycling and importantly identifies discrepancies between spatial and temporal models.

Themes that emerged across my dissertation chapters include the differential responses of dominant vegetation. For example, grasslands appear more sensitive to changes in precipitation (Chapter 2) and would be the fastest to acclimate and ecosystems dominated by long-lived woody vegetation would be the slowest (Chapter 4). Yet, my research also demonstrated that drylands exhibit resiliency in certain processes. Soil N stocks remain relatively stable overall, and plants continue to show non-detectable N limitation. As bias shifts away from deserts perceived as barren wastelands, this dissertation creatively integrates these important ecosystems into revised ecological and climate change frameworks.

REFERENCES

Aber, J., W. McDowell, K. Nadelhoffer, A. Magill, G. Berntson, M. Kamakea, S. McNulty, W. Currie, L. Rustad, and I. Fernandez. 1998. “Nitrogen saturation in temperate forest ecosystems.” *BioScience* 48:921–934.

Adole, T., J. Dash, V. Rodriguez-Galiano, and P. M. Atkinson. 2019. “Photoperiod controls vegetation phenology across Africa.” *Communications Biology* 2:391.

Ahlström, A., M. R. Raupach, G. Schurgers, B. Smith, A. Arneth, M. Jung, M. Reichstein, J. G. Canadell, P. Friedlingstein, A. K. Jain, E. Kato, B. Poulter, S. Sitch, B. D. Stocker, N. Viovy, Y. P. Wang, A. Wiltshire, S. Zaehle, and N. Zeng. 2015. “The dominant role of semi-arid ecosystems in the trend and variability of the land CO_2 sink.” *Science* 348:895–899.

Amundson, R., A. T. Austin, E. a. G. Schuur, K. Yoo, V. Matzek, C. Kendall, A. Uebersax, D. Brenner, and W. T. Baisden. 2003. “Global patterns of the isotopic composition of soil and plant nitrogen.” *Global Biogeochemical Cycles* 17.

Atlas, U. 1992. *World Atlas of Desertification*, Vol. 80. Kent: UNEP and E. Arnold Ltd.

Ault, T. R. 2020. “On the essentials of drought in a changing climate.” *Science* 368:256–260.

Austin, A. T., L. Yahdjian, J. M. Stark, J. Belnap, A. Porporato, U. Norton, D. A. Ravetta, and S. M. Schaeffer. 2004. “Water pulses and biogeochemical cycles in arid and semiarid ecosystems.” *Oecologia* 141:221–235.

Bandieri, L. M., R. J. Fernández, and A. J. Bisigato. 2020. “Risks of neglecting phenology when assessing climatic controls of primary production.” *Ecosystems* 23:164–174.

Bates, D., M. Maechler, B. Bolker, and S. Walker. 2014. “Lme4: Linear mixed-effects models using Eigen and S4.” R Package Version 1:1–23.

Beatley, J. C. 1974. “Phenological events and their environmental triggers in Mojave Desert ecosystems.” *Ecology* 55:856–863.

Berendse, F., and R. Aerts. 1987. “Nitrogen-use-efficiency: A biologically meaningful definition?” *Functional Ecology* 1:293–296.

Berg, A., and K. A. McColl. 2021. “No projected global drylands expansion under greenhouse warming.” *Nature Climate Change* 11:1–7.

Bingham, A. H., and M. F. Cotrufo. 2016. “Organic nitrogen storage in mineral soil: Implications for policy and management.” *Science of the Total Environment* 551–552:116–126.

Bolan, N. S., M. J. Hedley, and R. E. White. 1991. “Processes of soil acidification during nitrogen cycling with emphasis on legume based pastures.” *Plant and Soil* 134:53–63.

Bolker, B. M., M. E. Brooks, C. J. Clark, S. W. Geange, J. R. Poulsen, M. H. H. Stevens, and J.-S. S. White. 2009. “Generalized linear mixed models: a practical guide for ecology and evolution.” *Trends in Ecology and Evolution* 24:127–135.

Briske, D. D., editor. 2017. *Rangeland Systems: Processes, Management and Challenges*. New York, NY: Springer International Publishing.

Bolker, B. M., M. E. Brooks, C. J. Clark, S. W. Geange, J. R. Poulsen, M. H. H. Stevens, and J.-S. S. White. 2009. “Generalized linear mixed models: a practical guide for ecology and evolution.” *Trends in Ecology and Evolution* 24:127–135.

Bosshard, C., E. Frossard, D. Dubois, P. Mäder, I. Manolov, and A. Oberson. 2008. “Incorporation of nitrogen-15-labeled amendments into physically separated soil organic matter fractions.” *Soil Science Society of America Journal* 72:949–959.

Bowden, W. B. 1986. “Gaseous nitrogen emmissions from undisturbed terrestrial ecosystems: An assessment of their impacts on local and global nitrogen budgets.” *Biogeochemistry* 2:249–279.

Browning, D. M., J. W. Karl, D. Morin, A. D. Richardson, and C. E. Tweedie. 2017. “Phenocams bridge the gap between field and satellite observations in an arid grassland ecosystem.” *Remote Sensing* 9:1071.

Caldararu, S., T. Thum, L. Yu, M. Kern, R. Nair, and S. Zaehle. 2022. “Long-term ecosystem nitrogen limitation from foliar $\delta^{15}N$ data and a land surface model.” *Global Change Biology* 28:493–508.

Chapin, F. S. 1980. “The mineral nutrition of wild plants.” *Annual Review of Ecology and Systematics* 11:233–260.

Churkina, G., and S. W. Running. 1998. “Contrasting climatic controls on the estimated productivity of global terrestrial biomes.” *Ecosystems* 1:206–215.

Cleland, E., I. Chuine, A. Menzel, H. Mooney, and M. Schwartz. 2007. “Shifting plant phenology in response to global change.” *Trends in Ecology and Evolution* 22:357–365.

Cleland, E. E., J. M. Allen, T. M. Crimmins, J. A. Dunne, S. Pau, S. E. Travers, E. S. Zavaleta, and E. M. Wolkovich. 2012. “Phenological tracking enables positive species responses to climate change.” *Ecology* 93:1765–1771.

Collins, C. G., S. C. Elmendorf, R. D. Hollister, G. H. R. Henry, K. Clark, A. D. Bjorkman, I. H. Myers-Smith, J. S. Prevéy, I. W. Ashton, J. J. Assmann, J. M. Alatalo, M. Carbognani, C. Chisholm, E. J. Cooper, C. Forrester, I. S. Jónsdóttir, K. Klanderud, C. W. Kopp, C. Livensperger, M. Mauritz, J. L. May, U. Molau, S. F. Oberbauer, E. Ogburn, Z. A. Panchen, A. Petraglia, E. Post, C. Rixen, H. Rodenhizer, E. A. G. Schuur, P. Semenchuk, J. G. Smith, H. Steltzer, Ø. Totland, M. D. Walker, J. M. Welker, and K. N. Suding. 2021. “Experimental warming differentially affects vegetative and reproductive phenology of tundra plants.” *Nature Communications* 12:3442.

Collins, S. L., R. L. Sinsabaugh, C. Crenshaw, L. Green, A. Porras-Alfaro, M. Stursova, and L. H. Zeglin. 2008. “Pulse dynamics and microbial processes in aridland ecosystems: Pulse dynamics in aridland soils.” *Journal of Ecology* 96:413–420.

Collins, S. L., S. R. Carpenter, S. M. Swinton, D. E. Orenstein, D. L. Childers, T. L. Gragson, N. B. Grimm, J. M. Grove, S. L. Harlan, J. P. Kaye, A. K. Knapp, G. P. Kofinas, J. J. Magnuson, W. H. McDowell, J. M. Melack, L. A. Ogden, G. P. Robertson, M. D. Smith, and A. C. Whitmer. 2011. “An integrated conceptual framework for long-term social–ecological research.” *Frontiers in Ecology and the Environment* 9:351–357.

Collins, S. L., J. Belnap, N. B. Grimm, J. A. Rudgers, C. N. Dahm, P. D’Odorico, M. Litvak, D. O. Natvig, D. C. Peters, W. T. Pockman, R. L. Sinsabaugh, and B. O. Wolf. 2014. “A multiscale, hierarchical model of pulse dynamics in arid-land ecosystems.” *Annual Review of Ecology, Evolution, and Systematics* 45:397–419.

Collins, S. L., L. M. Ladwig, M. D. Petrie, S. K. Jones, J. M. Mulhouse, J. R. Thibault, and W. T. Pockman. 2017. “Press-pulse interactions: Effects of warming, N deposition, altered winter precipitation, and fire on desert grassland community structure and dynamics.” *Global Change Biology* 23:1095–1108.

Cook, B. I., E. M. Wolkovich, T. J. Davies, T. R. Ault, J. L. Betancourt, J. M. Allen, K. Bolmgren, E. E. Cleland, T. M. Crimmins, N. J. B. Kraft, L. T. Lancaster, S. J. Mazer, G. J. McCabe, B. J. McGill, C. Parmesan, S. Pau, J. Regetz, N. Salamin, M. D. Schwartz, and S. E. Travers. 2012. “Sensitivity of spring phenology to warming across temporal and spatial climate gradients in two independent databases.” *Ecosystems* 15:1283–1294.

Cook, C. S., B. R. Erkkila, S. Chakraborty, B. J. Tipple, T. E. Cerling, and J. R. Ehleringer. 2017. *Stable Isotope Biogeochemistry and Ecology: Laboratory Manual*. University of Utah.

Craine, J. M., A. J. Elmore, L. Wang, J. Aranibar, M. Bauters, P. Boeckx, B. E. Crowley, M. A. Dawes, S. Delzon, A. Fajardo, Y. Fang, L. Fujiyoshi, A. Gray, R. Guerrieri, M. J. Gundale, D. J. Hawke, P. Hietz, M. Jonard, E. Kearsley, T. Kenzo, M. Makarov, S. Marañón-Jiménez, T. P. McGlynn, B. E. McNeil, S. G. Mosher, D. M. Nelson, P. L. Peri, J. C. Roggy, R. Sanders-DeMott, M. Song, P. Szpak, P. H. Templer, D. Van der Colff, C. Werner, X. Xu, Y. Yang, G. Yu, and K. Zmudczyńska-Skarbek. 2018. "Isotopic evidence for oligotrophication of terrestrial ecosystems." *Nature Ecology and Evolution* 2:1735–1744.

Craine, J. M., A. J. Elmore, L. Wang, J. Aranibar, M. Bauters, P. Boeckx, B. E. Crowley, M. A. Dawes, S. Delzon, A. Fajardo, Y. Fang, L. Fujiyoshi, A. Gray, R. Guerrieri, M. J. Gundale, D. J. Hawke, P. Hietz, M. Jonard, E. Kearsley, T. Kenzo, M. Makarov, S. Marañón-Jiménez, T. P. McGlynn, B. E. McNeil, S. G. Mosher, D. M. Nelson, P. L. Peri, J. C. Roggy, R. Sanders-DeMott, M. Song, P. Szpak, P. H. Templer, D. Van Der Colff, C. Werner, X. Xu, Y. Yang, G. Yu, and K. Zmudczyńska-Skarbek. 2019. "Data from: Isotopic evidence for oligotrophication of terrestrial ecosystems." Dryad. https://doi.org/10.5061/dryad.v2k2607.

Crow, S. E., C. W. Swanston, K. Lajtha, J. R. Brooks, and H. Keirstead. 2007. "Density fractionation of forest soils: methodological questions and interpretation of incubation results and turnover time in an ecosystem context." *Biogeochemistry* 85:69–90.

Currier, C. M., and O. E. Sala. 2022. "Precipitation versus temperature as phenology controls in drylands." *Ecology*:e3793.

Daly, A. B., A. Jilling, T. M. Bowles, R. W. Buchkowski, S. D. Frey, C. M. Kallenbach, M. Keiluweit, M. Mooshammer, J. P. Schimel, and A. S. Grandy. 2021. "A holistic framework integrating plant-microbe-mineral regulation of soil bioavailable nitrogen." *Biogeochemistry* 154:211–229.

Duniway, M. C., M. D. Petrie, D. P. C. Peters, J. P. Anderson, K. Crossland, and J. E. Herrick. 2018. "Soil water dynamics at 15 locations distributed across a desert landscape: insights from a 27-yr dataset." *Ecosphere* 9:e02335.

Epstein, H. E., W. K. Lauenroth, I. C. Burke, and D. P. Coffin. 1996. "Ecological responses of dominant grasses along two climatic gradients in the Great Plains of the United States." *Journal of Vegetation Science* 7:777–788.

Esch, E. H., D. A. Lipson, and E. E. Cleland. 2019. "Invasion and drought alter phenological sensitivity and synergistically lower ecosystem production." *Ecology* 100:e02802.

F. A. O. 2019. "Forests and Land Use in Drylands: The First Global Assessment—Full Report." *FAO Forestry Paper* 184.

Felton, A. J., A. K. Knapp, and M. D. Smith. 2020. “Precipitation-productivity relationships and the duration of precipitation anomalies: An underappreciated dimension of climate change.” *Global Change Biology* 27:1127–1140.

Felton, A. J., R. K. Shriver, M. Stemkovski, J. B. Bradford, K. N. Suding, and P. B. Adler. 2022. “Climate disequilibrium dominates uncertainty in long-term projections of primary productivity.” *Ecology Letters* 25:2688–2698.

Field, C. B., M. J. Behrenfeld, J. T. Randerson, and P. Falkowski. 1998. “Primary production of the biosphere: Integrating terrestrial and oceanic components.” *Science* 281:237–240.

Filippa, G., E. Cremonese, M. Migliavacca, M. Galvagno, M. Forkel, L. Wingate, E. Tomelleri, U. Morra di Cella, and A. D. Richardson. 2016. “Phenopix: A R package for image-based vegetation phenology.” *Agricultural and Forest Meteorology* 220:141–150.

Finger-Higgens, R., T. B. B. Bishop, J. Belnap, E. L. Geiger, E. E. Grote, D. L. Hoover, S. Reed, and M. C. Duniway. 2023. “Droughting a megadrought: Ecological consequences of a decade of experimental drought atop aridification on the Colorado Plateau.” *Global Change Biology* n/a.

Garcia-Pichel, F., and O. E. Sala. 2022. “Expanding the pulse-reserve paradigm to microorganisms on the basis of differential reserve management strategies.” *BioScience* 72:638–650.

Gherardi, L. A., and O. E. Sala. 2013. “Automated rainfall manipulation system: a reliable and inexpensive tool for ecologists.” *Ecosphere* 4:art18.

Gherardi, L. A., and O. E. Sala. 2019. “Effect of inter-annual precipitation variability on dryland productivity: A global synthesis.” *Global Change Biology* 25:269–276.

Gibbens, R. P., and J. M. Lenz. 2001. “Root systems of some Chihuahuan Desert plants.” *Journal of Arid Environments* 49:221–263.

Gile, L. H. 1981. “Soils and geomorphology in the basin and range area of southern New Mexico: Guidebook to the Desert Project, New Mexico.” *Bureau of Mines and Mineral Resources Memoir* 39:222.

Goulden, M. L., J. W. Munger, S.-M. Fan, B. C. Daube, and S. C. Wofsy. 1996. “Exchange of carbon dioxide by a deciduous forest: Response to interannual climate variability.” *Science* 271:1576–1578.

Grime, J. P. 1973. “Competitive exclusion in herbaceous vegetation.” *Nature* 242:344–347.

Gu, L., W. M. Post, D. D. Baldocchi, T. A. Black, A. E. Suyker, S. B. Verma, T. Vesala, and S. C. Wofsy. 2009. "Characterizing the seasonal dynamics of plant community photosynthesis across a range of vegetation types." In *Phenology of Ecosystem Processes*, edited by A. Noormets, 35–58 . New York, NY: Springer.

Handley, L. L., A. T. Austin, G. R. Stewart, D. Robinson, C. M. Scrimgeour, J. A. Raven, T. H. E. Heaton, and S. Schmidt. 1999. "The ^{15}N natural abundance (δ15N) of ecosystem samples reflects measures of water availability." *Functional Plant Biology* 26:185.

Havstad, K. M., L. F. Huenneke, and W. H. Schlesinger, editors. 2006. *Structure and Function of a Chihuahuan Desert Ecosystem: The Jornada Basin Long-Term Ecological Research Site*. New York, NY: Oxford University Press.

Homyak, P. M., J. O. Sickman, A. E. Miller, J. M. Melack, T. Meixner, and J. P. Schimel. 2014. "Assessing nitrogen-saturation in a seasonally dry chaparral watershed: Limitations of traditional indicators of N-saturation." *Ecosystems* 17:1286–1305.

Homyak, P. M., S. D. Allison, T. E. Huxman, M. L. Goulden, and K. K. Treseder. 2017. "Effects of drought manipulation on soil nitrogen cycling: A meta-analysis." *Journal of Geophysical Research: Biogeosciences* 122:3260–3272.

Homyak, P. M., E. W. Slessarev, S. Hagerty, A. C. Greene, K. Marchus, K. Dowdy, S. Iverson, and J. P. Schimel. 2021. "Amino acids dominate diffusive nitrogen fluxes across soil depths in acidic tussock tundra." *New Phytologist* 231:2162–2173.

Hooper, D. U., and L. Johnson. 1999. "Nitrogen limitation in dryland ecosystems: Responses to geographical and temporal variation in precipitation." *Biogeochemistry* 46:47.

Hu, H.-W., P. Trivedi, J.-Z. He, and B. K. Singh. 2017. "Microbial nitrous oxide emissions in dryland ecosystems: mechanisms, microbiome and mitigation." *Environmental Microbiology* 19:4808–4828.

Huang, J., H. Yu, X. Guan, G. Wang, and R. Guo. 2016. "Accelerated dryland expansion under climate change." *Nature Climate Change* 6:166–171.

Huenneke, L. F., J. P. Anderson, M. Remmenga, and W. H. Schlesinger. 2002. "Desertification alters patterns of aboveground net primary production in Chihuahuan ecosystems." *Global Change Biology* 8:247–264.

Ibrahim, S., J. Kaduk, K. Tansey, H. Balzter, and U. M. Lawal. 2021. "Detecting phenological changes in plant functional types over West African savannah dominated landscape." *International Journal Of Remote Sensing* 42:567–594.

Inselsbacher, E., O. A. Oyewole, and T. Näsholm. 2014. “Early season dynamics of soil nitrogen fluxes in fertilized and unfertilized boreal forests.” *Soil Biology and Biochemistry* 74:167–176.

Jackson, R. B., J. Canadell, J. R. Ehleringer, H. A. Mooney, O. E. Sala, and E. D. Schulze. 1996. “A global analysis of root distributions for terrestrial biomes.” *Oecologia* 108:389–411.

Jackson, R. B., M. J. Lechowicz, X. Li, and H. A. Mooney. 2001. “Phenology, growth, and allocation in global terrestrial productivity.” In *Terrestrial Global Productivity*, edited by J. Roy, B. Saugier, and H. A. Mooney, 61–82. Cambridge, MA: Academic Press.

Jackson, S. D. 2009. “Plant responses to photoperiod.” *New Phytologist* 181:517–531.

Jilling, A., M. Keiluweit, A. R. Contosta, S. Frey, J. Schimel, J. Schnecker, R. G. Smith, L. Tiemann, and A. S. Grandy. 2018. “Minerals in the rhizosphere: Overlooked mediators of soil nitrogen availability to plants and microbes.” *Biogeochemistry* 139:103–122.

Keller, A. B., E. T. Borer, S. L. Collins, L. C. DeLancey, P. A. Fay, K. S. Hofmockel, A. D. B. Leakey, M. A. Mayes, E. W. Seabloom, C. A. Walter, Y. Wang, Q. Zhao, and S. E. Hobbie. 2022. “Soil carbon stocks in temperate grasslands differ strongly across sites but are insensitive to decade-long fertilization.” *Global Change Biology* 28:1659–1677.

Kikuzawa, K. 1991. “A cost-benefit analysis of leaf habit and leaf longevity of trees and their geographical pattern.” *The American Naturalist* 138:1250–1263.

Kikuzawa, K. 1995. “Leaf phenology as an optimal strategy for carbon gain in plants.” *Canadian Journal of Botany* 73:158–163.

Kleber, M., P. S. Nico, A. Plante, T. Filley, M. Kramer, C. Swanston, and P. Sollins. 2011. “Old and stable soil organic matter is not necessarily chemically recalcitrant: Implications for modeling concepts and temperature sensitivity.” *Global Change Biology* 17:1097–1107.

Kleber, M., K. Eusterhues, M. Keiluweit, C. Mikutta, R. Mikutta, and P. S. Nico. 2015. “Mineral–organic associations: Formation, properties, and relevance in soil environments.” In *Advances in Agronomy*, edited by D. L. Sparks, 1–140. San Diego, CA: Elsevier.

Klosterman, S. T., K. Hufkens, J. M. Gray, E. Melaas, O. Sonnentag, I. Lavine, L. Mitchell, R. Norman, M. A. Friedl, and A. D. Richardson. 2014. “Evaluating remote sensing of deciduous forest phenology at multiple spatial scales using PhenoCam imagery.” *Biogeosciences* 11:4305–4320.

Kraft, N. J. B., O. Godoy, and J. M. Levine. 2015. “Plant functional traits and the multidimensional nature of species coexistence.” *Proceedings of the National Academy of Sciences* 112:797–802.

Kramer, M. G., K. Lajtha, G. Thomas, and P. Sollins. 2009. “Contamination effects on soil density fractions from high N or C content sodium polytungstate.” *Biogeochemistry* 92:177–181.

Kramer, K., I. Leinonen, and D. Loustau. 2000. “The importance of phenology for the evaluation of impact of climate change on growth of boreal, temperate and Mediterranean forests ecosystems: An overview.” *International Journal of Biometeorology* 44:67–75.

Lal, R. 2004. “Carbon sequestration in dryland ecosystems.” *Environmental Management* 33:528–544.

Lauenroth, W. K., O. E. Sala, D. G. Milchunas, and R. W. Lathrop. 1987. “Root dynamics of Bouteloua gracilis during short-term recovery from drought.” *Functional Ecology* 1:117–124.

Lauenroth, W. K., and O. E. Sala. 1992. “Long-term forage production of North American shortgrass steppe.” *Ecological Applications* 2:397–403.

LeBauer, D. S., and K. K. Treseder. 2008. “Nitrogen limitation of net primary productivity in terrestrial ecosystems is globally distributed.” *Ecology* 89:371–379.

Liao, J. D., T. W. Boutton, and J. D. Jastrow. 2006. “Storage and dynamics of carbon and nitrogen in soil physical fractions following woody plant invasion of grassland.” *Soil Biology and Biochemistry* 38:3184–3196.

Liu, D., W. Zhu, X. Wang, Y. Pan, C. Wang, D. Xi, E. Bai, Y. Wang, X. Han, and Y. Fang. 2017. “Abiotic versus biotic controls on soil nitrogen cycling in drylands along a 3200 km transect.” *Biogeosciences* 14:989–1001.

Lovett, G. M., and C. L. Goodale. 2011. “A new conceptual model of nitrogen saturation based on experimental nitrogen addition to an oak forest.” *Ecosystems* 14:615–631.

MacBean, N., R. L. Scott, J. A. Biederman, P. Peylin, T. Kolb, M. E. Litvak, P. Krishnan, T. P. Meyers, V. K. Arora, V. Bastrikov, D. Goll, D. L. Lombardozzi, J. E. M. S. Nabel, J. Pongratz, S. Sitch, A. P. Walker, S. Zaehle, and D. J. P. Moore. 2021. “Dynamic global vegetation models underestimate net CO_2 flux mean and inter-annual variability in dryland ecosystems.” *Environmental Research Letters* 16:094023.

Maestre, F. T., J. L. Quero, N. J. Gotelli, A. Escudero, V. Ochoa, M. Delgado-Baquerizo, M. Garcia-Gomez, M. A. Bowker, S. Soliveres, C. Escolar, P. Garcia-Palacios, M. Berdugo, E. Valencia, B. Gozalo, A. Gallardo, L. Aguilera, T. Arredondo, J. Blones, B. Boeken, D. Bran, A. A. Conceicao, O. Cabrera, M. Chaieb, M. Derak, D. J. Eldridge, C. I. Espinosa, A. Florentino, J. Gaitan, M. G. Gatica, W. Ghiloufi, S. Gomez-Gonzalez, J. R. Gutierrez, R. M. Hernandez, X. Huang, E. Huber-Sannwald, M. Jankju, M. Miriti, J. Monerris, R. L. Mau, E. Morici, K. Naseri, A. Ospina, V. Polo, A. Prina, E. Pucheta, D. A. Ramirez-Collantes, R. Romao, M. Tighe, C. Torres-Diaz, J. Val, J. P. Veiga, D. Wang, and E. Zaady. 2012. "Plant species richness and ecosystem multifunctionality in global drylands." *Science* 335:214–218.

Maestre, F. T., B. M. Benito, M. Berdugo, L. Concostrina-Zubiri, M. Delgado-Baquerizo, D. J. Eldridge, E. Guirado, N. Gross, S. Kéfi, and Y. Le Bagousse-Pinguet. 2021. "Biogeography of global drylands." *New Phytologist* 231:540–558.

Mack, M. C., E. A. G. Schuur, M. S. Bret-Harte, G. R. Shaver, and F. S. Chapin. 2004. "Ecosystem carbon storage in arctic tundra reduced by long-term nutrient fertilization." *Nature* 431:440–443.

Marschner, P., and Z. Rengel, editors. 2007. *Nutrient Cycling in Terrestrial Ecosystems*. New York, NY: Springer.

Mason, R. E., J. M. Craine, N. K. Lany, M. Jonard, S. V. Ollinger, P. M. Groffman, R. W. Fulweiler, J. Angerer, Q. D. Read, P. B. Reich, P. H. Templer, and A. J. Elmore. 2022. "Evidence, causes, and consequences of declining nitrogen availability in terrestrial ecosystems." *Science* 376:eabh3767.

McCalley, C. K., and J. P. Sparks. 2009. "Abiotic gas formation drives nitrogen loss from a desert ecosystem." *Science* 326:837–840.

McHugh, T. A., E. M. Morrissey, R. C. Mueller, L. V. Gallegos-Graves, C. R. Kuske, and S. C. Reed. 2017. "Bacterial, fungal, and plant communities exhibit no biomass or compositional response to two years of simulated nitrogen deposition in a semiarid grassland." *Environmental Microbiology* 19:1600–1611.

Medeiros, J. S., and W. T. Pockman. 2014. "Freezing regime and trade-offs with water transport efficiency generate variation in xylem structure across diploid populations of Larrea sp. (Zygophyllaceae)." *American Journal of Botany* 101:598–607.

Monger, H. C. 2006. "Soil development in the Jornada Basin." In *Structure and Function of a Chihuahuan Desert Ecosystem: The Jornada Basin Long-Term Ecological Research Site*, edited by K. M. Havstad, L. F. Huenneke, and W. H. Schlesinger, 81–106. New York, NY: Oxford University Press.

Monger, C., O. E. Sala, M. C. Duniway, H. Goldfus, I. A. Meir, R. M. Poch, H. L. Throop, and E. R. Vivoni. 2015. “Legacy effects in linked ecological–soil–geomorphic systems of drylands.” *Frontiers in Ecology and the Environment* 13:13–19.

Moore, J. C., K. McCann, H. Setälä, and P. C. De Ruiter. 2003. “Top-down is bottom-up: Does predation in the rhizosphere regulate aboveground dynamics?” *Ecology* 84:846–857.

Morellato, L. P. C. 2003. “South America.” in *Phenology: An Integrative Environmental Science*, edited by M. D. Schwartz, 75–92. Dordrecht: Kluwer Academic Press.

Neff, J. C., A. R. Townsend, G. Gleixner, S. J. Lehman, J. Turnbull, and W. D. Bowman. 2002. “Variable effects of nitrogen additions on the stability and turnover of soil carbon.” *Nature* 419:915–917.

Nemani, R. R., C. D. Keeling, H. Hashimoto, W. M. Jolly, S. C. Piper, C. J. Tucker, R. B. Myneni, and S. W. Running. 2003. “Climate-driven increases in global terrestrial net primary production from 1982 to 1999.” *Science* 300:1560–1563.

NEON (National Ecological Observatory Network). 2022. “Plant foliar traits (DP1.10026.001).” https://doi.org/10.48443/kmc7-8g05.

NEON (National Ecological Observatory Network). 2022. “Explore field sites.” https://www.neonscience.org/field-sites/explore-field-sites.

New, M., D. Lister, M. Hulme, and I. Makin. 2002. “A high-resolution data set of surface climate over global land areas.” *Climate Research* 21:1–25.

Noy-Meir, I. 1973. “Desert ecosystems: Environment and producers.” *Annual Review of Ecology and Systematics* 4:25–51.

Occurrence records of Bouteloua eriopoda (Torr.) Torr. 2021. “GBIF Secretariat.” https://www.gbif.org/species/5289847.

Occurrence records of Bouteloua Lag. 2021. “GBIF Secretariat.” https://www.gbif.org/species/7557664.

Occurrence records of Prosopis glandulosa Torr. 2021. “GBIF Secretariat.” https://www.gbif.org/species/5358457.

Occurrence records of Prosopis L. 2021. “GBIF Secretariat.” https://www.gbif.org/species/2970763.

Okin, G. S., O. E. Sala, E. R. Vivoni, J. Zhang, and A. Bhattachan. 2018. “The interactive role of wind and water in functioning of drylands: What does the future hold?” *BioScience* 68:670–677.

Osborne, B. B., B. T. Bestelmeyer, C. M. Currier, P. M. Homyak, H. L. Throop, K. Young, and S. C. Reed. 2022. “The consequences of climate change for dryland biogeochemistry.” *New Phytologist* 236:15–20.

Parmesan, C. 2007. “Influences of species, latitudes and methodologies on estimates of phenological response to global warming.” *Global Change Biology* 13:1860–1872.

Paul, E. A. 2016. “The nature and dynamics of soil organic matter: Plant inputs, microbial transformations, and organic matter stabilization.” *Soil Biology and Biochemistry* 98:109–126.

Peñuelas, J., T. Rutishauser, and I. Filella. 2009. “Phenology feedbacks on climate change.” *Science* 324:887–888.

Petrie, M. D., S. L. Collins, D. S. Gutzler, and D. M. Moore. 2014. “Regional trends and local variability in monsoon precipitation in the northern Chihuahuan Desert, USA.” *Journal of Arid Environments* 103:63–70.

Pörtner, H. O., D. C. Roberts, H. Adams, C. Adler, P. Aldunce, E. Ali, R. A. Begum, R. Betts, R. B. Kerr, and R. Biesbroek, editors. 2022. *Climate Change 2022: Impacts, Adaptation and Vulnerability. Contribution of Working Group II to the Sixth Assessment Report of the Intergovernmental Panel on Climate Change*. Geneva, Switzerland: IPCC.

Poulter, B., D. Frank, P. Ciais, R. B. Myneni, N. Andela, J. Bi, G. Broquet, J. G. Canadell, F. Chevallier, Y. Y. Liu, S. W. Running, S. Sitch, and G. R. van der Werf. 2014. “Contribution of semi-arid ecosystems to interannual variability of the global carbon cycle.” *Nature* 509:600–603.

Prăvălie, R. 2016. “Drylands extent and environmental issues. A global approach.” *Earth-Science Reviews* 161:259–278.

Püspök, J. F., S. Zhao, A. D. Calma, G. L. Vourlitis, S. D. Allison, E. L. Aronson, J. P. Schimel, E. J. Hanan, and P. M. Homyak. 2022. “Effects of experimental nitrogen deposition on soil organic carbon storage in Southern California drylands.” *Global Change Biology* 00:1–20.

R Core Team. 2018. “R: A language and environment for statistical computing.” R Foundation for Statistical Computing, Vienna, Austria. https://www.R-project.org/.

Ramirez, G. A., G. Ramirez, and C. Tweedie. 2021. “Phenoanalyzer.” System Ecology Lab, University of Texas El Paso. https://selutep.squarespace.com/.

Rathcke, B., and E. P. Lacey. 1985. “Phenological patterns of terrestrial plants.” *Annual Review of Ecology and Systematics* 16:179–214.

Reich, P. B. 1995. “Phenology of tropical forests: patterns, causes, and consequences.” *Canadian Journal of Botany* 73:164–174.

Reichmann, L. G., O. E. Sala, and D. P. C. Peters. 2013. “Precipitation legacies in desert grassland primary production occur through previous-year tiller density.” *Ecology* 94:435–443.

Reichmann, L. G., O. E. Sala, and D. P. Peters. 2013. “Water controls on nitrogen transformations and stocks in an arid ecosystem.” *Ecosphere* 4:1–17.

Richardson, A. D., K. Hufkens, T. Milliman, D. M. Aubrecht, M. Chen, J. M. Gray, M. R. Johnston, T. F. Keenan, S. T. Klosterman, M. Kosmala, E. K. Melaas, M. A. Friedl, and S. Frolking. 2018a. “Tracking vegetation phenology across diverse North American biomes using PhenoCam imagery.” *Scientific Data* 5:180028.

Richardson, A. D., K. Hufkens, T. Milliman, D. M. Aubrecht, M. E. Furze, B. Seyednasrollah, M. B. Krassovski, J. M. Latimer, W. R. Nettles, R. R. Heiderman, J. M. Warren, and P. J. Hanson. 2018b. “Ecosystem warming extends vegetation activity but heightens vulnerability to cold temperatures.” *Nature* 560:368–371.

Richardson, A. D., T. F. Keenan, M. Migliavacca, Y. Ryu, O. Sonnentag, and M. Toomey. 2013. “Climate change, phenology, and phenological control of vegetation feedbacks to the climate system.” *Agricultural and Forest Meteorology* 169:156–173.

Rockström, J., W. Steffen, K. Noone, Å. Persson, F. S. Chapin, E. F. Lambin, T. M. Lenton, M. Scheffer, C. Folke, H. J. Schellnhuber, B. Nykvist, C. A. de Wit, T. Hughes, S. van der Leeuw, H. Rodhe, S. Sörlin, P. K. Snyder, R. Costanza, U. Svedin, M. Falkenmark, L. Karlberg, R. W. Corell, V. J. Fabry, J. Hansen, B. Walker, D. Liverman, K. Richardson, P. Crutzen, and J. A. Foley. 2009. “A safe operating space for humanity.” *Nature* 461:472–475.

Römermann, C., S. F. Bucher, M. Hahn, and M. Bernhardt-Römermann. 2016. “Plant functional traits – fixed facts or variable depending on the season?” *Folia Geobotanica* 51:143–159.

Rowley, M. C., S. Grand, and É. P. Verrecchia. 2018. “Calcium-mediated stabilisation of soil organic carbon.” *Biogeochemistry* 137:27–49.

Safriel, U., Z. Adeel, D. Niemeijer, J. Puigdefabregas, R. White, R. Lal, and D. Mcnab. 2005. “Dryland Systems, Millenium Ecosystem Assessment.” in *Ecosystems and Human Well-Being: Current State and Trends,* 623–662. Washington D.C.: Island Press.

Sakamoto, Y., M. Ishiguro, and G. Kitagawa. 1986. “Akaike information criterion statistics.” *Dordrecht, The Netherlands: D. Reidel* 81:26853.

Sala, O. E., R. A. Golluscio, W. K. Lauenroth, and P. A. Roset. 2012. “Contrasting nutrient-capture strategies in shrubs and grasses of a Patagonian arid ecosystem.” *Journal of Arid Environments* 82:130–135.

Sala, O. E., L. A. Gherardi, L. Reichmann, E. Jobbagy, and D. Peters. 2012. “Legacies of precipitation fluctuations on primary production: Theory and data synthesis.” *Philosophical Transactions of the Royal Society B: Biological Sciences* 367:3135–3144.

Sala, O. E., and W. K. Lauenroth. 1982. “Small rainfall events: An ecological role in semiarid regions.” *Oecologia* 53:301–304.

Schlesinger, W. H., editor. 2005. *Biogeochemistry*. Amsterdam: Elsevier.

Schulze, K., W. Borken, J. Muhr, and E. Matzner. 2009. “Stock, turnover time and accumulation of organic matter in bulk and density fractions of a Podzol soil.” *European Journal Of Soil Science* 60:567–577.

Scott, J. D., M. A. Alexander, D. R. Murray, D. Swales, and J. Eischeid. 2016. “The climate change web portal: A system to access and display climate and Earth system model output from the CMIP5 archive.” *Bulletin of the American Meteorological Society* 97:523–530.

Schwinning, S., and O. E. Sala. 2004. “Hierarchy of responses to resource pulses in arid and semi-arid ecosystems.” *Oecologia* 141:211–220.

Seyednasrollah, B., A. M. Young, K. Hufkens, T. Milliman, M. A. Friedl, S. Frolking, and A. D. Richardson. 2019. “Tracking vegetation phenology across diverse biomes using Version 2.0 of the PhenoCam Dataset.” *Scientific Data* 6:222.

Shea, K., and P. Chesson. 2002. “Community ecology theory as a framework for biological invasions.” *Trends in Ecology and Evolution* 17:170–176.

Shukla, J., C. Nobre, and P. Sellers. 1990. “Amazon deforestation and climate change.” *Science* 247:1322–1325.

Smith, M. D., A. K. Knapp, and S. L. Collins. 2009. “A framework for assessing ecosystem dynamics in response to chronic resource alterations induced by global change.” *Ecology* 90:3279–3289.

Sollins, P., C. Swanston, M. Kleber, T. Filley, M. Kramer, S. Crow, B. A. Caldwell, K. Lajtha, and R. Bowden. 2006. “Organic C and N stabilization in a forest soil: Evidence from sequential density fractionation.” *Soil Biology and Biochemistry* 38:3313–3324.

Sonnentag, O., K. Hufkens, C. Teshera-Sterne, A. M. Young, M. Friedl, B. H. Braswell, T. Milliman, J. O’Keefe, and A. D. Richardson. 2012. “Digital repeat photography for phenological research in forest ecosystems.” *Agricultural and Forest Meteorology* 152:159–177.

Sperber, C. von, O. A. Chadwick, K. L. Casciotti, K. G. Peay, C. A. Francis, A. E. Kim, and P. M. Vitousek. 2017. “Controls of nitrogen cycling evaluated along a well-characterized climate gradient.” *Ecology* 98:1117–1129.

Sterner, R. W., and J. J. Elser. 2002. *Ecological Stoichiometry: The Biology of Elements from Molecules to the Biosphere*. Princeton, NJ: Princeton University Press.

Thatcher, D. and Bestelmeyer, B. 2021. “Monthly precipitation data from a network of standard gauges at the Jornada Experimental Range (Jornada Basin LTER) in southern New Mexico, January 1916 - ongoing ver 739.” Environmental Data Initiative.https://doi.org/10.6073/pasta/3086f4fa60f1e0ec807c269490d47ed3.

Throop, H. L., L. G. Reichmann, O. E. Sala, and S. R. Archer. 2012. “Response of dominant grass and shrub species to water manipulation: an ecophysiological basis for shrub invasion in a Chihuahuan Desert grassland.” *Oecologia* 169:373–383.

Throop, H. L., K. Lajtha, and M. Kramer. 2013. “Density fractionation and ^{13}C reveal changes in soil carbon following woody encroachment in a desert ecosystem.” *Biogeochemistry* 112:409–422.

Trenberth, K. E., A. Dai, R. M. Rasmussen, and D. B. Parsons. 2003. “The changing character of precipitation.” *Bulletin of the American Meteorological Society* 84:1205–1218.

Torn, M. S., C. W. Swanston, C. Castanha, and S. E. Trumbore. 2009. “Storage and turnover of organic matter in soil.” In *Biophysico-Chemical Processes Involving Natural Nonliving Organic Matter in Environmental Systems*, edited by N. Senesi, B. Xing, and P. M. Huang, 219–272. Hoboken, NJ: John Wiley & Sons, Inc.

Vitousek, P. 1982. “Nutrient cycling and nutrient use efficiency.” *The American Naturalist* 119:553–572.

Vitousek, P. M., and R. W. Howarth. 1991. “Nitrogen limitation on land and in the sea: How can it occur?” *Biogeochemistry* 13:87–115.

Wang, C., X. Wang, D. Liu, H. Wu, X. Lü, Y. Fang, W. Cheng, W. Luo, P. Jiang, J. Shi, H. Yin, J. Zhou, X. Han, and E. Bai. 2014. “Aridity threshold in controlling ecosystem nitrogen cycling in arid and semi-arid grasslands.” *Nature Communications* 5:4799.

Westoby, M. 1972. “Problem-oriented modelling: A conceptual framework.” *Page IBP/Desert Biome*, Information Meeting, Tempe, Arizona.

Whittaker, R. H., and W. A. Niering. 1965. “Vegetation of the Santa Catalina Mountains, Arizona: A gradient analysis of the south slope.” *Ecology* 46:429–452.

Wilson, R. S., and C. E. Franklin. 2002. “Testing the beneficial acclimation hypothesis.” *Trends in Ecology and Evolution* 17:66–70.

Wingate, L., J. Ogée, E. Cremonese, G. Filippa, T. Mizunuma, M. Migliavacca, C. Moisy, M. Wilkinson, C. Moureaux, and G. Wohlfahrt. 2015. “Interpreting canopy development and physiology using a European phenology camera network at flux sites.” *Biogeosciences* 12:5995–6015.

Wuebbles, D., G. Meehl, K. Hayhoe, T. R. Karl, K. Kunkel, B. Santer, M. Wehner, B. Colle, E. M. Fischer, R. Fu, A. Goodman, E. Janssen, V. Kharin, H. Lee, W. Li, L. N. Long, S. C. Olsen, Z. Pan, A. Seth, J. Sheffield, and L. Sun. 2014. “CMIP5 climate model analyses: Climate extremes in the United States.” *Bulletin of the American Meteorological Society* 95:571–583.

Yahdjian, L., and O. E. Sala. 2002. “A rainout shelter design for intercepting different amounts of rainfall.” *Oecologia* 133:95–101.

Yahdjian, L., and O. E. Sala. 2010. “Size of precipitation pulses controls nitrogen transformation and losses in an arid Patagonian ecosystem.” *Ecosystems* 13:575–585.

Yahdjian, L., L. Gherardi, and O. E. Sala. 2011. “Nitrogen limitation in arid-subhumid ecosystems: A meta-analysis of fertilization studies.” *Journal of Arid Environments* 75:675–680.

Yao, J., H. Liu, J. Huang, Z. Gao, G. Wang, D. Li, H. Yu, and X. Chen. 2020. “Accelerated dryland expansion regulates future variability in dryland gross primary production.” *Nature Communications* 11:1665.

Yao, J., J. J. Anderson, H. Savoy, and D. Peters. 2020. “Gap-filled daily precipitation at the 15 long-term NPP sites at Jornada Basin LTER, 1980-ongoing ver 75.” Environmental Data Initiative. https://doi.org/10.6073/pasta/cf3c45e5480551453f1f9041d664a28f.

Zani, D., T. W. Crowther, L. Mo, S. S. Renner, and C. M. Zohner. 2020. “Increased growing-season productivity drives earlier autumn leaf senescence in temperate trees.” *Science* 370:1066–1071.

Zhang, X., M. A. Friedl, C. B. Schaaf, A. H. Strahler, J. C. F. Hodges, F. Gao, B. C. Reed, and A. Huete. 2003. “Monitoring vegetation phenology using MODIS.” *Remote Sensing of the Environment* 84:471–475.

APPENDIX A

ACKNOWLEDGMENT OF PREVIOUSLY PUBLISHED WORK

This appendix serves to acknowledge that Chapter 2 entitled “Precipitation versus temperature as phenology controls in drylands” has been previously published in the peer-reviewed journal *Ecology,* with Courtney Currier as the lead author and the chair of her Ph.D. supervisory committee, Osvaldo Sala, as the second co-author. Permission has been granted from the co-author to use this previously published material as a research chapter within the culminating dissertation document. The citation for this published work is: “Currier, C. M., and O. E. Sala. 2022. Precipitation versus temperature as phenology controls in drylands. *Ecology* 103:e3793.”